From the: *Max Planck Institute of Psychiatry*

Dissertation zum Erwerb des Doctor of Philosophy
(Ph.D.)

an der Medizinischen Fakultät

der Ludwig-Maximilians-Universität zu München

Non-cell autonomous mechanisms in neurodevelopment and neurological disorders

vorgelegt von:

Fabrizia Pipicelli

aus:

Neapel, Italien

Jahr:

2023

Mit Genehmigung der Medizinischen Fakultät der

Ludwig-Maximilians-Universität zu München

First evaluator (1. TAC member): Prof. Dr. Dr. Elisabeth Binder

Second evaluator (2. TAC member): Prof. Dr. Silvia Cappello

Third evaluator: Prof. Dr. Moritz Rossner

Fourth evaluator: Dr. Jan Deussing

Dean: **Prof. Dr. med. Thomas Gudermann**

date of the defense:
08/03/2023

Table of Contents

Abstract

The cerebral cortex is a complex structure that controls human features, including language and cognition. During brain development, many processes important for the assembly of functional cortical circuits occur, including neurogenesis and neuronal migration. Defects in neurogenesis and neuronal migration might cause neurological diseases such as cortical malformations, epilepsy, and autism spectrum disorders. In particular, interneurons (or inhibitory neurons) play a crucial role in the construction of cortical circuits, and alteration in their specification, as well as migration, leads to neurological disorders.

The aim of this thesis is to shed new light on how the extracellular environment modulates brain development and how it can relate to neurological and neuropsychiatric disorders.

This thesis combined three different projects. The first project focuses on the role of *cystatin B (CSTB)* during neurogenesis. *CSTB* mutation is causative of EPM1, the most common form of progressive myoclonus epilepsy. Here, using both *in vivo* developing mouse brain and *in vitro* 3D human cerebral organoids and assembloids, derived from two EPM1 patients, I investigated the role of CSTB in brain development and EPM1. The results here presented show a non-cell-autonomous function of CSTB in cell proliferation, distribution, neurogenesis, and interneuron recruitment mediated via secretion by extracellular vesicles.

The model system used in the second project are ventrally patterned organoids and dorso-ventral assembloids, presenting mutations in the extracellular matrix glycoprotein LGALS3BP. Mutations in the *LGALS3BP* gene have been identified in patients with neurological disorders and brain malformations. We previously showed that *LGALS3BP*, a human-brain-specific gene, enriched in human RG cells, is important for human cortical development, modifying and regulating the extracellular matrix composition. The results here presented show that the molecular differentiation of interneuron precursors and interneurons can be influenced by altering the composition of the extracellular environment and, changes in cell identity result in defects in interneuron migration and recruitment. Moreover, it has been reported that LGALS3BP regulates progenitor cell delamination and neuronal migration, and its secretion in the extracellular environment is mediated by extracellular vesicles. In this thesis I show that interneuron precursor molecular differentiation and interneuron migration are regulated by short- and long-distance factors released into the extracellular environment by extracellular vesicles.

I, therefore, studied the protein content of extracellular vesicles during brain development. Every cell secretes extracellular vesicles which carry extracellular matrix components that regulate cell growth and differentiation. The knowledge regarding extracellular vesicles in brain development is very little, therefore, in my thesis, I analyzed the role of EVs in neurodevelopment in both physiological and pathological conditions. I characterized EV content, in 3D human cerebral organoids at different time points and in 2D cell cultures (neuronal progenitor cells, neurons, and astrocytes). My results indicate that extracellular vesicles collected from cerebral organoids and neuronal progenitor cells, neurons, and astrocytes, show changes in protein contents according to their developmental stage and cell types.

Moreover, I analyzed the protein content of organoids derived from EPM1 patients and organoids with the LGALS3BP mutation found in an individual with neuropsychiatric diseases.

Interestingly, mutant extracellular vesicles present altered protein content, dysregulated proteins associated with vesicles biogenesis, cell-fate decision, extracellular matrix composition, and axonogenesis, suggesting a non-cell-autonomous role of CSTB and LGALS3BP in these mechanisms.

This thesis proposes novel mechanisms of non-cell autonomous regulation during neurodevelopmental and neurological disorders.

1 Introduction

1.1 Brain and Cortical Development

The human cerebral cortex is a complex structure that regulates behavioral functions, such as language, sociability, cognition and motor skills (Florio and Huttner, 2014; Klingler et al., 2021). The nervous system generates from the ectoderm, one of three layers (endoderm, mesoderm, and ectoderm) produced during the very early mammalian embryonic development. The ectoderm generates the neural crest, which will produce neurons of the peripheral nervous system, and the neural tube, which will give rise to the entire central nervous system. During its differentiation, the neural tube divides into three main areas: the prosencephalon (or forebrain), the mesencephalon (or midbrain), and the rhombencephalon (or hindbrain) (Grace-Dutton, 2005).

During forebrain development, telencephalon, diencephalon, and optic vesicles are formed. The telencephalon will develop the two cerebral hemispheres and, therefore, the cerebral cortex (Grace-Dutton, 2005).

In mammals, cortical development is a highly regulated and coordinated event. The right functioning of cortical activities depends on the two neuronal types that populate the neocortex: glutamatergic or excitatory neurons and GABAergic or inhibitory neurons (Tatti et al., 2017). Neuronal migration and neurogenesis are important processes for cortical development, especially for the correct formation of neuronal circuits, thus the disruption of one or more of these events can lead to a wide range of neurodevelopmental disorders.

1.1.1 Cortical Neurogenesis

Cortical neurogenesis defines the process in which neurons are generated from neural stem cells (NSCs) and neural progenitor cells (NPCs). Three main progenitor cell types that inhabit the mammalian cortex have been classified: apical radial glial cells, basal progenitors, and basal progenitors (Florio and Huttner, 2014) (Figure 1-1).

Neuroepithelial cells

Neuroepithelial cells (NECs) of the neural plate generate cortical neurons (Florio and Huttner, 2014). NECs are characteristic for their symmetric proliferative divisions, which result in the thickening of the neuroepithelium. During cell division, the nucleus of NECs migrates through the cytoplasm along the apical-basal axis of the cell, in a process called interkinetic nuclear migration (INM), resulting in the pseudo-stratification of the neuroepithelium (Sauer and Walker, 1959, Taverna and Huttner, 2010).

NECs are highly polarized and connected to inner and outer surfaces generating the ventricular (VZ) zone and cortical plate (CP); (Stiles and Jernigan, 2010). After the symmetric, self-renewing proliferation, NECs undergo asymmetric differentiative divisions becoming apical radial glia cells (aRGs). The transition from NECs to aRGs appears around embryonic day (E) 9 in mice and at approximately gestational week (GW) 5-6 in humans (Beattie and Hippenmeyer, 2017; Florio and Huttner, 2014; Howard et al., 2008; Rashighi and Harris, 2017).

Cortical apical radial glial cells

aRGs are NPCs with apical-basal polarity, with processes that contact both the ventricle and the basal lamina (Götz and Huttner, 2005). This cell type of progenitors is characterized by the expression of the marker Pax6 (Götz et al., 1998; Lui et al., 2011; Rakic, 1972; Stiles and Jernigan, 2010) and functions as a scaffold for the migration of cortical neurons within the cortical layers. In humans, aRGs will give rise to the majority of cortical cells: neurons and glia (Götz and Huttner, 2005). Indeed, they undergo either symmetric proliferative division, increasing the stem cell pool in the VZ, or asymmetric differentiative division producing basal progenitors (BPs).

Cortical basal progenitors

Basal progenitors are generated from aRGs that retract their apical process, delaminate, and migrate into the subventricular zone (SVZ). BPs are composed by basal intermediate progenitors (bIPs) and basal radial glia cells (bRGs).

Cortical basal intermediate progenitors

Basal intermediate progenitors (bIPs) originate from aRGs or NECs and are localized at the SVZ, where they divide basally. This population of progenitors starts downregulating PAX6 and expresses the marker EOMES (known also as TBR2) and produces only neurons (Götz and Huttner, 2005; Haubensak et al., 2004; Kriegstein et al., 2006; Miyata et al.,

2004; Noctor et al., 2004). Basal intermediate progenitors present different behaviour in different species. In the mouse and in other lissencephalic species, with a "smooth brain", bIPs divide asymmetrically and directly generated neurons (Florio and Huttner, 2014; Haubensak et al., 2004; Kriegstein and Noctor, 2004; Miyata et al., 2004). While in gyrencephalic species, including primates and humans, bIPs divide also symmetrically to increase the bIPs pool before asymmetrical division which will produce neurons (Fietz and Huttner, 2010; Florio and Huttner, 2014; Lui et al., 2011).

Cortical basal radial glial progenitors

Basal radial glial progenitors are localized in the outer subventricular zone (oSVZ), an additional germinal zone enriched in humans. Indeed, bRGs are human enriched progenitors, essential for cerebral cortex expansion and generation of folds, typical of gyrencephalic species. (Buchsbaum and Cappello, 2019; Götz and Huttner, 2005; Hansen et al., 2010; Lui et al., 2011; Pilz et al., 2013; Taverna and Götz, 2014). Most bRGs express PAX6, but some can also express EOMES (Betizeau et al., 2013; Florio and Huttner, 2014; Florio et al., 2017). Basal radial glial progenitors are monopolar cells characterized by the absence of apical junctions, typical of aRGs (Borrell and Götz, 2014; Cappello et al., 2012a; Fish et al., 2008; Götz and Huttner, 2005). They also have basal process that contacts the pial surface of the cortex (Arai and Taverna, 2017; Fietz et al., 2010; Nowakowski et al., 2016).

1.1.2 Migration of Excitatory Neurons

Neuronal migration is a highly coordinated process that permits the establishment of the typical multilayer organization of the mammalian cortex. The mammalian cortex consists of six cellular layers which are generated in an "inside-out" fashion: early-born neurons are localized in cortical deep layers, while late-born neurons colonize the superficial layers of the cortex (Alvarez-buylla and Nottebohm; Rakic, 2009).

During early neurogenesis, newborn excitatory neurons migrate basally from their place of origin (VZ) to the marginal zone (MG) with a movement called somal translocation (Buchsbaum and Cappello, 2019a). From the VZ, excitatory neurons extend a radially directed leading process that reaches the pial surface. Once the leading process shortens, the soma is pulled up to the cortical plate (Nadarajah and Parnavelas, 2002a; Nadarajah et al., 2001).

With the increase of cortical thickness, neurons shift from somal translocation to multipolar migration, where they extend and retract multiple processes resulting in an undirected migration mode, reaching the intermediate zone (IZ). In the IZ, they undergo a multipolar-to-bipolar transition and begin the radial migration using the basal process of RGs as a migratory scaffold and migrate through the cortical layers (Buchsbaum and Cappello, 2019b; Nadarajah et al., 2001; Pipicelli et al., 2022). RG-dependent neuronal migration is regulated by cilia/centrosome and nuclear movements, called nucleokinesis (Marín, 2013). Neurons that migrate with this type of migration display saltatory movements and are slower compared to neurons that migrate with somal translocation (Nadarajah and Parnavelas, 2002b; Nadarajah et al., 2001). Once migrating neurons reach the MZ, they detach from the RG fibers (terminal translocation) and terminate their migration (Sekine et al., 2011). The six cortical layers are formed in a birth-date-dependent and inside-out manner (Sun and Hevner, 2014) (Figure 1-1)

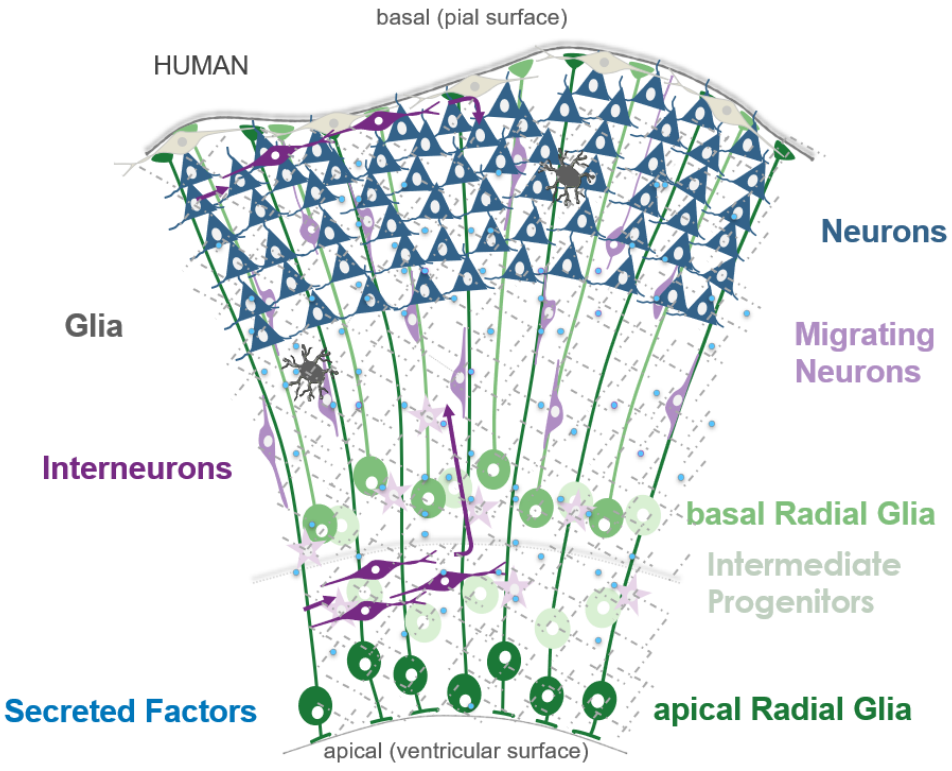

Figure 1-1: Neuronal migration in the developing brain

Schematic of the developing human cerebral cortex. Cell composition is shown, including migrating excitatory neurons and interneurons. Figure adapted from Buchsbaum and Cappello, 2019.

1.1.3 Genesis of Interneurons

During neurogenesis, interneurons (INs) generate from the germinal area of the ganglionic eminences (GEs), located in the ventral forebrain (also known as subpallium). The ventral forebrain includes distinct proliferative areas: the GEs are indeed divided in, medial (MGE), lateral (LGE), annd caudal (CGE). Moreover, the preoptic area (POA) is also part of the ventral forebrain. (Peyre et al., 2015). MGE and CGE give rise to most of interneuron subtypes, while LGE gives rise to striatal neurons (Flames et al., 2007; Miura et al., 2020; Rubin et al., 2010; Yun et al., 2003)

As in the cortex, in the GEs, radial glial cells (RGs) are generated from neuroepithelial cells. This differentiation occurs around mouse embryonic day 10 (E10) in the forebrain (Anthony et al., 2004; Turrero García and Harwell, 2017). GEs are organized in ventricular (VZ) and subventricular (SVZ) zones. Postmitotic cells derived from VZ and SVZ move to the marginal zone (MZ) (Turrero García and Harwell, 2017).

Ventral radial glial cells (RGs) are located in the VZ and divide asymmetrically to generate other progenitor types, as well as self-renewing progenies (Peyre et al., 2015). The cell bodies of ventral RGs occupy the VZ, the germinal region that faces the ventricle, of the GEs, where they proliferate (Turrero García and Harwell, 2017). They also display a bipolar morphology, with apical and basal processes that contact the ventricular and basal surfaces, respectively. During development, RGs from MGE and LGE divide at basal regions, and this results in the formation of the SVZ. At this point, the SVZ will become the main proliferative area in the GEs. Differently from cortical RGs, ventral RGs do not contact the pia, but the blood vessels of the SVZ or MZ (Turrero García and Harwell, 2017). Ventral RGs divide either symmetrically or asymmetrically, as was described for cortical RGs. With the differentiative asymmetrical division, they produce other populations of progenitors, including intermediate progenitors (IPs) and basal radial glia (bRGs) (Figure 1-2).

Ventral IPs, as well as cortical IPs, have a multipolar morphology and populate the SVZ. They differentiate into neurons, after undergoing a single round of division (Brown et al., 2011). Ventral IPs undergo symmetrical proliferative divisions expanding the IPs pool, and asymmetrical differentiative divisions resulting in the interneuron population (Buchsbaum and Cappello, 2019a; Pilz et al., 2013).

Ventral bRGs also display a monopolar morphology, as do cortical bRGs, and they have been recently identified in the LGE. They maintain their basal process and derive from the asymmetrical division of RGs (Pilz et al., 2013). Ventral bRGs self-renew and their abundance in the brain correlates with the expansion of the cortex in gyrencephalic species (Borrell and Götz, 2014).

The development of GEs is guided by morphogens and transcription factors that will define their ventral identity. The MGE is organized into two domains, dorsal MGE which gives rise to somatostatin (SST) INs, and ventral MGE that generates parvalbumin (PV) INs (Cobos et al., 2005; Peyre et al., 2015; Yu et al., 2021). The transcription factors NKX2-1, LHX6, and DLX genes control MGE-derived INs specification and maturation (Flames et al., 2007; Flandin et al., 2011; Peyre et al., 2015). The CGE contributes to the generation of calretinin (CR), vasoactive intestinal peptide (VIP), and LAMP5 INs (Butt et al., 2005; Krienen et al., 2020; Pleasure et al., 2000). The specification of CGE-derived INs is controlled by the homeobox transcription factors GSH or GSX, MASH1 and NRF2F1, and NRF2F2 (Lodato et al., 2011; Xu et al., 2011). During embryogenesis, the ventralization of GE is induced by morphogens and transcription factors, including forkhead G1 factor (FOXG1), fibroblast growth factors (FGFs), and Sonic hedgehog (SHH) (Briscoe and Ericson, 2001; Jessell TM, 2000; Martynoga et al., 2005; Peyre et al., 2015).

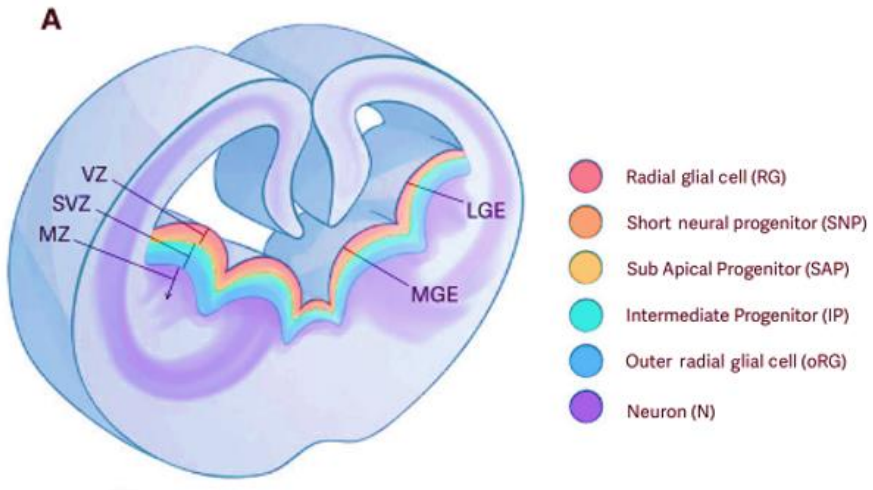

Figure 1-2: Cell progenitor types and proliferative areas in the ganglionic eminences (GEs)

Schematic of a coronal section of a mouse forebrain. Ventrcular (VZ), subventricular (SVZ) and marginal (MZ) zones of GEs are show. Figure adapted from Turrero and Harwell, 2017.

1.1.4 Migration of Interneurons

Inhibitory neurons (or interneurons, INs) are generated in the GEs and migrate long distances from their place of birth in the ventral forebrain to reach the cortex in the dorsal forebrain (Lim et al., 2018; Mayer et al., 2018).

After mitosis, INs start migrating tangentially displaying their typical cycling movement. First, INs extend multiple, diverging branches from the leading process to better sense the extracellular cues. The branch that senses the cues will be stabilized, while the other branches will be retracted. At this point, the nucleus will move in the same direction of the leading process, defining the direction of the migration. The cycling movement of INs is characterized by a cycle of two-phase nucleokinesis. After the stabilization of the leading process, a transient swelling close to the cell body occurs (Guo and Anton, 2014). At this point, the INs move forward by nuclear translocation into the swelling, while the trailing process is retracting (Guo and Anton, 2014; Peyre et al., 2015). After nucleokinesis, the cycle starts again.

INs are highly polarized and can change their direction of migration by inverting polarity via extension and retraction of leading and trailing processes. Characteristic of INs migration is the jumping, saltatory migratory behavior, resulting from sharp periods of pauses (when the leading process is extended and exploring), and movement (when the soma translocates towards new directions) (Bellion et al., 2005; Guo and Anton, 2014; Nadarajah et al., 2001; Peyre et al., 2015; Silva et al., 2018).

Newborn interneurons sense several cues that promote their tangential migration to the cortex. The migration starts after the repulsion of INs from the GEs by repulsive cues (SLIT, netrin1, and ephrin A5) (Hamasaki et al., 2001; Zimmer et al., 2008). Consequently, they integrate and move in tangential migratory streams to reach the cortex. Interneurons are attracted by gradients of molecules including NRG1 and CXCL12, released by IP in the cortex. Indeed, it has been shown that the presence of TBR2+ bIPs facilitates the migration of INs into the IZ (Sessa et al., 2010). Two migratory streams have been identified: the intermediate zone (IZ) stream, located at the cortical IZ, and the marginal zone (MZ) stream, located at the marginal zone (Lavdas et al., 1999; Nadarajah and Parnavelas, 2002a; Sessa et al., 2010; Silva et al., 2018).

It has been shown that the choice of a specific migratory path is correlated with the temporal origin and fate of INs, and is controlled by attractive and repulsive cues (Flames et al., 2004; Tiveron et al., 2006). Specifically, INs express CXCR4 and CXCR7 receptors that sense CXCL12, permitting INs to migrate in streams and reach the cortex (Marin 2013)

By the end of embryogenesis, INs sensing SHH gradients reach the cortex (Baudoin et al., 2012), where they switch to radial migration to disperse into cortical layers, differentiating and establishing functional dendritic and axonal connections (Ohnuma and Harris, 2003; Tanaka et al., 2004). It has been reported that the tangential-radial migration switch is regulated by the responsiveness to CXCL12: specifically, the exit from the tangential migratory stream coincides with a loss of response to CXCL121 as a chemoattract (Li et al., 2008).

In the cortex, INs of both streams actively contact the radial glial processes, and then switch to radial migration and migrate up to the developing cortical plate. Some INs of the IZ stream can also display a "ventricle-oriented migration" (Bellion et al., 2005; Guo and Anton, 2014), characterized by radial migration into the VZ, resting, an extension of multiple processes in the VZ, and then migration towards the cortical plate.

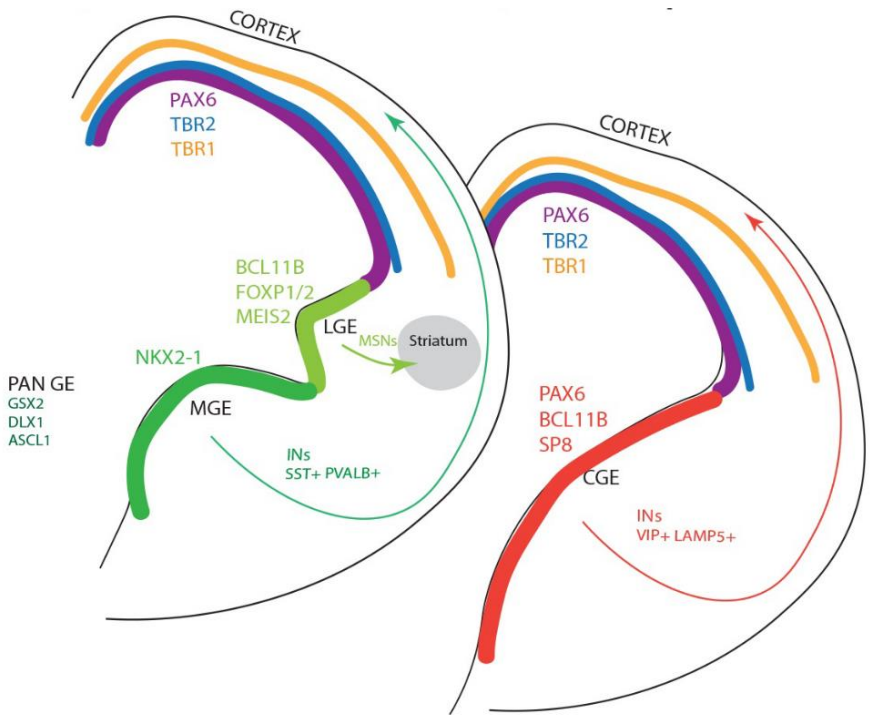

Figure 1-3: Tangential migration of interneurons

Schematic of a coronal section of mouse developing brain showing tangential migration of interneurons with representative molecular markers.

Interneurons reach the cortex following a lateral-medial gradient: young INs arrive at the lateral cortical domains earlier than the medial regions. Different subtypes of INs follow different ways for cortical positioning. MGE-derived SST and PV INs display a time-dependent, inside-out manner; CGE-derived CR INs display an outside-in fashion; and VIP localize to superficial layers or display a scattered positioning within the developing cortex (Guo and Anton, 2014; Métin et al., 2006; Peyre et al., 2015; Romero-grimaldi and Moreno-lo, 2008) (**Error! Reference source not found.**).

1.2 Extracellular Matrix in Neurodevelopment

Neurogenesis and neuronal migration are highly regulated, especially by the extracellular matrix (ECM). The ECM is a complex and dynamic structure of proteins that surround cells within a tissue (Long and Huttner, 2019). It is an essential part that forms the cellular microenvironment during corticogenesis (Amin and Borrell, 2020). The ECM components include macromolecules such as integrin and syndecans, involved in cell adhesion and signaling; or proteoglycans, laminins, fibronectins, elastins, and tenascins that function as cellular structural support (Frantz et al., 2010; Hynes, 2009).

During neurodevelopment, the ECM has other fundamental functions. It has been shown that the ECM regulates cell proliferation, morphology, migration, and differentiation via signal pathways (Amin and Borrell, 2020; Long et al., 2018). Many molecules, including morphogens, and proteins are released by cells in the ECM and their presence in the extracellular environment is crucial for regulating patterning and cellular behavior, especially migration and recruitment of neurons.

The proteoglycan reelin (RELN) has been described to be crucial for neuronal migration, promoting the interaction of migrating neurons with ECM and RG scaffold. Reelin is secreted by Cajal-Retzius cells in the MZ. (Amin and Borrell, 2020; Long and Huttner, 2019).

Moreover, many morphogens critical for patterning are released in the ECM. Sonic hedgehog (Shh) is known to define the ventral identity of the subpallium and it is mostly secreted by postmitotic MGE-derived INs (Chiang et al., 1996; Ericson et al., 1995; Flandin et al., 2011). Retinoic acid (RA) is also secreted in the ECM and is involved in the patterning of the developing cortex (Rhinn and Dollé, 2012; Siegenthaler and Pleasure,

2011). The early patterning of the telencephalon is also determined by Wnt proteins, secreted by the cortex. Wnt proteins maintain cell proliferation and determine cell fate switch in MGE progenitors via the canonical Wnt pathway through activation of b-catenin. (Bielen and Houart, 2014; Zhong et al., 2011). Fibroblast growth factors (FGF) determine telencephalon formation as well as patterning and migration of cortical neurons (Borello et al., 2008; Martynoga et al., 2005).

Moreover, previous works have demonstrated that ECM plays a role in human cortex expansion and gyrification (Albert et al., 2017; Fietz et al., 2012; Karzbrun et al., 2018). Human ECM reveals a different expression and composition compared to mouse during cortex development, specifically, different sets of collagens, proteoglycans, integrins and laminins are expressed in increased amounts in the human cortex (Fietz et al., 2012; Florio and Huttner, 2014; Florio et al., 2017; Long and Huttner, 2019; Long et al., 2018). A previous study has demonstrated that the ECM components HAPLN1, lumican, and collagen I induce folding of the cortical plate in human fetal cortical explants, suggesting the fundamental role of ECM in human cortical expansion and gyrification (Long et al., 2018).

1.3 Extracellular Vesicles in Neurodevelopment

The extracellular environment is crucial for the right functioning of the human brain by regulating cell-cell communication and transport of molecules or proteins.

In this thesis, I will focus on the role of extracellular vesicles (EVs) in neurodevelopment. Extracellular vesicles are secreted by all cells and transport various cargos such as proteins, nucleic acid, including, DNA, mRNAs and microRNAs, metabolites, lipids (Shah et al., 2018). Extracellular vesicles are classified as ectosomes and exosomes. Ectosomes are generated by the direct budding of the plasma membrane and produce microvesicles, with a diameter between 50 nm and 1 um (Kalluri and LeBleu, 2020; Van Niel et al., 2018). Exosomes, instead, generate from multivesicular bodies (MVBs), an accumulation of vesicles originated from an endocytic cisterna. MVBs fuse with the plasma membrane in a process called exocytosis, mediated by G proteins, such as Ral1, Rab27 and Rab27b (Hyenne et al., 2018; Ostrowski et al., 2010), followed by the release of MVBs content in the extracellular environment (Meldolesi, 2018). Exosomes, instead, are vesicles of 30-200 nm diameter (Kalluri and LeBleu, 2020). Among the complexes and proteins involved in exosome biogenesis, Rab, Syntentin1, TSG101, syndecan-1, ESCT proteins, tetraspanins and SNARE complex have been described (Ciardiello et al., 2016; Mathieu et al., 2019).

Extracellular vesicles differ in their origin, size, content, and function on receiving cells. The effect on receiving cells could be determined by expression of specific surface receptors which can induce survival or apoptosis, for example. EV heterogeneity has been described in macrophages, hepatocytes, adipocytes, endothelial cells and smooth and skeletal muscle fibers (Meldolesi, 2018) and refers to EV cargoes and membrane composition. EV membranes are composed of cholesterol and sphingomyelin, important for MVB biogenesis; tetraspanins involved in luminal cargo loading, such as surface and intracellular signaling proteins (E-cadherin, b-catenin and Wnt) (Van Niel et al., 2018; Urbanelli et al., 2016), by interacting with cytosolic proteins (Perez-Hernandez et al., 2013; Vyas and Dhawan, 2017). Other EV cargoes identified are cytoskeletal and microtubules associated proteins, such as annexin and actin; chaperones, enzymes, GTPases, nucleic acids, especially miRNAs (Figure 1-4).

It has been shown that EVs play a role in cell physiology, regulating the maintenance and plasticity of stem cells, proliferation, apoptosis, repair of damaged tissue, mediating cell-

to-cell communication (Kalluri and LeBleu, 2020). EV release and uptake can affect both the parent and receiving cell at the protein and transcriptomic level (Meldolesi, 2018).

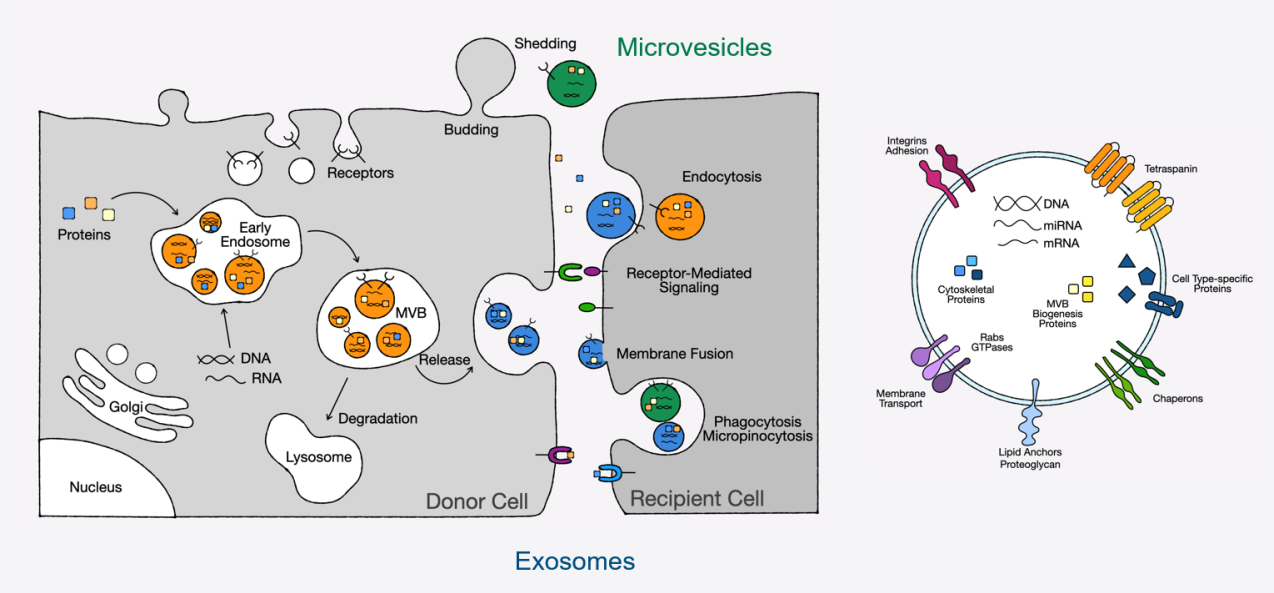

Figure 1-4:EV biogenesis and content

Schematic representing biogenesis and content of extracellular vesicles (EVs). EVs can be released either by direct budding from the plasma membrane (microvesicles) or by fusion of internal multivesicular compartments (MVB) with the plasma membrane (exosomes). EVs carry nucleic acids, proteins, lipids, and metabolites.

EVs have been studied in many tissues and organs. In the brain, they are involved in neuronal plasticity, myelination, synapses and neuronal-glia communication (Montecalvo et al., 2012). The role of EVs in disease has been described in cancer, where EVs transfer oncogenes (Chen et al., 2017; Muralidharan-Chari et al., 2010), and in neurodegeneration. EVs can promote neurodegeneration via transfer of miRNA and proteins in Alzheimer's disease and amyotrophic lateral sclerosis. The role of EVs during brain development is poorly understood, in this thesis, I will show some crucial events regulated by EVs, in both physiological and pathological conditions.

1.4 Neurological and Neuropsychiatric Disorders

The generation of the human cortex is a complex and highly regulated process, it is not surprising that any disruption in neurogenesis, neuronal migration, extracellular matrix composition and/or secretion might lead to diseases. Neurological and neuropsychiatric disorders are characterized as chronic diseases that affect the central nervous system during development. They constitute a wide range of disorders characterized by impairments in learning, communication, motor, and attention (Mullin et al., 2013). The most known and studied neurological and neuropsychiatric disorders include cortical malformations, epilepsy, developmental delay and regression, intellectual disability, autism spectrum disorder, and specific learning disabilities (Ismail and Shapiro, 2019). In this thesis, I will focus on cortical malformations and epilepsy.

1.4.1 Cortical Malformations

Cortical malformations (CMs) can be developed from environmental factors, including drug or alcohol abuse or infections of Zika virus during pregnancy, maternal seizures, or radiation exposure. However, many studies revealed that genetic factors are involved role in the onset of CMs.

Cortical malformations are caused by deregulation of mechanisms of cortical development at both the cellular and molecular level. They are highly heterogeneous, however, the most known causes of CMs are mutations in genes associated with cytoskeletal regulation.

The classification of CMs is very complex considering the level of heterogeneity of these diseases. In fact, the identification of the causes of CMs is very challenging. The relationship between genetic variants and phenotypes is complicated: in same cases a mutation in a single gene can lead to different clinical outcomes; while, in others, mutations in different genes can lead to a same phenotype (Klingler et al., 2021). For this reason, the study of genetic causes leading to CMs is very complicated.

This group of neurodevelopmental disorders can be classified in malformations due to defects in cell proliferation or apoptosis, defects in cell migration or in post-migration development (Barkovich et al., 2012; Hu et al., 2014) (Figure 1-5).

Malformations due to defects in cell proliferation or apoptosis

In this category belong diseases characterized by decrease in proliferation and increase in apoptosis, in case of microcephaly; increase in proliferation and decrease in apoptosis, in case of megalocephaly; and defects in progenitor proliferation in dysplastic malformations. Patients with microcephaly present a smaller brain size compared to healthy individuals (Gilmore and Walsh, 2013). Many genes associated with regulation of neurogenesis, cell proliferation, but also chromosomal segregation and cell division have been identified as causative of microcephaly (Desikan and Barkovich, 2016). These genes include: *ASPM* (Bond et al., 2002; Létard et al., 2018; Nicholas et al., 2009), *CENPJ* (Hung et al., 2000), *CDK5RAP2* (Megraw et al., 2011; Thornton and Woods, 2009).

Individuals affected with megalocephaly present an overgrow brain (DeMyer, 1986; Pirozzi et al., 2018). and it can be associated with polymicrogyria (PMG) (Barkovich et al., 2012; Leventer et al., 2010). It has been reported that the mTOR pathway is involved in megalocephaly, indeed mutations in *AKT3*, *PIK3CA* and *PIK3R2* genes lead to this malformation (Desikan and Barkovich, 2016;Rivière et al., 2013). Moreover, these mutations are also associated with focal cortical dysplasia (FCD) and nodular periventricular heterotopia (NPH). (Alcantara et al., 2017; D'Gama et al., 2015; Desikan and Barkovich, 2016).

Malformations due to defects in neuronal migration

Abnormal neuronal migration can lead to lissencephaly, type I and II; subcortical band heterotopia (SBH) and periventricular heterotopia (PH) (Desikan and Barkovich, 2016; Lee, 2017). Lissencephaly type I is the most common CM, characterized by loss of the gyral patterning resulting in a "smooth brain". Patients with lissencephaly present increased brain thickness. Mutations in the *LIS1* gene can lead to lissencephaly (Pilz, 1998). *LIS1* regulates the proliferation of neuroepithelial cell, permitting the correct spindle orientation and symmetric division (Yingling et al., 2008). Also, *TUBA1A* has been identified as associated with lissencephaly. *TUBA1A* is a neuronal alpha-tubulin involved in cell migration and motility (Keays et al., 2007). Individuals with mutation in *TUBA1A* manifest microcephaly and mental retardation (Bahi-Buisson et al., 2008; Barkovich et al., 2012; Jansen et al., 2011). Mutations in *Reelin* have also been identified in individual with lissencephaly (Hong et al., 2000). Lissencephaly type II, known also as cobblestone lissencephaly, is a CM where patients present an increased migration of neurons at the pial surface (Bizzotto and Francis, 2015). In this condition, the basal membrane is disrupted

which prevents the basal process of the RGs to attach to it and the neurons continue their migration. Mutations in genes encoding for glycosyltransferases and for ECM components such as *LAMB1* and *COL4A1* have been described to be associated with lissencephaly type II.

Individuals diagnosed with subventricular heterotopia (SBH) present a band of grey matter between the ventricle and the cortex resulting in the so-called "double cortex". In 85% of the cases, SBH is associated with mutations in the *DCX* gene, a microtubule-associated gene important for the correct stabilization of the cytoskeleton (Cappello et al., 2012b)**.** Subventricular heterotopia can be caused by disruption in RGs which will ultimately affect neuronal migration within the cortex.

Another gene involved in the onset of SBH is *EML1*, codifying for a microtubule-associated protein and important for spindle orientation. Patients with mutations in this gene have ectopic neurons in their brain (Bizzotto et al., 2017; Kielar et al., 2014).

Like SBH, also periventricular heterotopia (PH) is a condition characterized by ectopic neurons in the brain. In the case of nodular periventricular heterotopia (PVNH), the most common of the PHs, neurons are organized in nodules in the SVZ, lining the ventricles (Barkovich and Kuzniecky, 2000; Barkovich et al., 2012). Interestingly, most of the patients diagnosed with PVNH present epileptic seizures (Dubeau et al., 1995; Pang et al., 2008) at the level of the ectopic neuronal nodules (Scherer et al., 2005). Periventricular heterotopia can be caused by altered morphology of RGs which will impact neuronal migration, or by defects in neuronal motility (Desikan and Barkovich, 2016; Ferland et al., 2009; Klaus et al., 2019).

Patients with PH have shown to have mutations in *FAT4* and *DCHS1* genes, codifying for two protocadherins involved in cell migration, proliferation, and polarity (Cappello et al., 2013; Ishiuchi et al., 2009; Klaus et al., 2019).

Mutations in the gene *FLNA* are also associated with PH. *FLNA*, filamin A actin-binding protein, is involved in RG proliferation and polarity (Carabalona et al., 2012), remodeling the cytoskeleton (Ekşioğlu et al., 1996; Fox et al., 1998; Parrini et al., 2006). Other mutations that can lead to PH occur in the genes *MOB2* (O'Neill et al., 2018a), part of the Hippo pathway, and *ARFGEF2*, involved in vesicle trafficking (Desikan and Barkovich, 2016; Ferland et al., 2009).

LGALS3BP, galectin-3 binding protein, is involved in neuronal progenitor delamination and localization of neurons and mutations of this gene have been identified in patients with PH (Kyrousi et al., 2021; O'Neill et al., 2018b).

Among the transcription factors (TFs) involved in the onset of CMs, mutation of *EOMES*, *FOXG1*, *PAX6* genes have been found in patients with microcephaly (Guerrini and Dobyns, 2014).

The study of the causes of CMs is very challenging, considering that they are associated with neuropsychiatric disorders, mostly epilepsy.

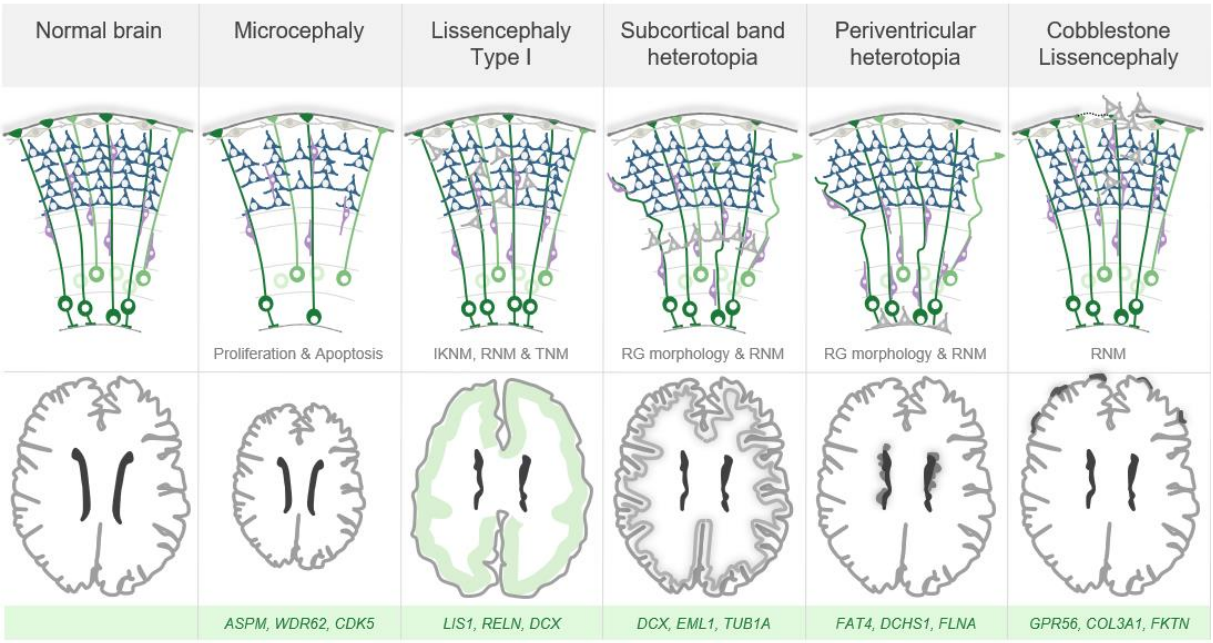

Figure 1-5: Cellular and anatomical defects associated with cortical malformations

Schematics showing cellular and anatomical features of CMs Cortical layers and migratory pattern are shown. Figure adapted from Buchsbaum and Cappello, 2019.

1.4.2 Epilepsy

Clinical studies show that many individuals with cortical malformations present epileptic seizures. Epilepsy is a neuropsychiatric condition characterized by a predisposition to generate repeated spontaneous bursts of neuronal activity, known as seizures (Bozzi et al., 2012). Many factors can lead to epilepsy, including cortical malformations, moreover disruption in neurogenesis, neuronal migration and differentiation can alter the excitatory/inhibitory balance resulting in neuronal hyperexcitability and onset of seizures.

Many genes, whose mutations are associated with CMs, are also causative of epilepsy. *RELN*, *DCX*, *DLX* and *ARX* play a role in excitatory and inhibitory neuron migration and, several studies have shown their involvement in altering the excitation/inhibition ratio and generating seizures (Bozzi et al., 2012; Guerrini and Dobyns, 2014).

Epilepsy can also occur when the assembly of excitatory and inhibitory synapses is perturbated. During development, the immature neuronal circuits are refined into organized and mature circuits. In the refining process, many connections are eliminated, and the remaining synapses mature functionally (Katz and Shatz, 1996). The correct functioning of different channels and the control of neurotransmitter release are necessary for a proper assembly and maturation of synapses. Mutations in sodium, potassium and calcium channels lead to a group of epilepsies called 'channelopathies', while disruption of synapsins (SYN1, SYN2 and SYN3) and SNAP-25 leads to defects in neurotransmitter release and synapse formation (Bozzi et al., 2012).

Epileptic seizures can be classified as focal, generalized, and unknown. Focal seizures are limited to one side of the hemisphere, and they can be motor (associated with muscle movement) or non-motor (without muscle movement). Generalized seizures, instead, start from both hemispheres spreading to other brain regions and they can also be motor or non-motor. The motor seizures include myoclonic-tonic-clonic, characterized by arms jerking, tonic stiffening and irregular rhythmical jerking; and myoclonic-atonic epileptic spasm, characterized by brief jerking of limbs and limp drop (Sarmast et al., 2020).

In this thesis, I will focus on a specific group of epilepsies: myoclonic epilepsy. This group of epilepsies present brief and sudden seizures combined with muscle contractions and they are generalized (Leppik, 2003) as described above. The classification of myoclonic epilepsy is very complex since they can occur unilaterally or bilaterally, and, in this last case, also symmetrically or asymmetrically.

Many genetic studies shed light in the understanding of myoclonic epilepsies. Some of them can be acquired after specific events, including tumors, anoxia, head trauma or stroke. But most of them are inherited and include benign primary epilepsy syndromes (JMEs) and progressive myoclonic epilepsies (PMEs) (Leppik, 2003).

Benign primary epilepsies

This group of epilepsies occur in the early childhood and they present both tonic (stiffening) and clonic (jerking) generalized seizures (Leppik, 2003), and, about one third of patients

do not suffer from seizures. Genetic studies identified many families where JME has been linked to chrosome 6p and 15q (Leppik, 2003).

Progressive myoclonic epilepsies

This rare group of epilepsies are severed neurological disorders with genetic basis. The most common PME is Unverricht-Lundborg disease (EPM1), an autosomal recessive disorder with the onset of symptoms starting in early childhood and adolescence (Kälviäinen et al., 2008) with a slow progression (Leppik, 2003). It is a rare disease, with an incidence of 1:20000 in Finland. EPM1 patients present ataxia, dysarthria, and tremor. Moreover, they show irregular and asynchronous seizures and problems with walking, swallowing, and speaking which will worsened with the progression of the disease. Mutations in the gene *cystatin B* are responsible for EPM1. The role of *CSTB* will be discussed in chapter 3.

Neurological and neuropsychiatric disorders are a very complex group of diseases, mostly because they include a wide range of clinical expressions and comorbidities, including epileptic and autistic features. Altogether, these features make the identification of the cause(s) of the diseases very challenging (Guerrini and Dobyns, 2014; Klingler et al., 2021) (Klinger et al., 2021, Guerrini and Dobyns, 2014).

1.5 How can we study brain development and neurological and neuropsychiatric disorders?

The human brain is an extremely complex structure, which makes its study very challenging. Ideally, research on human brain development and disease would be carried out using human tissue. However, the availability of human tissues, including post-mortem tissues or biopsies, is limited. For this purpose, researchers have developed and use different suitable model systems.

1.5.1 *In vivo* models

The most common *in vivo* animal model used to study brain development and diseases is the mouse. This system allows to study specific genes described in patients with neurological disorders and to understand mechanisms underlying neurodevelopment by generating knockouts of disease-associated genes, for example. However, it has been shown that few models have recapitulated the exact phenotype described in patients with CMs, like in the case of the Eml1 KO model for SBH (Bizzotto et al., 2017; Kielar et al., 2014) or in the Flna conditional cKO model for PH (Feng et al., 2006). This is not surprising, considering the species differences between mouse and primate, including human, brain development.

The human and the mouse brains present macroscopic differences, including size, progenitor cell number and composition of the ECM (Pollen et al., 2015). The mouse brain is smaller and lissencephalic, “smooth”, while the human brain is larger and gyrified. Moreover, the human cortex is characterized by the abundance of bRGs that populate the outer SVZ, absent in the mouse cortex (Figure 1-6).

These specie-specific aspects should be taken in account when choosing the model system to study human brain development and disease. For this purpose, ferrets, and non-human primates, such as macaque or marmosets, are also used. The cortex of the ferret contains abundant bRGs and is gyrified (Fietz and Huttner, 2010), moreover the migration modes of neurons is like the ones observed in primates (Gertz and Kriegstein, 2015). The brain of the macaque shares some features with the human brain in terms of size, abundance of bRGs, number of neurons and gyrification. Marmosets are lissencephalic like the mouse, but their cortex is abundant in bRGs.

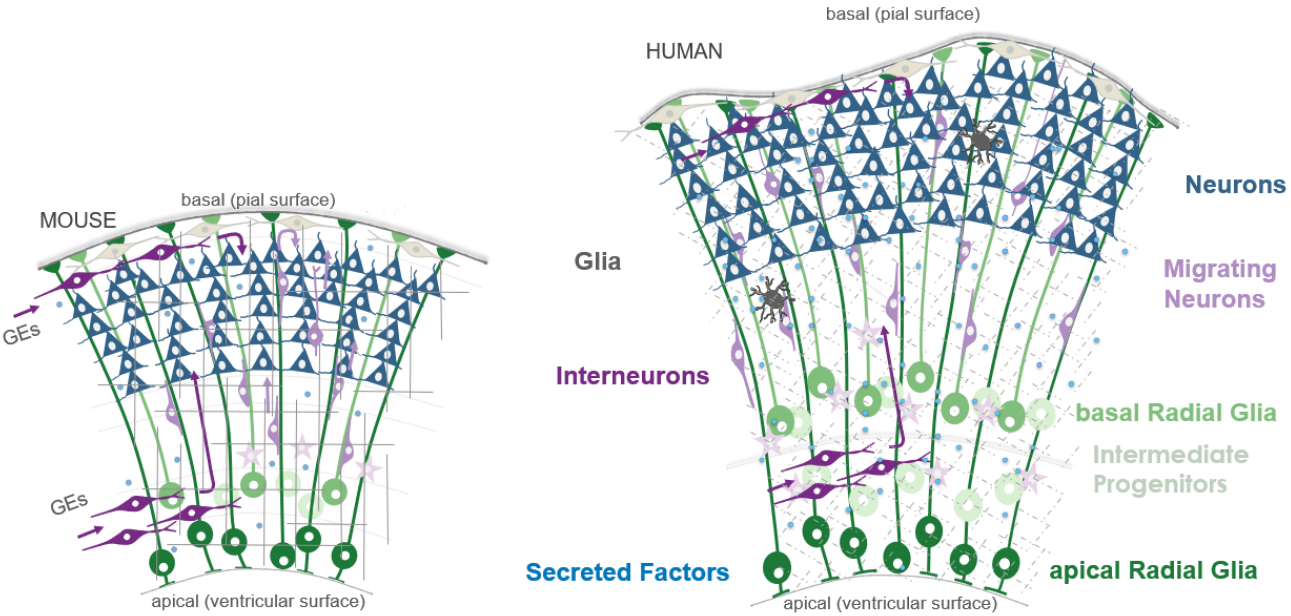

Figure 1-6 Cortex during mouse and humanl development

Cell composition in the developing mouse -lissencephalic- (left) and -gyrified- human (right) cerebral cortex is shown Figure adapted from Buchsbaum and Cappello, 2019.

However, animal models alone do not allow a full recapitulation of human brain development, due to still important differences compared to human. For this reason, in *vitro* models were established.

1.5.2 2D *in vitro* models

The advances in stem cell technology have brought many advantages in the study of human brain development. Many protocols have established techniques to differentiate stem cells into neural progenitor cells, neurons, and glial cells. The stem cells used in these protocols are either human embryonic stem cell (hESCs) or induced pluripotent stem cell (iPSCs). hESCs derive directly from human blastocysts (Thomson, 1998), while iPSCs derive from somatic cells, like peripheral blood mononuclear cells or fibroblasts, and are reprogrammed into a stem cell state (Staerk et al., 2010; Takahashi and Yamanaka, 2006; Yu et al., 2007) (Figure 1-7)

The in *vitro* protocols used for the 2D generation of neural progenitors and neurons require neuroepithelial cells to organize themselves in neuronal rosettes, maintaining the apicobasal polarity observed in *vivo* (Elkabetz et al., 2008; Shi et al., 2012a, 2012b). Neural progenitor cells (NPCs) can be developed from hESCs or iPSCs, and they can be differentiated into neurons, obtaining many mature neurons (Boyer et al., 2012; Brennand

et al., 2011; Chambers et al., 2009; Gunhanlar et al., 2017a; Shi et al., 2012a, 2012b). These models allow to investigate cell morphology, migration and maturation (Buchsbaum and Cappello, 2019), however, they are characterized by a restricted spatial organization and lack of the extracellular space complexity organization. For this reason, scientists have developed 3D *in vitro* systems that exploit the capacity of cells to self-organize.

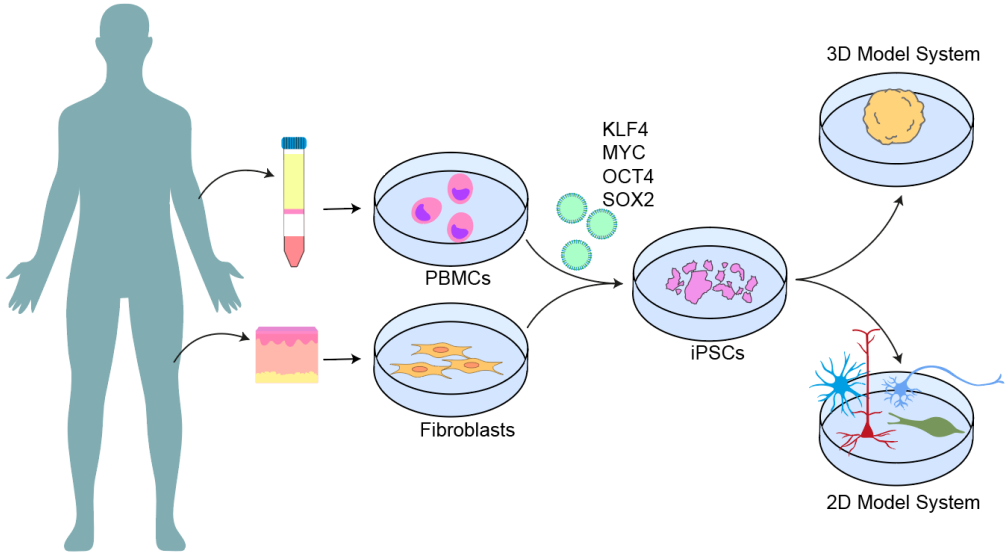

Figure 1-7 Generation of neural model systems from human induced pluripotent stem cells (iPSCs)
Reprogramming of human peripheral blood mononuclear cells (PBMCs) or fibroblasts into iPSCs, using Yamaka factors (KLF4, MYC, OCT4, SOX2). Figure adapted from Forero Echeverry and Cappello, 2022.

1.5.3 3D *in vitro* models

3D in *vitro* models were established to generate a system that can resemble the in *vivo* human neuronal tissue. Neurospheres were the first 3D system to be generated and they are the result of the aggregation of neural stem cells (NSCs) cultured in low attachment plate. An initial protocol for the generation of cerebral organoids was based on culturing hESCs or iPSCs (Kadoshima et al., 2013; Mariani et al., 2012) in suspension. This led to the quick aggregation of the cells in floating embryoid bodies (EBs) (Kadoshima et al., 2013; Mariani et al., 2012). The cells self-organize into apico-basally polarized tissue, resembling the neuroepithelium of the human cortex.

The protocol was improved by embedding the EBs in Matrigel. The Matrigel, a matrix containing membrane proteins, supports the organoids functioning as a scaffold, giving them a more complex 3D organization (Lancaster and Knoblich, 2014a; Lancaster et al.,

2013a). The cerebral organoids are kept in agitation using an orbital shaker or a spinning bioreactor and are characterized by their self-assembly capacity which leads to the formation of well-defined progenitor zones and more differentiative zones.

Two main protocols for the generation of cerebral organoids have been developed and they can be divided in whole-brain (also called unpattern) and regionalized (also called patterned or guided) cerebral organoids.

The approach to generate whole-brain organoids consists in the spontaneous differentiation of the neuroepithelium into different brain regions, mostly dorsal forebrain, without using signaling molecules or growth factors (Kyrousi and Cappello, 2019; Lancaster and Knoblich, 2014b). This protocol has the advantage of studying human brain development and disease in a more complete and complex system, including different brain regions (Kyrousi and Cappello, 2019). With this protocol, the generated organoids form many cavities filled with fluid that resemble small ventricles. Progenitor cells face the ventricles, resembling the VZ and SVZ of the human cortex. They also display the typical multilayer organization of the human brain, and the neurons migrate following the same migratory routes observed in *vivo*. Whole-brain organoids present also mature neural networks with formation of dendritic spines and spontaneous activity (Quadrato et al., 2017) (Figure 1-8).

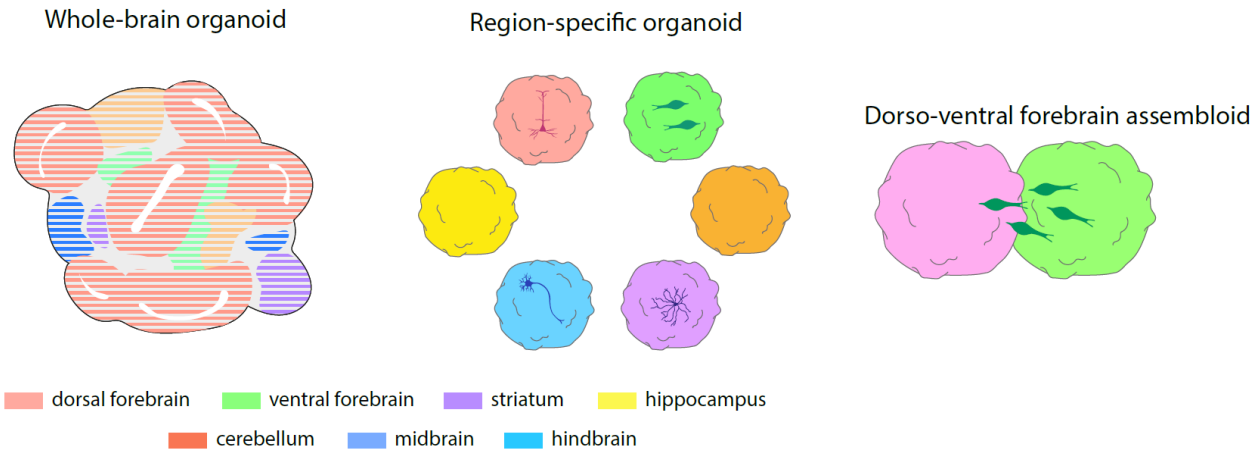

Figure 1-8: Whole-brain organoids, region-specific organoids and dorso-ventral forebrain assembloids

Schematic of whole brain organoids including different cell types (left); region-specific organoids generated with patterning molecules to determine a specific regional identity (middle); dorso-ventral forebrain organoids resembling the dorsal and ventral forebrain. Figure adapted from Forero Echeverry and Cappello, 2022.

Regionalized organoids are generated by adding small molecules during the early step of the protocol and many protocols have been established for different region-specific

organoids. Dorsal cortical organoids are obtained by dual SMAD inhibition with FGF2 and EGF (Birey et al., 2017; Pașca et al., 2015) and they present both upper layer as well as deep layer neurons; ventral organoids are generated by adding Wnt inhibitors and SHH agonist (Bagley et al., 2017a; Birey et al., 2017; Sloan et al., 2018; Xiang et al., 2017) and they resemble the ganglionic eminences (GEs), with ventral progenitor cells and interneuron precursors. Moreover, protocols for generating mesencephalic, hippocampus-, striatum-, midbrain- and cerebellum- like organoids have also been developed (Jo et al., 2016; Miura et al., 2020; Qian et al., 2016; Sakaguchi et al., 2015) (Figure 1-8)

However, whole-brain and regionalized organoids lack the assembly of cortical circuits. To address this issue, assembloids were generated. This model requires the fusion of independent regionalized organoids to integrate two or more component of a cerebral circuit.

The first assembloid system developed was the dorso-ventral system. Here, the dorsal organoids are fused with ventral organoids to resemble the dorsal-ventral axis in *vivo*. This system allows the study of the migration of interneurons, generated in the ventral organoids, to the cortical organoids. Migratory interneurons in dorso-ventral assembloids display the same saltatory migratory mode observed in *vivo*.

The other assembled systems generated are the cortico-striatal and cortico-motor assembloids. These two models will not be discussed as, in this work, these models were not used.

In *vitro* model can be used to investigate neurological disorders by culturing cells derived from patients. Specifically, cerebral organoids and assembloids can be used to study a wide range of neurological and neuropsychiatric disorders, including ASD (Mariani et al., 2015), epilepsy (Di Matteo et al.) and different cortical malformations. Several studies show that cerebral organoids can recapitulate PH (Buchsbaum et al., 2020; Klaus et al. 2019), microcephaly Lancaster et al., 2013; R. Li et al., 2017; W. Zhang et al., 2019) and lissencephaly (Bershteyn et al., 2017; Iefremova et al., 2017; Karzbrun et al., 2018) (Figure 1-8).

1.6 Candidate genes in Neurological and Neuropsychiatric Disorders

In this thesis, I will focus on two genes that have been associated with neurological and neuropsychiatric disorders: *Cystatin B (CSTB)*, whose mutations are causative of EPM1; and *Galectin-3 binding protein (LGALS3BP)* whose mutations have been described in individuals with PH and neuropsychiatric disorders.

1.6.1 Cystatin B (CSTB)

The *CSTB* gene is on chromosome 21q22.3 and codes for a cysteine protease inhibitor part of the large superfamily of cystatins. The *CSTB mRNA* is ubiquitously expressed in most cell types and tissue (Joensuu et al.). The 5' region of the CSTB gene includes two potential transcription start sites localized after the 12-nucleotide dodecamer repeat element(5'-CCCCGCCCCGCG-3') (Lalioti et al., 1997). Human *CSTB* was identified in lymphatic tissue, liver and isolated from mouse, rat, sheep, and bovine (Joensuu et al.; Lehesjoki, 2003). It is conserved between species and the human *CSTB* codifies for a 98 amino-acid sequence with a molecular weight of circa 11 kDa (Lehesjoki, 2003). Studies of experiments performed in *vitro* showed that CSTB inhibits several papain-family cysteine proteases, including cathepsins B, H, L and S via binding. The function of cathepsins is to degrade intracellular proteins and they are involved in antigen processions and apoptosis (Rinne et al., 2002; Turk et al., 2000). *CSTB* is known to be associated with EPM1, the most common type of progressive myoclonic epilepsies.

CSTB and EPM1

Mutations in the *CSTB* gene are causative of EPM1 (Figure 1-9). The most common mutation identified is the expansion of an unstable dodecamer in the promoter. This mutation is mostly found in homozygosis, in 90% of the EPM1 patients; but it can also be found in heterozygosis with an allele carrying a point mutation (Canafoglia et al., 2012; Lafrenière et al., 1997; Lalioti et al., 1997; Virtaneva et al., 1997). The expansion of the dodecamer results in downregulation of the expression of CSTB. However, this is not the only mutation causing EPM1. There are other nine mutations causative of EPM1 and they all affect splice sites leading to truncated proteins or amino acid

changes. Only one patient without the expansion has been identified and he is homozygous for a missense mutation (pG4R) (Joensuu et al.).

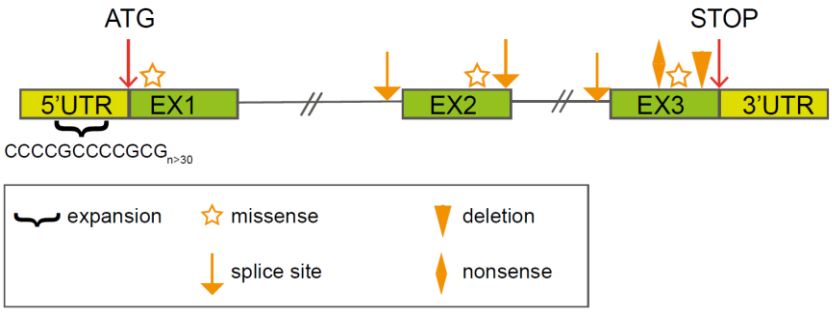

Figure 1-9: Structure of CSTB gene

Schematic structure of the CSTB gene showing the positions of mutations described in EPM1. Figure adapted from Joensuu et al., 2008.

Moreover, studies using the mouse in *vivo* model with the knockout (KO) of *Cstb* showed that the model could recapitulate only part of the human EPM1 symptoms, including the neuronal atrophy in the cerebellum, in the cortex and in the hippocampus, and loss of GABAergic neuronal terminals (Buzzi et al., 2012a; Pennacchio et al., 1996). It has also described a role of *Cstb* in regulating autophagy in mouse astrocytes (Polajnar et al., 2014)**,** and in vesicular trafficking and synapse physiology (Joensuu et al.)

In this thesis, I will focus on the nonsense mutation c.202C>T, identified in homozygous EPM1 patients (Chapter 3). The CSTB mutant form is a truncated form of the protein, refers as R68X. These patients have been diagnosed with microcephaly, developmental delay, and dyskinesia in very early childhood (Mancini et al., 2016).

1.6.2 Galectin 3-binding protein (LGALS3BP)

Galectin 3-binding protein, also known as LGALS3BP, is a soluble glycoprotein secreted in the ECM, where it organizes in large ring-like oligomers composed of subunits of 55-90 kDa (Fogeron et al., 2013; Müller et al., 1999). LGALS3BP belongs to the scavenger receptor cysteine-rich superfamily, a group of both membrane and secreted proteins involved in the regulation of the immune system (Martínez et al., 2011).

Human *LGALS3BP* codes for a 567-amino acid sequence with four domains, preceded by a signal peptide at the N-terminus. The leader peptide is proteolytically cleaved during the maturation of the protein, and it is important for its secretion. The signal peptide is followed by the scavenger receptor cysteine rich (SRCR) domain (domain 1), a highly conserved domain of circa 110 residues (Loimaranta et al., 2018); a BTB/POZ domain and a BACK domain (domains 2 and 3) important for interaction with the ECM and oligomerization. The C-terminal sequence (or domain 4) is inactive (Figure 1-10).

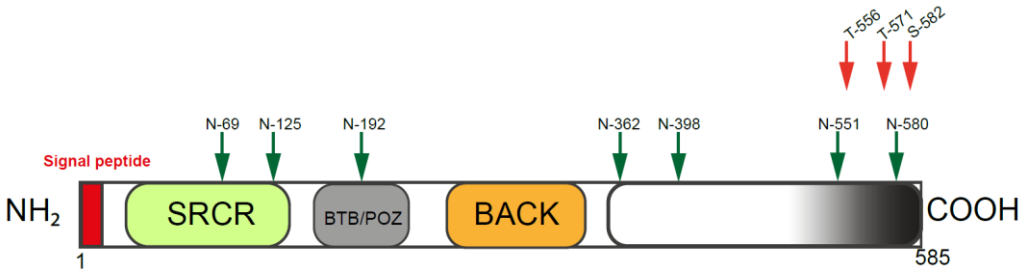

Figure 1-10: Structure of LGALS3BP protein

Schematic structure of LGALS3BP domains, N and O glycosylation sites are shown. N: Asparagine; T: Threonine; S: Serine.Figure adapted from Capone et al., 2021.

LGALS3BP purified from human tissues and fluids revealed three different forms of 25, 75 and 90 kDa, suggesting that this protein can be proteolytically cleaved by proteases (Capone et al., 2020, 2021a). Once secreted in the ECM, LGALS3BP interacts with integrin, collagens IV, V and VI, fibronectins, galectins, laminins, and tetraspanins (Lee et al., 2010; Stampolidis et al., 2015) and regulates cell-adhesion (Larsen et al., 2011) .

Many studies report the role of LGALS3PB in the immune system and in cancer. For example, in the activation of natural killer cells for the production and secretion of interleukin 1, 2, 6, and tumor necrosis factor alpha (TNFα). High levels of LGALS3BP can be detected in human body fluids after viral infections, including hepatitis C virus (Loimaranta et al., 2018) and HIV (Grassadonia et al., 2002), and in many types of cancer (i.e. neuroblastoma, ovarian carcinoma, melanoma) where it promotes the metastatic phase via regulating cell motility and chemoresistance (Batista et al., 2011; Capone et al., 2020; Escrevente et al., 2013; Song et al., 2020). Cancer studies demonstrated that LGALS3BP can be secreted directly in the extracellular environment interacting with the ERGIC-53 system (Capone et al., 2021b) or via EVs being expressed on EV surfaceome (Capone et al., 2020; Liang et al., 2014). Moreover, LGALS3BP is enriched in cerebrospinal fluid (CSF) from patients with neurological disorders (Costa et al., 2020).

LGALS3BP and the brain

The function of *LGALS3BP* in the brain is still poorly understood. The availability of sequencing data in mouse and human brain tissues made the characterization of the expression level of this gene possible.

Interestingly, *LGALS3BP* is almost undetectable in mouse developing cortex (Telley et al., 2019, http://www.humous.org/), while it is enriched in human progenitor cells, both in fetal brain tissue and in cerebral organoids (Kyrousi et al., 2021; Telley et al., 2019) (**Error! Reference source not found.**).

Figure 1-11: LGALS3BP expression level in mouse developing cortex, human brain fetal tissue and cerebral organoids.

Expression of LGALS3BP obtained from single-cell RNA-seq data of mouse developing cortex (left), human brain fetal tissue(middle) and cerebral organoids (right). Data from Telley et al., 2019, http://www.humous.org/

Moreover, studies in cerebral organoids derived from macaque and chimp, revealed that *LGALS3BP* is expressed at lower levels in macaque, while its expression is higher in chimp (Kanton et al., 2019). This information could suggest a role of *LGALS3BP* in evolution. Indeed, it has been shown that the forced expression of the wild-type isoform of *LGALS3BP* induces folds in the developing mouse cortex (Kyrousi et al., 2021).

The function of *LGALS3BP* in human neurodevelopment was studied in human cerebral organoids (COs). This study, carried out in our lab (Kyrousi et al., 2021), showed that *LGALS3BP* is important for neuronal progenitor cell delamination, regulating the thickness of the apical belt. Moreover, it can explain its function in a non-cell autonomous way via secretion and transport in EVs. *LGALS3BP* is crucial for human brain development, organizing the extracellular space and regulating progenitors delamination and neuronal migration.

De novo mutations in LGALS3BP lead to cortical malformation

Given the importance of *LGALS3BP* in brain development, it is not surprising that mutations in this gene can lead to neurodevelopmental disorders. *De novo* variants in the exon 5 of *LGALS3BP* gene have been identified in individuals with nodular periventricular heterotopia (Kyrousi et al., 2021; O'Neill et al., 2018b).

A patient with a *de novo* missense variant in *LGALS3BP* has autism, developmental delay, ataxia and focal seizures. Moreover, gyrification index (GI) changes were reported in this patient. The *de novo* missense variation implicates a substitution of the glutamic acid in position 370 with a lysin (E370K).

Another patient was diagnosed with prenatal microcephaly and neurodevelopmental delay, in this case, the mutation implicates substitution of the glutamic acid in position 294 with a lysis. From the other individual identified with mutation in LGALS3BP (substitution of glutamic acid in position 527 with a glycine), no clinical data could be obtained (Kyrousi et al., 2021).

This information suggests that the exon 5 of *LGALS3BP* might be crucial for brain development. Study in mouse and COs demonstrate that the mutant form of *LGALS3BP* (E370K) disrupt the apical belt resulting in defects in delamination and localization of migrating neurons (Kyrousi et al.,2021).

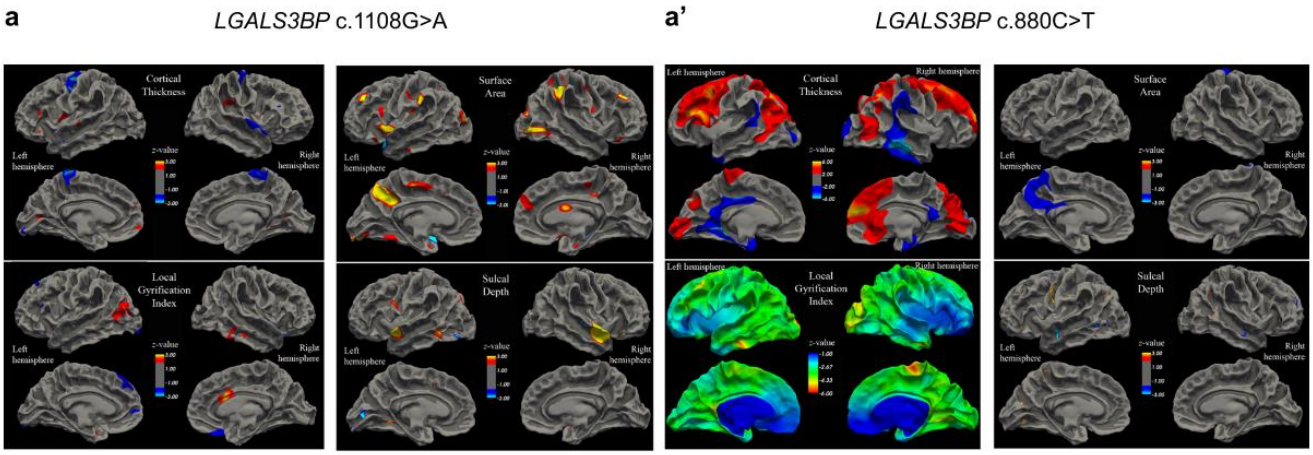

Figure 1-12 Morphometric analysis of MRIs of individuals with genetic variants in LGALS3BP

Individuals with c.1108G>A (a) and c.880C>T (a') mutations in LGALS3BP, showing difference in cortical thickness, gyrification index, surface area and sulcal depth in different positions of the cortex. Figure adapted from Kyrousi et al., 2021.

2 Scope of this thesis

This thesis combines three projects with the goal of investigating mechanisms involved in brain development and in neurological and neuropsychiatric disorders, including epilepsy and cortical malformations. Using both *in vivo* mouse and 3D *in vitro* human model systems, I investigated neurogenesis, neuronal migration, and differentiation in both physiological and pathological conditions.

Given the complexity of neurological diseases and cortical malformations, many of the molecular and cellular mechanisms underlying this group of disorders are poorly understood. In this thesis I will analyze the role of two genes associated with neurological disorders with the aim to identify common mechanisms that could help in understanding the pathologies also for diagnostic purposes.

I will show the importance of *CSTB* and *LGALS3BP* in neurogenesis and neuronal migration during brain development, identifying novel non-cell autonomous mechanisms of regulation of cell proliferation and specification.

It has been shown that extrinsic factors released in the extracellular environment can affect cellular behavior, including proliferation, motility, and morphogenesis. Moreover, extrinsic factors can be secreted by cells and tissues via extracellular vesicles (EVs).

However, their role in neurodevelopment and disease is still unknow. For this reason, having found that both CSTB and LGALS3BP have non-cell autonomous functions, are secreted and transported by extracellular vesicles, I will show how EVs can be important for cell proliferation and cell fate decision.

In **Chapter 3**, part of the results of manuscript published in the journal EMBO Molecular Medicine are shown.

"Cystatin B is essential for proliferation and interneuron migration in individuals with EPM1 epilepsy"

"Francesco Di Matteo[1,2],†, **Fabrizia Pipicelli[1,2],†**, Christina Kyrousi[1], Isabella Tovecci[1,3], Eduardo Penna[3], Marianna Crispino[3], Angela Chambery[4], Rosita Russo[4], Ane Cristina Ayo-Martin[1,2], Martina Giordano[1], Anke Hoffmann[1], Emilio Ciusani[5], Laura Canafoglia[5], Magdalena Götz[6,7,8], Rossella Di Giaimo[1,3],*& Silvia Cappello[1]**"

†The authors contributed equally to this work

Data not included in the manuscript is also presented.

Some of the figures, figure legends and results in this chapter are adapted from the manuscript with the permission of the Journal under the copyright:

"This is an open access article distributed under the terms of the Creative Commons CC BY license, which permits unrestricted use, distribution, and reproduction in any medium, provided the original work is properly cited. Citation: (Di Matteo et al., 2020).

You are not required to obtain permission to reuse this article"

"© 2020 The Authors. Published under the terms of the CC BY 4.0 license."

Most of the work, including experiments, quantifications and data analysis and visualization, on cerebral organoids presented in this project was done by me. In particular: immunohistochemistry for characterization of CSTB expression (

Figure 3-1, B); overexpression of CSTB and mutant form in cerebral organoids (Figure 3-2, A and B; Figure 3-6, B), migration of interneuron in cerebral assembloids (Figure 3-8, A and B).

Treatment of EVs on NPCs and differential expression analysis including data visualization was performed by me (Figure 3-10, A and B; Figure 3-12, A, B and C).

Part of the work, including experiments, quantification and data analysis and visualization, on mice presented in this work was done by me. In particular cell cycle analysis on E14-E16 mice and proliferation analysis on E14-E16 including immunohistochemistry and quantifications of Ki67+, CcndD1+, Pax6+, Tbr2+ cells (Figure 3-2, C-I, Figure 3-3, Figure 3-6, B, C, D and H)

Part of the experiments of this project here presented has been done in collaboration with:

1) Rossella Di Giaimo, from the Max Planck Institute of Psychiatry in Munich, and Martina Giordano from the University of Naples Federico II, who performed part of the mouse work.

2) Rossella Di Giaimo, from the Max Planck Institute of Psychiatry in Munich, and Isabella Tovecci, from the University of Naples Federico II, who performed part of the work on cerebral organoids

2) Marianna Crispino, Eduardo Penna, from the University of Naples Federico II, Angela Chambery, Rosita Russo, from the University of Campania Luigi Vanvitelli, who prepared sample for proteomic and performed proteomic analysis

5) Filippo Cernilogar from the Biomedical Center in Munich who performed the pre-processing (alignment) for the bulk RNA sequencing

3 Cystatin B role in proliferation and interneuron migration in EPM1 epilepsy

This work focused on the function of *cystatin B (CSTB)* during brain development. *CSTB* mutation is causative of Unverricht-Lundbord-type (EPM1) epilepsy, a common form of progressive myoclonus epilepsy (PME).

In our study, we used both *in vivo* developing mouse brain and *in vitro* 3D human cerebral organoids (COs), derived from two EPM1 patients, to investigate the role of CSTB in brain development. We showed that the alteration of physiological levels of CSTB affected cell proliferation and progenitors' distribution in a cell non-autonomous way.

It was previously shown that CSTB is secreted from synaptosomes, therefore, we investigated CSTB secretion in our model systems. Our findings revealed that CSTB is secreted in both mouse cerebral spinal fluid (CSF) and in organoids conditioned media (CM) which explained the cell non-autonomous effect. Interestingly, we found that the pathological form of CSTB was not secreted in the extracellular environment.

Then, we generated COs from 2 EPM1 patient induced pluripotent stem cells (IPCs) and observed a reduction in size and in proliferation, and increased neurogenesis. The extrinsic function of CSTB on proliferation was assessed by exchanging media between control and EPM1 COs. Control COs exposed to EPM1 media showed a decrease in proliferation, while EPM1 COs exposed to control media rescued the phenotype. We showed that CSTB is secreted via extracellular vesicles (EVs). We demonstrated that EVs derived from EPM1 organoids can modify the transcriptome profile of progenitor cells, dysregulating genes associated with WNT signaling or extracellular space.

These results suggested a novel role of CSTB in the extracellular environment during neurogenesis, shedding new light on mechanisms of the neurobiology of EPM1.

3.1 CSTB is expressed in COs and in the mouse developing brain

To investigate the role of *CSTB* during neurodevelopment, we characterized its level of expression in iPSCs-derived COs at different time points. In COs, *CSTB* is expressed from day 16 to day 140, with higher expression level at day 50 and 85 of culture (

Figure 3-1, A); while immunohistochemistry analysis shows that the protein is detected from

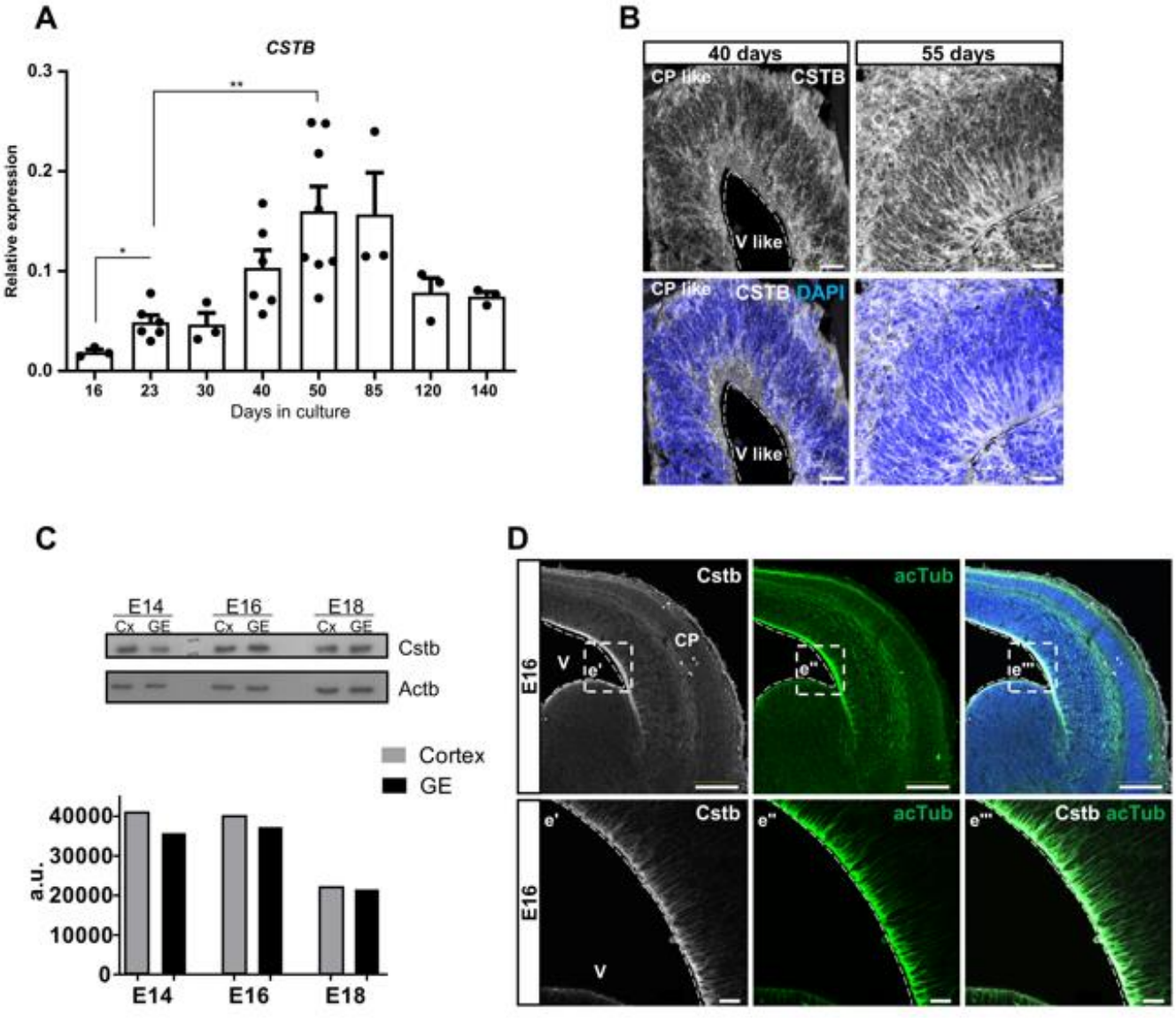

day 40 (**Error! Reference source not found.**, B). CSTB was also detected in the mouse d eveloping cortex and ganglionic eminence (GE) from embryonic day 14 (E14).

Figure 3-1: CSTB is expressed in COs and in mouse developing brain

A. Gene expression levels in COs at different timepoints.
B. Representative pictures of 40- and 55-days old COs immunostained for CSTB.
C. WB of protein extracts from mouse cortical (Cx) and ganglionic eminence (GE) tissues for Cstb at different timepoints. Actb is used as loading control.
D. Representative pictures of coronal sections of E16 mouse cerebral cortices immunostained for Cstb and acetylated tubulin (acTub).
Ventricle (V) and cortical plate (CP) are shown. Apical surface of the ventricles is represented by dashed lines. Scale bars: 50 µm in (B); 100 µm in (E); 20 µm in (e', e'' and e''').
Figure and figure legend adapted from Di Matteo, Pipicelli et al., 2020."

3.2 CSTB overexpression increases progenitor cell proliferation

To assess the role of *CSTB* in brain development, we overexpressed the wild-type form of *CSTB* labeled with GFP in 35 days old COs and in E14 mouse embryos. Interestingly we found changes in proliferation. We observed a significant increase in total KI67+ cells upon overexpression of *CSTB* compared to control in COs. The analysis was performed 5 days post electroporation (dpe) (Figure 3-2, A and B). The same outcome was observed in the mouse cortex as well, at 2 dpe (Figure 3-2, C and D).

With the aim to analyze cell cycle dynamics, bromodeoxyuridine (BrdU) was injected in pregnant mice intraperitoneally. After 30 minutes, cells in the S-phase can be detected. Moreover, we looked for Ki67+ proliferating cells, Phospho-Histone H3 (PH3) + M-phase cells, and CyclinD1 (CcndD1) + G1-phase cells.

Interestingly, upon overexpression of *Cstb*, we noticed a significant increase of cells in S-phase (BrdU+Ki67+) (Figure 3-2C-D-E) and an increase in the number of cells in M-Phase (PH3+) (Figure 3-2 F-G) and G1-Phase (CcnD1+), but not significant (Figure 3-2, H and I). These results showed that *Cstb* has a role in regulating proliferation affecting cells in S-phase in the developing mouse cortex.

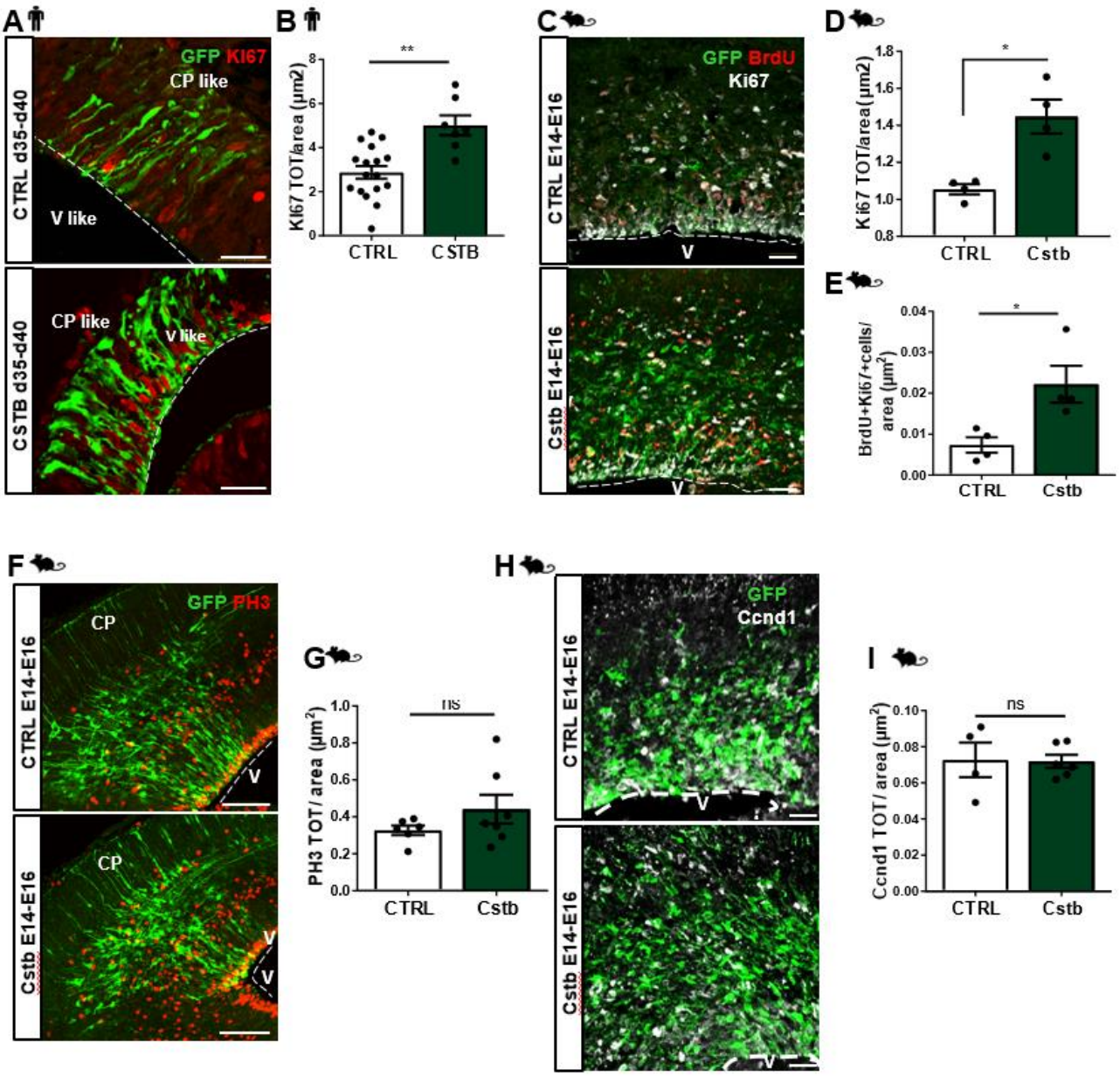

Figure 3-2: CSTB overexpression increases progenitor cells' proliferation

"A. Representative pictures of 40-days old COs electroporated with GFP-empty vector control or GFP-CSTB. Immunostaining for GFP and KI67 are shown.
B. Quantification of total KI67+ cells/area (µm2)
C. Representative pictures of coronal sections of E16 mouse cerebral cortices electroporated at E14 with GFP-empty vector or GFP-Cstb. Immunostaining for GFP, Ki67 and BrdU are shown.
D,E. Quantifications of total Ki67+ cells/area(µm2) and Ki67+Brdu+ cells/area(µm2)
F,G. Representative pictures of coronal sections of E16 mouse cerebral cortices electroporated at E14 with GFP-empty vector or GFP-Cstb. Immunostaining for GFP and PH3 are shown.
H,I. Representative pictures of coronal sections of E16 mouse cerebral cortices electroporated at E14 with GFP-empty vector or *Cstb* . Immunostaining for GFP and Ccnd1 are shown.
Ventricle (V) is indicated. Apical surface of the ventricles is represented by dashed lines.
Scale bars: 50 µm in (A); 100 µm in (C, F, H). Figure and figure legend adapted from Di Matteo, Pipicelli et al., 2020."

Therefore, the analysis of cells in transition from the apical radial glial state to intermediate progenitors (Pax6+/Tbr2+ cells) did not show any difference compared to control, suggesting that *Cstb* is crucial for cell proliferation rather than cell fate (Figure 3-3, A and B).

We found an increase of Ki67+ and BrdU+ cycling progenitors, therefore we analyzed the distribution of the proliferating cells. The analysis was performed by dividing the electroporated cerebral cortex area in 5 equally-distributed bins and it revealed an accumulation of Ki67+ and BrdU+ cells at the level of bin3 (**Error! Reference source not found.** C), which corresponds t o the IZ. Also, Tbr2+ Ips and Pax6+/Tbr2+ cells accumulated in bin3 (Figure 3-3, D and E); while we have not observed changes in Pax6+ RGs distribution (Figure 3-3, F). Interestingly, PH3+/GFP- cells also showed an accumulation in bin3, suggesting a non-cell autonomous mechanism of *Cstb* (Figure 3-3, G).

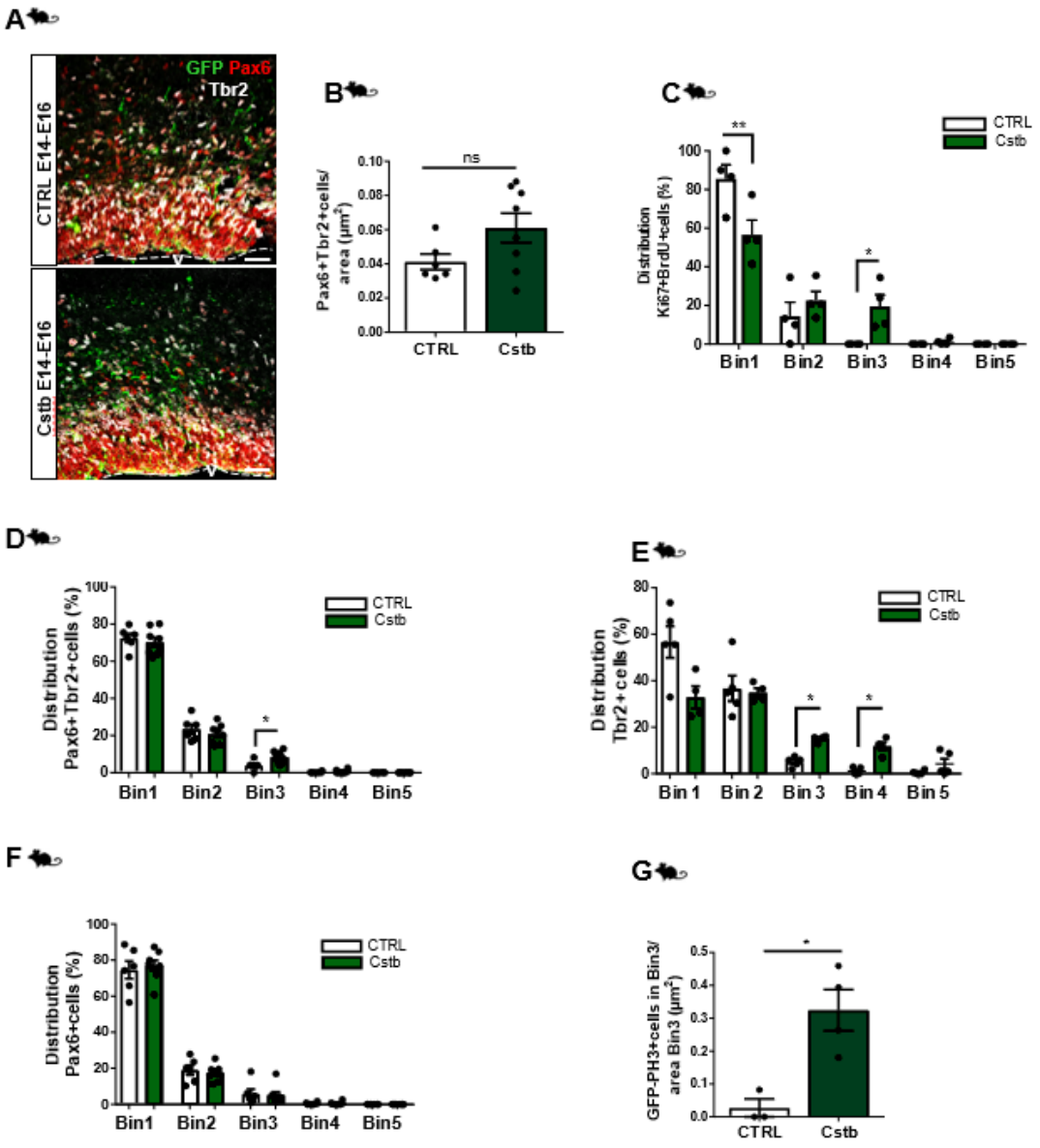

Figure 3-3: CSTB overexpression increases progenitor cells' proliferation (II)

A, B. Representative pictures of E16 mouse cerebral cortices electroporated at E14 with GFP-empty vector or GFP-Cstb. Immunostaining for GFP, Pax6 and Tbr2 are shown. (B).

C. Distribution of Ki67+/BrdU+cells in the mouse cortex, divided in 5 equal Bins.

D, E, F Distributions of Pax6+Tbr2+ cells, Tbr2+ and Pax6+cells in the mouse cortex, divided in 5 equal Bins.

G. Quantification of total PH3+ GFP negative cells/ area of in E16 mouse cerebral cortices electroporated at E14 with GFP-empty vector or Cstb .

Ventricle (V) is indicated. Apical surface of the ventricles is represented by dashed lines.

Scale bars: 50 µm in (A). Figure ad figure legend adapted from Di Matteo, Pipicelli et al., 2020.

3.3 CSTB is secreted in both mouse CSF and CO conditioned media

It was recently showed that CSTB is secreted from synaptosomes and it might have a role in synaptic plasticity (Penna et al., 2019). To confirm the secretion of CSTB in the mouse cortex and COs, we collected and analyzed mouse cerebral spinal fluid (CSF) and conditioned media (CM) from mouse cortical cells and COs. We found that CSTB is detected in both the CSF of E14 mouse embryos and CM (both mouse cells and COs) at different time points (Figure 3-4, A, B and C).

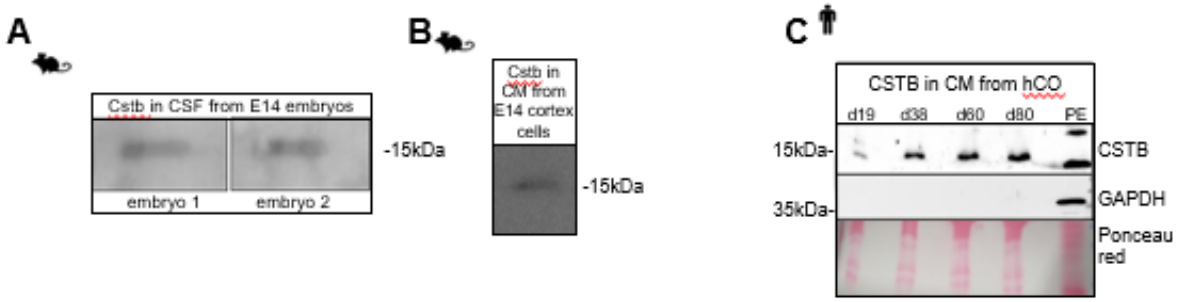

Figure 3-4: CSTB is secreted in both mouse CSF and CO conditioned media

A. WB for CSTB in the CSF from 2 different E14 mouse embryos.
B. WB for CSTB in the CM from E14 cortical cells in culture for 4 days.
C. WB for CSTB in the CM from COs after 4 days in culture.
Figure and figure legend adapted from Di Matteo, Pipicelli et al., 2020.

3.4 CSTB regulates interneuron recruitment

Studies on *Cstb*-KO mouse model and EPM1 patients revealed a loss of interneuron GABA synaptic terminals (Buzzi et al., 2012a). Therefore, we hypothesized that *Cstb* might be involved in regulation in interneuron migration and recruitment from the ganglionic eminence to the cortex (Silva et al.).

To analyzed the migration of interneurons, we used of 2 transgenic reporter mouse lines: the GAD65-GFP transgenic mouse line (López-Bendito et al., 2004), and GAD67-GFP knock-in mouse line (Tamamaki et al., 2003). We co-electroporated the plasmid expressing *Cstb*, fused to the HA, with a plasmid expressing *mCherry* in the E14 embryos cortex. Upon electroporation (3dpe), we analyzed the number and distribution of interneurons migrated from the ventral to the dorsal forebrain. Despite no difference in terms of total number of GAD65-GFP+ or GAD67-GFP+ interneurons in the cortex (Figure 3-5, A, B, C and D), their distribution was

affected. Specifically, GAD65 and GAD67 GFP+ interneurons were localized close to the Cstb+ expressing cells (Figure 3-5, E and F). These findings propose a role of *Cstb* in recruitment of interneurons during brain development.

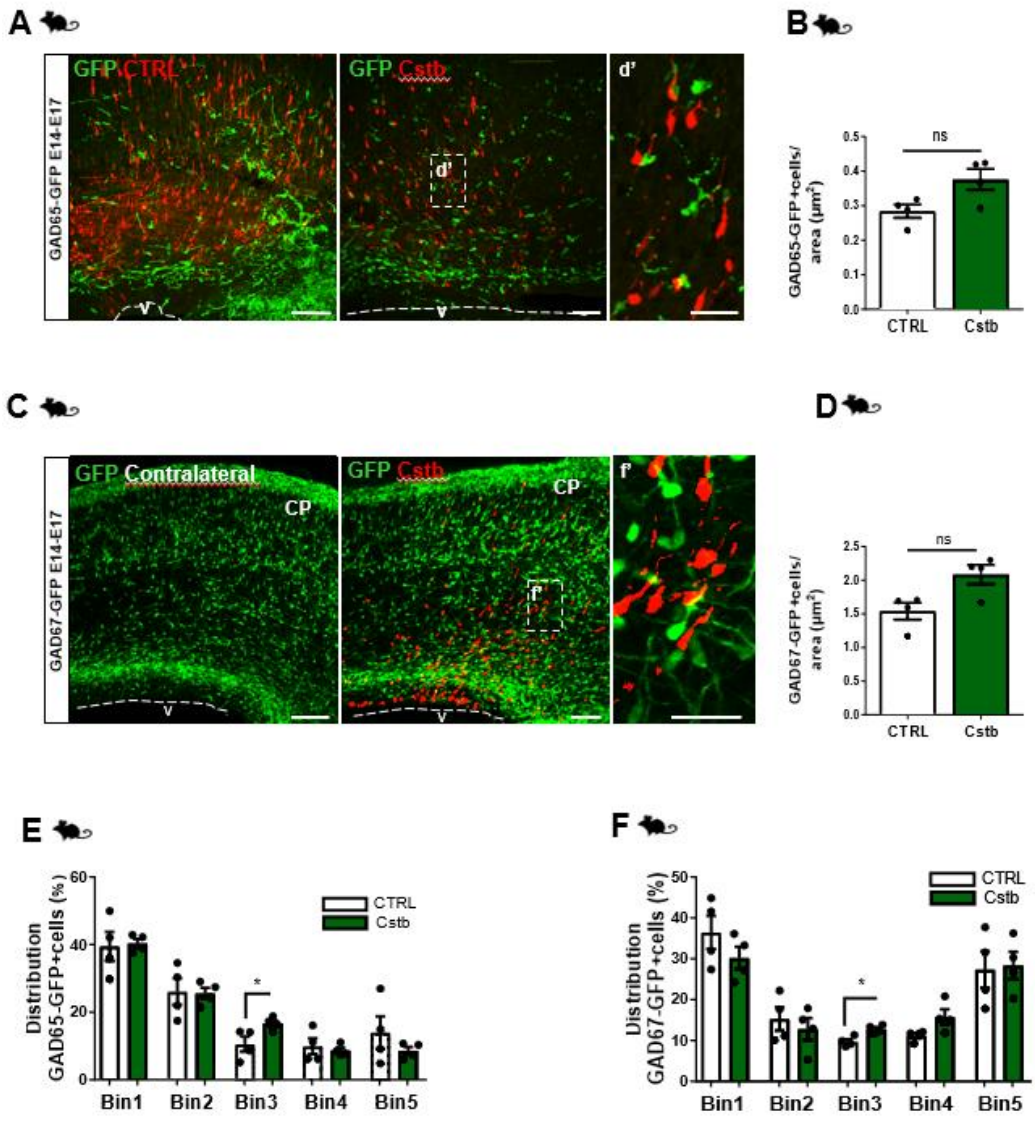

Figure 3-5: CSTB regulates interneuron recruitment

A. Representative pictures of coronal sections of E17 mouse cerebral cortices electroporated at E14 co-electroporated with mCherry expressing vector and HA-empty vector or -*Cstb*.
B. Quantification of total GAD67-GFP interneurons/area ($\mu m^{2)}$.
C. Representative pcitures of coronal sections of E17 mouse cerebral cortices electroporated at E14 co-electroporated with mCherry and HA-*Cstb* expressing vector.
D. Quantification of total of GAD65-GFP interneurons/area, ($\mu m^{2)}$.
E. Distribution of GFP+ interneurons in mouse developing cortex, divided in 3 equally distributed Bins.
F. Distribution of GFP+ interneurons in mouse developing cortex, divided in 3 equally distributed Bins.
Data information: Scale bars: 100 µm (A and C), 20 µm in (d' and f').
Figure and figure legend adapted from Di Matteo, Pipicelli et al., 2020."

Altogether, these results revealed that increased levels of CSTB can interfere with physiological cell proliferation during neurogenesis in COs and in the developing mouse cortex.

3.5 R68X pathological form reduces cell proliferation and recruitment of interneurons

Different types of mutations in *CSTB* causative of EPM1 have been described, including homozygous nonsense mutation (Mancini et al., 2016).

These patients have been diagnosed with microcephaly, dyskinesia and developmental delay, starting at 3 months of age and they are homozygous for a c.202C>T mutation. This mutation, called R68X, leads to a truncated form of the CSTB protein.

We first evaluated if the truncated form was secreted in the CM from mouse cortical cells. For this aim, we overexpressed the pathological form in E14 primary cells and analyzed the CM 4dpe. Surprisingly, the overexpressed R68X form was not found in the CM of E14 primary cells, while the endogenous CSTB was always present (Figure 3-6, A).

We, then, overexpressed the wild-type and R68X pathological forms in 35 days old COs and analyzed the number of KI67+ proliferating cells in the electroporated area at 5dpe. As expected, we observed a significant reduction in proliferating cells compared to control and overexpression of *CSTB*, suggesting that the truncated form has an opposite effect on cell proliferation compared to the wild -type form (Figure 3-6, B, C and D).

Moreover, R68X overexpression affected the distribution of the GFP+ electroporated cells. R68X-GFP cells localized mostly in bin1 at the expenses of bin2 and bin3 (Figure 3-6, E and F). Same behavior was observed in PH3+ mitotic cells. However, the total number of PH3+ cell was not changed (Figure 3-6, G and H).

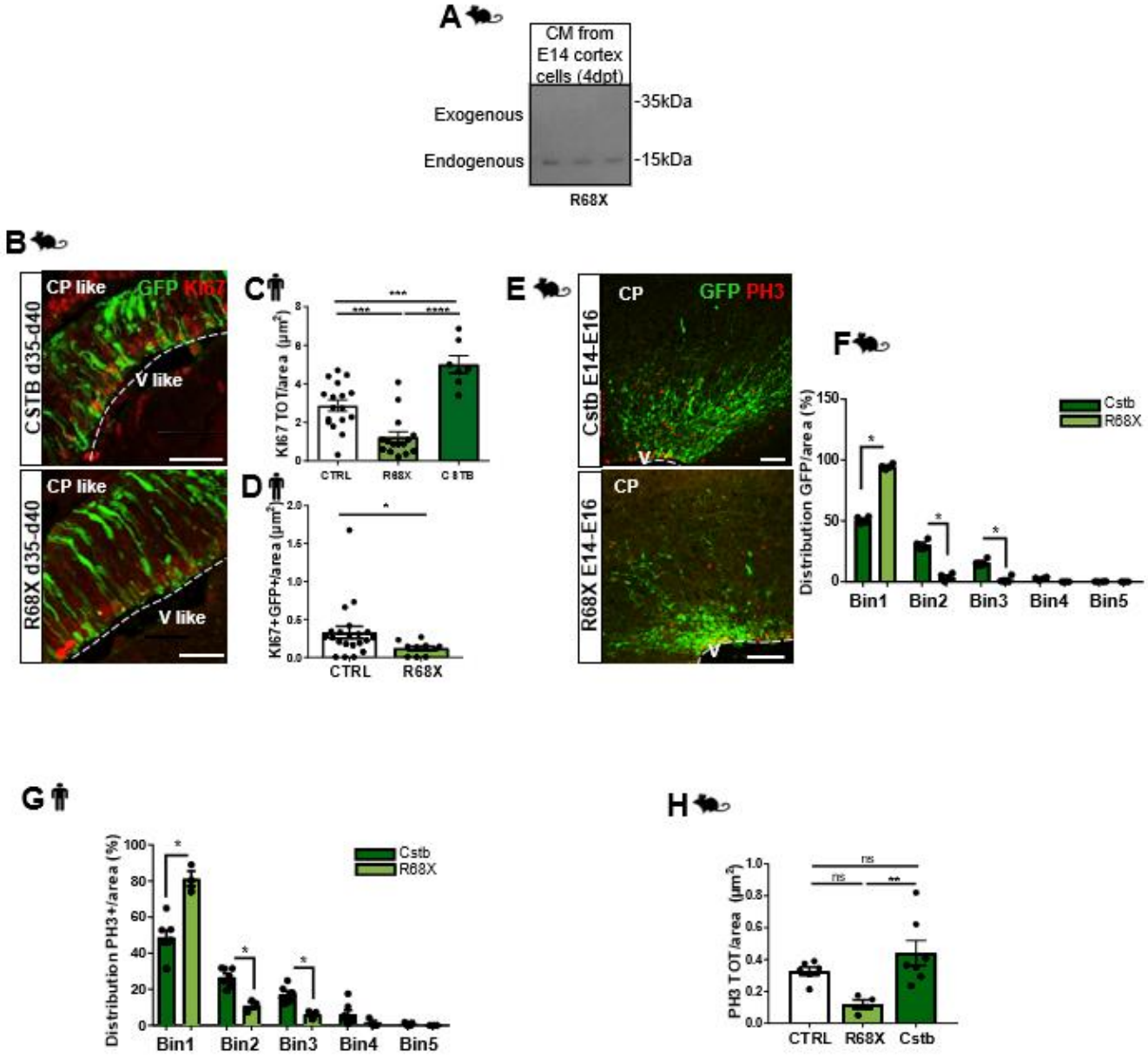

Figure 3-6: R68X pathological form reduces cell proliferation and recruitment of interneuron

A. WB analysis for Cstb in the CM collected from E14 cortical cells.
B. Representative pictures of 40-days old COs electroporated with GFP-Cstb-expressing vector or GFP-R68X mutant. Immunostaining for GFP and Ki67 are shown.
C, D. Quantification of total KI67+ cells/area (C) (µm2) and Ki67+GFP+ cells/area (D) (µm2) of ventricles electroporated with GFP-empty vector control, GFP-Cstb or GFP-R68X mutant.
E. Representative pictures of coronal sections of E16 mouse cerebral cortices electroporated at E14 with GFP-empty vector control, GFP-Cstb, or GFP-R68X, Immunostaining for GFP and PH3 are shown.
F, G. Distributions of electroporated GFP+ cells (F) and PH3+ cells (G) in the mouse cortex, divided in 5 equally distributed Bins.
H. Quantification of total PH3+ cells/area (µm2) of ventricles electroporated with GFP-empty vector control, GFP-Cstb, or GFP-R68X mutant.
Scale bars: 50 µm.
Figure and figure legend adapted from Di Matteo, Pipicelli et al., 2020.

We, therefore, looked at the number of Tbr2+ IPs after overexpression of the R68X form finding a significant decreased in this population of cells, compared to the wild-type CSTB (

Figure 3-7, A and B).

As previously showed, overexpressing *CSTB* results in a change of interneuron distribution in the mouse cortex. We then hypothesized that the pathological variant could retain its function. Interestingly, we noticed that R68X overexpression affected the migration of interneurons, suggesting a dominant effect of the pathological form (

Figure 3-7, C and D). Altogether, these results suggest contrary effects of wild-type *CSTB* and the pathological R68X variant on cell proliferation and neuronal migration in both mouse and COs.

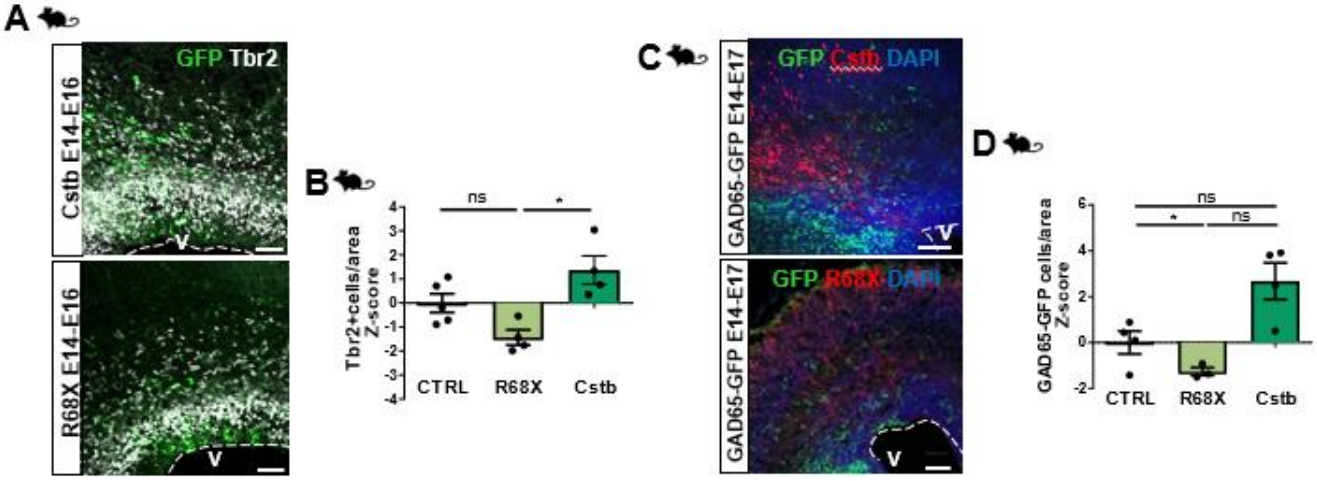

Figure 3-7: R68X pathological form reduces cell proliferation and recruitment of interneuron (II)

A. Representative pictures of coronal sections of E16 mouse cerebral cortices electroporated at E14 with GFP-empty vector control, GFP-Cstb or GFP-R68X mutant. Immunostaining for GFP and Tbr2 are shown.
B. Quantification of total Tbr2+ cells/ cortical area (µm2) in (L). Data shown as Z-scores relative to the mean of GFP control vector.
C. Representative pictures of coronal sections of E17 mouse cerebral cortices electroporated at E14 co-electroporated with mCherry expressing vector and HA-Cstb or R68X. Ventricle (V) is indicated. The dashed lines represent the apical surface of the ventricles.
D. Quantification of total GAD65-GFP interneurons/ cortical area (µm2) in (N). Data shown as Z-scores relative to the mean of GFP control vector.
Ventricle (V) is indicated. Apical surface of the ventricles is represented by the dashed lines. Scale bars: 100 µm in. Figure and figure legend adapted from Di Matteo, Pipicelli et al., 2020."

3.6 Generation and analysis of EPM1 COs

The experiments presented in this paragraph have been performed by Francesco Di Matteo, who has equally contributed to this work. For this reason, they will be briefly reported since these findings are fundamental for the understanding of the next paragraphs. For more details, refer to (Di Matteo et al., 2020)

EPM1 COs were generated from 2 patient cell lines, referred here as UL1 (homozygous amplification in the *CSTB* promoter) and UL4 (with a heterozygous mutation of the dodecamer repeat and a point mutation leading to skipping of exon 2).

Patient COs revealed a reduction in size and in proliferation, and increased neurogenesis. The extrinsic function of CSTB on proliferation was assessed by exchanging media between control and EPM1 COs. Control COs exposed to EPM1 media showed a decrease in proliferation, while EPM1 COs exposed to control media showed a recued phenotype.

These findings suggested that secreted CSTB play an important role in cell proliferation in a non-cell autonomous regulation.

3.7 EPM1 assembloids show changes in interneuron migration

We showed that, in *vivo*, both *CSTB* wild-type and pathological variant regulate distribution and recruitment of interneurons. Therefore, we tested the role of *CSTB* in interneuron migration also in a human *in vitro* model, generating human cerebral assembloids. I this protocol, patterned ventral and dorsal organoids are combined to specifically reproduce the dorso-ventral forebrain axis *in vitro*. With this model it is possible to analyzed the tangential migration of ventral interneurons (Bagley et al., 2017b).

We generated dorsal organoids from CTRL or UL1 cells and ventral organoids from CTRL cells, labeled with GFP, and fused them together (Figure 3-8, A). At day 30, we looked the number of GFP+ ventral cells that had migrated into the dorsal area of the assembloid. For the quantification of migrated cell, we quantified cells that at 100um distance from the dorso-ventral boundary.

We observed a significant reduction in the number of ventral GFP+ cells in the UL1 dorsal part, compare to control, indicating a function of *CSTB* in the process of recruitment of interneurons also in human assembloids (Figure 3-8, B and C).

Overall, these results suggested a function of *CSTB* in brain development, proposing that *CSTB* might regulate the correct migration and recruitment of interneurons, a crucial developmental event often altered in epilepsy.

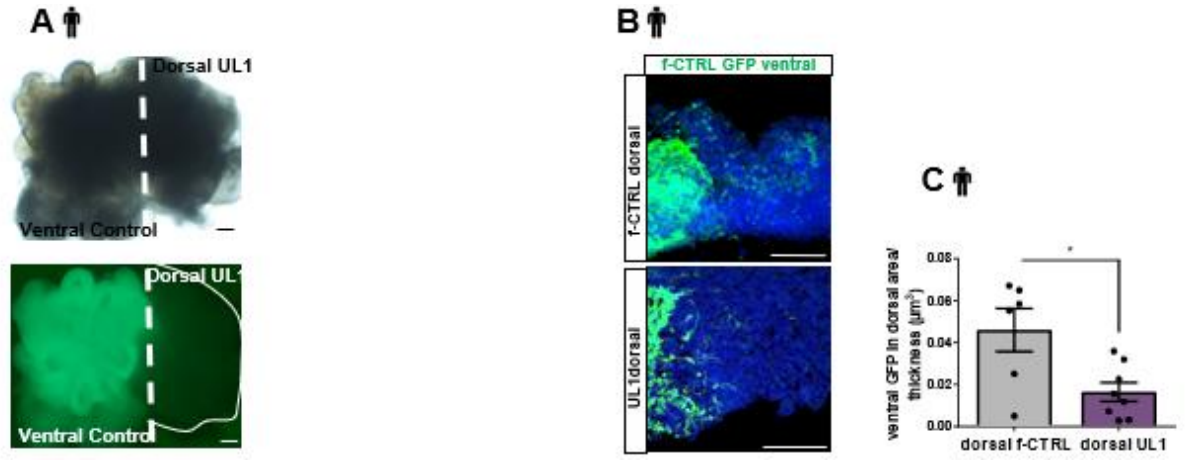

Figure 3-8: EPM1 assembloids show changes in interneuron migration

A. Representative pictures of d30 fused-organoid; ventral GFP-f-CTRL and dorsal UL1.
B. Representative pictures of sections from30-days old assembloids, showing ventral GFP+ cells in the dorsal area.
C. Quantification of ventrally derived GFP+ cells in dorsal area/thickness of the counted area (µm3). Every dot represents a different hCOs and different areas were counted for each hCO.
Scale bars: 200 µm in (A) and 100 µm in (B). Figure and figure legend adapted from Di Matteo, Pipicelli et al., 2020.

3.8 EPM1 COs dysregulate proteins involved in extracellular space organization

We, then investigates the molecular mechanisms that could explain the non-cell autonomous phenotypes. To this end, we performed proteomic analysis of 40 days old EPM1 COs.

We identified 178 differentially regulated proteins, including down-regulation of CSTB (Figure 3-9, A). Interestingly, some of these proteins were associated with biological processes including oxido-reduction stress (Lehtinen et al, 2009; Butinar et al, 2014) (Fig 6J). Moreover, biological processes such as protein-lipid assembly, cell-cell adhesion and secretion, were also dysregulated, indicating a role of CSTB in secretory pathways and cell-cell contact. Specifically, EPM1 COs altered proteins associated with the formation of the extracellular matrix (Figure 3-9, B).

These finding propose that neurogenesis and neuronal migration, which are affected in EPM1 COs, can be altered by changes in the extracellular environment.

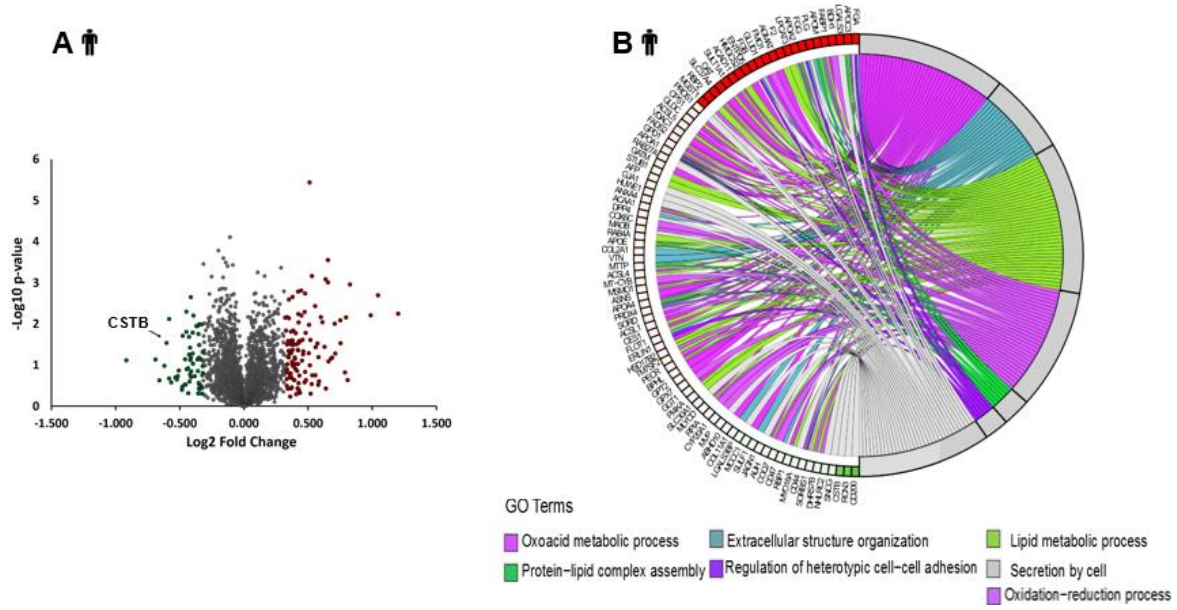

Figure 3-9: EPM1 COs dysregulate proteins involved in extracellular space organization

A. Volcano plot showing differentially expressed proteins identified in COs, (-0.3≥log2FC≥0.3; UL1 vs CTRL).
B. GOChord plot showing relationships between selected biological process and differentially expressed proteins identified in COs.
Figure and figure legend adapted from Di Matteo, Pipicelli et al., 2020.

3.9 Non-cell autonomous function of CSTB is mediated by EVs

To gain more insight in the non-cell autonomous function of CSTB in brain development, we hypothesized that CSTB might be secreted and transported by extracellular vesicles (EVs), secreted vesicles important for cell-cell communication and ECM composition (Peruzzotti-Jametti et al., 2021; Sharma et al., 2019; Taverna and Huttner, 2010).

For this purpose, we first investigated transcriptional changes on cells treated with EVs. We isolated EVs from dorsal and ventral control COs (dCOs and vCOs). We, then, performed RNA-seq analysis on neural progenitor cells (NPCs) acutely treated (12 hours) with EVs from dCOs and vCOs (Figure 3-10, A).

NPC transcriptome was significantly altered upon EV treatment, particularly upon treatment with dorsal EVs (dEVs) compared to ventral EVs (vEVs) (Figure 3-10, A). We found that genes associated with the WNT/TGFb/MAPK pathways and with extracellular space were altered, suggesting a role of EVs in these processes (Figure 3-10, B).

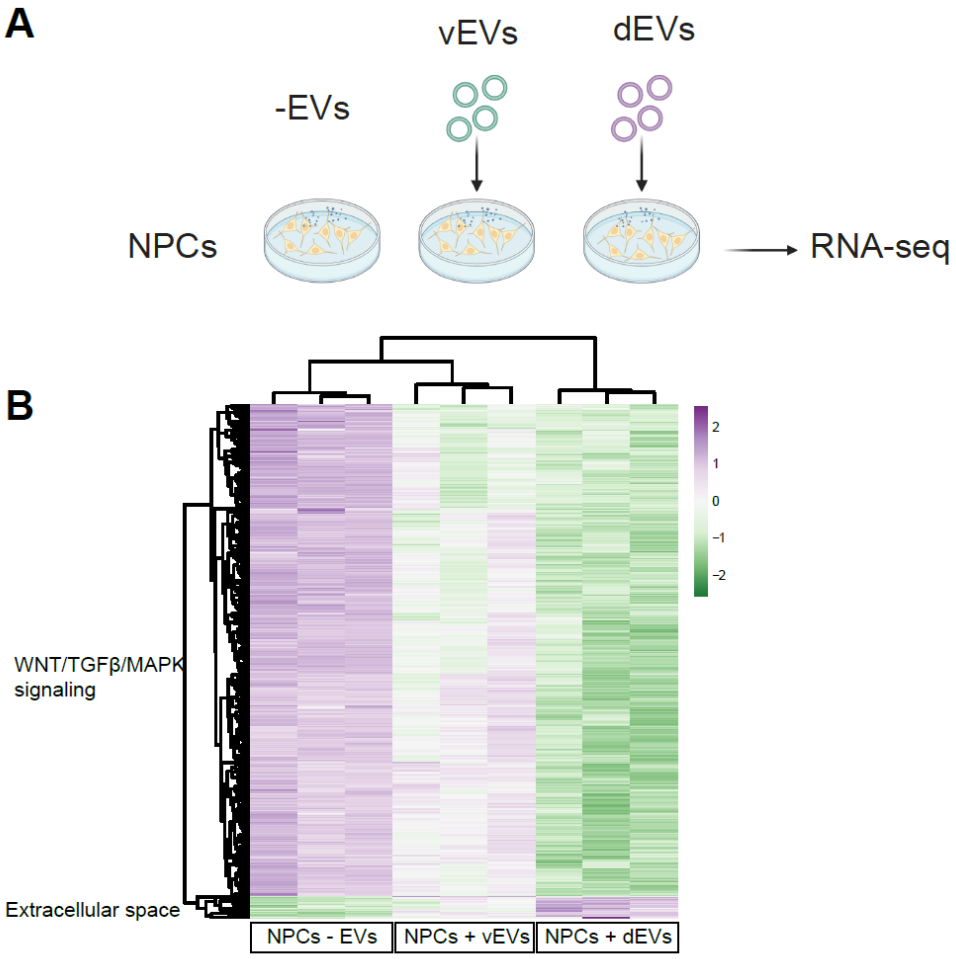

Figure 3-10: Non-cell autonomous function of CSTB is mediated by EVs

A. Schematic of 12 h treatment of NPCs with brain-region-specific CO EVs (vEVs, ventral, green; dEVs, dorsal, purple) or no EVs (-EVs).Created with BioRender.com.
B. Heatmap showing differentially regulated genes in NPCs after treatment with ventral (vEVs) and dorsal (dEVs) versus no EVs.

Then, we investigated if CSTB can contribute to signaling mechanisms mediated by EVs. To this end, we performed immuno-EM on EVs and confirmed the presence of CSTB in EVs (identified with the expression of the EV marker CD81 (D'Acunzo et al., 2021)) (Figure 3-11, A).

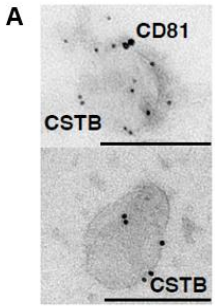

Figure 3-11: Non-cell autonomous function of CSTB is mediated by EVs (II)

A. CD81 (large dots) and CSTB (small dots) immuno-electron micrographs in EVs collected from COs. Scale bar: 100nm.

Therefore, we assessed the functional role of EVs in EPM1 epilepsy. We collected EVs from EPM1 dCOs and vCOs and treated control NPCs acutely for 12 hours with the collected EVs (Figure 3-12, A).

Upon treatment with EPM1-EVs, both dorsal and ventral, genes involved in neurogenesis and cell proliferation were altered compared to exposure to control EVs, confirming a non- cell autonomous role of CSTB, mediated by EVs, in these processes (Figure 3-12, C and D).

Overall, these findings suggest a non-cell autonomous role of CSTB in regulating cell proliferation and neurogenesis during brain development.

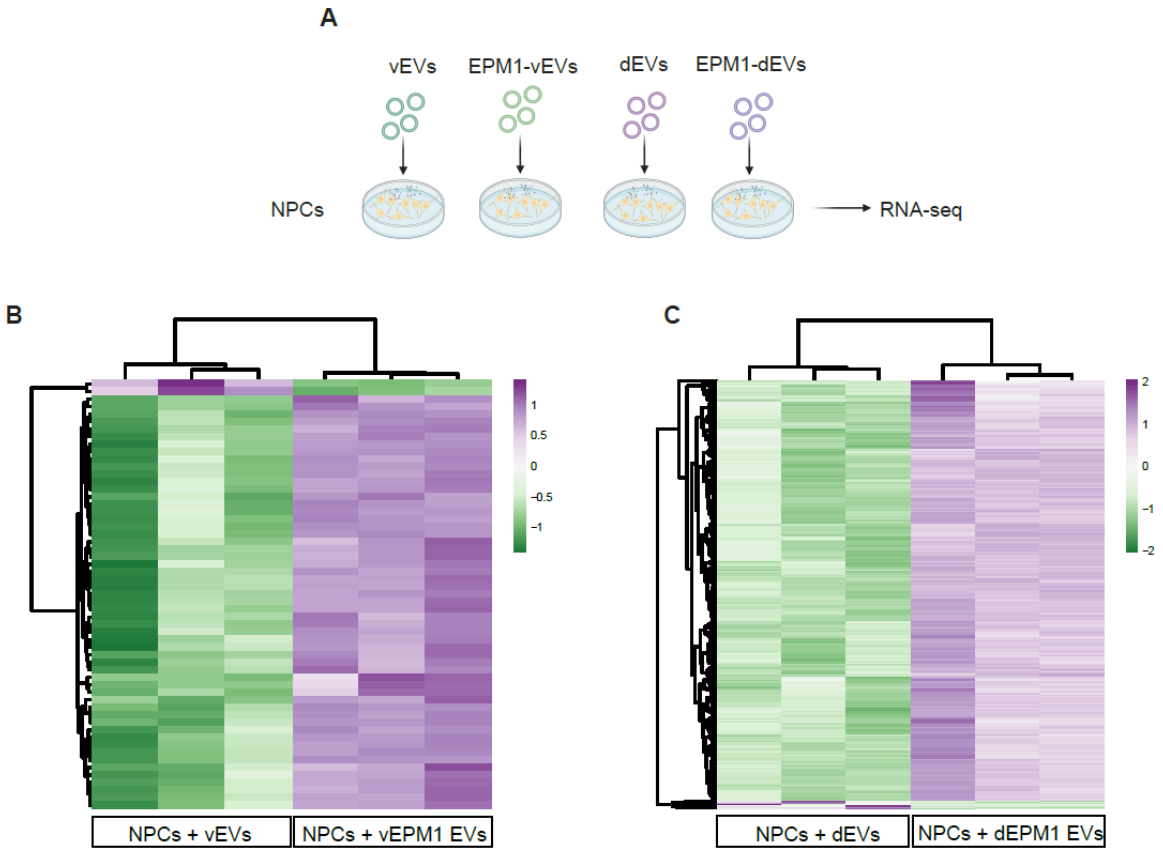

Figure 3-12: Non-cell autonomous function of CSTB is mediated by EVs (III)

A. Experimental setup of bulk-RNA seq performed on NPCs acutely treated (12h) with no EVs (-EVs), control ventral EVs (+ vEVs), control dorsal EVs (+dEVs), EPM1 ventral EVs (+vEPM1 EVs) and EPM1 dorsal EVs (+dEPM1 EVs). Created with BioRender.com.
B. Heatmap showing differentially regulated genes in NPCs after acute treatment (12 h) with control ventral (vEVs) and EPM1 ventral (vEPM1 EVs) EVs.
C. Heatmap showing differentially regulated genes in NPCs after acute treatment (12 h) with **(c)** control dorsal (dEVs) and EPM1 dorsal (dEPM1 EVs) EVs.

In **Chapter 4**, I will show part of the results of the project published on bioRxiv:

"Short- and long-distance extrinsic regulation of interneuron specification and migration"

Fabrizia Pipicelli[1,2], Natalia Baumann[3], Rossella Di Giaimo[1,4], Christina Kyrousi[1,5], Rebecca Bonrath[1], Denis Jabaudon[3], & Silvia Cappello[1]*

Data not included in the preprint manuscript is also presented.

Some of the figures, figure legends and results in this chapter are adapted from the manuscript. "The copyright holder for this preprint is the author/funder, who has granted bioRxiv a license to display the preprint in perpetuity". Citation (Pipicelli et al., 2022)

The work presented in this project contains all original work done by me, including design of the experiments, immunohistochemistry, quantifications, data analysis of transcriptomics (single-cell RNA-seq, bulk RNA-seq) and proteomics and data visualization.

Part of this project has been done in collaboration with Natalia Baumann and Denis Jabaudon from the University of Geneva who performed the pre-processing (alignment) for the single-cell RNA-seq analysis and established the dorso-ventral model used in this project.

Rossella Di Giaimo, Christina Kyrousi and Rebecca Bonrath from the Max Planck Institute of Pyschiatry in Munich have contributed to this work with technical help in performing bulk-RNAseq, live imaging and immunohistochemistry.

4 Short- and long-distance extrinsic regulation of interneuron specification and migration

In this project, we focused on the role of *LGALS3BP* in the regulation of the excitation/inhibition balance during neurodevelopment.

The construction of functional neuronal circuits relies on correct neurogenesis and neuronal migration, coordinated by excitatory and inhibitory neurons. Disruptions in these processes can lead to sever neurological disorders, such as epilepsy and autism spectrum disorder (ASD). Mutation of *LGALS3BP (E370K)* has been described in individual with several pathological conditions including periventricular heterotopia (PH), epilepsy and ASD.

Previous results obtained in the lab (Kyrousi et al., 2021) showed that *LGALS3BP*, a human-brain-specific gene, enriched in human RG cells, is crucial for human corticogenesis, shaping the ECM composition. Moreover, it has been reported that LGALS3BP regulates progenitor cell delamination and neuronal migration, and that its secretion in the extracellular environment is mediated by extracellular vesicles (EVs).

The project here presented aims at the investigation of the role of *LGALS3BP* in interneuron progenitor specification and interneuron migration and recruitment.

To this end, we generated dorso-ventral cerebral assembloids (dvCAs) and ventral and dorsal COs (vCOs and dCOs) derived from genome edited IPSC lines carrying the *LGALS3BP* variant (E370K) described in the patient. We found that the E370K variant affected migrating interneuron recruitment and distribution, and migratory dynamics in a short- and long- distance extrinsic manner. Moreover, E370K-vCOs showed altered cellular identity, expressing cortical dorsal genes. Single-cell RNA-seq analysis revealed that E370K ventral progenitors, intermediate progenitors (IP) and interneurons (INs) acquired also dorsal molecular identity and dysregulated genes associated with dorsal-ventral patterning, neurogenesis, and axon guidance. To investigate the short-distance non-cell autonomous regulation of LGALS3BP in ventral progenitor specification, we generated ventral mosaic organoids (vMOs). This model contains both isogenic control and E370K IPSCs. We found that LGALS3BP can partially rescue the altered identity of mutant progenitors and interneurons, confirming an extrinsic effect of LGALS3BP.

Moreover, our results indicate that E370K dCOs have altered cell proportions, which might lead to changes in the extracellular matrix composition, ultimately altering the attractive cues

that guide interneuron tangential migration. Considering that LGALS3BP is secreted via EVs, we looked at their function on NPCs, finding that they can modify their gene expression. Specifically, mutant ventrally originated EVs can activate pathways involved in patterning and cell fate decision, while mutant dorsally originated EVs can activate axon guidance and chemotaxis.

All together these results showed a novel role of LGALS3BP in maintenance of the excitatory/inhibitory balance, regulating interneuron specification and migration in both a short- and long- distance manner, mediated by EVs.

4.1 *LGALS3BP* variation affects interneuron distribution and migratory dynamics

We investigated it the E/I balance might be influenced by secreted factors. To this end, we chose *LGALS3BP* as a model to study short- and long-distance effects, considering that its protein is secreted and has crucial function in brain development (Kyrousi et al., 2021).

We, then generated human dorso-ventral cerebral assembloids (dvCAs), following the protocol descrived in (Bagley Joshua A , Reumann Daniel , Bian Shan, 2017). This model allows to study interneuron migration by resembling the ventral-dorsal forebrain axis in *vitro*. (

Figure 4-1, A).

We observed that our dvCAs express the ventral forebrain marker NKX2-1 in the ventral area (vCAs), and the dorsal forebrain markers TBR1 in the dorsal area (dCAs), as expected (Bagley Joshua A , Reumann Daniel , Bian Shan, 2017).

To investigate the role of LGALS3BP in interneuron migration, we used an iPSC line carrying the *LGALS3BP* variant in heterozygosity (E370K) (Kyrousi et al., 2021). We then generated dvCAs from isogenic control and genetically edited iPSCs, *LGALS3BP*-E370K (E370K). As a secreted protein, LGALS3BP acts extrinsically, possibly in both short- and/or long-distance. Thus, we generated dvCAs with different combinations of ventral and dorsal CAs (vCTRL-dCTRL, vE370K-dCTRL, vCTRL-dE370K, vE370K-dE370K) to focus on the local (ventral) and distant (dorsal) effects mediated by LGALS3BP in IN migration.

The vE370K-dCTRL condition carries the E370K variation only in the ventral region; therefore, this is used as a model for the short-distance effect on IN specification and migration;

while the vCTRL-dE370K condition, with the mutation in the dorsal region only, is a model for the long-distance effect on IN recruitment.

The vE370K-dE370K condition in which both ventral and dorsal regions carry the E370K variant is a model to assess short- and long-distance effects (Figure 4-1, B).

Next, we looked at INs migrated into the dorsal area and quantified the number of cells migrating from the ventral (GFP+, in green) to the dorsal (RFP+, in magenta) areas in 60-day old dvCAs in all four conditions. Interestingly, we found changes in INs localization within the dorsal area of CAs. The localization of GFP+ cells migrated from the ventral to the dorsal region of Cas was analyzed by subdividing the dorsal area (dCAs) into three equally distributed bins.

In the control condition, vCTRL-dCTRL dvCAs, circa 45% of GFP+ migrating cells mostly localized in bin2, while circa 55% in bin3 of the CTRL-dCAs.

On the contrary, in the vE370K-dCTRL condition (mimicking the short-distance effect of ventral E370K on migratory dynamics), 70% of the cells localized in bin2 and only 10% in bin3 of CTRL-dCAs.

In the vCTRL-dE370K condition (mimicking the long-distance effect of dorsal E370K on migratory dynamics of CTRL interneurons), 30-35% of control cells were distributed in bin1 and bin2 and ~25% in bin3 when migrated into E370K-dCAs.

In the vE370K-dE370K condition, we found that 70% of E370K cells localize in bin1, 20% in bin2, and 10% in bin3 of E370K dCAs (

Figure *4-1*, C).

In every condition that included the E370K variant, the distribution of INs within the dorsal regions was altered, suggesting that LGALS3BP is crucial for both migration and recruitment of INs. In the vE370K-dCTRL condition, migrated cells were primarily localized in bin2, suggesting an altered short-distance regulatory mechanism.

In both vCTRL-dE370K and vE370K-dE370K conditions, migrated cells were distributed primarily in bin1, indicating altered extrinsic long-distance mechanisms of recruitment mediated by the E370K mutation. These two last conditions both had LGALS3BP variants in the dCAs, demonstrating the strong extrinsic long-distance role of LGALS3BP in recruiting INs.

These results suggest that LGALS3BP E370K mutation affects IN migration and recruitment in the dorsal forebrain by influencing the local and remote extracellular environment.

We, next analyzed the migratory behavior of INs, looking at the trajectories of GFP+cells migrated into the dorsal area. This was done in all four conditions. To this end, we tracked GFP+ ventral migrating cells within dCAs in live imaging experiment. We measured three parameters described already in Klaus et al.,2019 (

Figure *4-1*, D). In particular, we looked at speed of migration (velocity), pausing (resting timepoints) and directionality (tortuosity).

For all three parameters, where LGALS3BP was mutated in at least one region of the dvCAs (vE370K-dCTRL, vCTRL-dE370K, vE370K-dE370K), we observed a significant difference compared with the vCTRL-dCTRL condition. In all three conditions, speed of migration decreased, and resting timepoints increased, suggesting that velocity and sliding movement are regulated in a short and long-distance manner.

Interestingly, E370K cells migrating into the control dorsal region showed more tortuous trajectories when migrating in CTRL-dCAs, suggesting that tortuosity is regulated in an intrinsic or extrinsic short-distance way. Altogether, these results show that LGALS3BP influences IN migration by regulating their migratory dynamics, in particular directionality, but also sliding movement and speed (

Figure *4-1*, E).

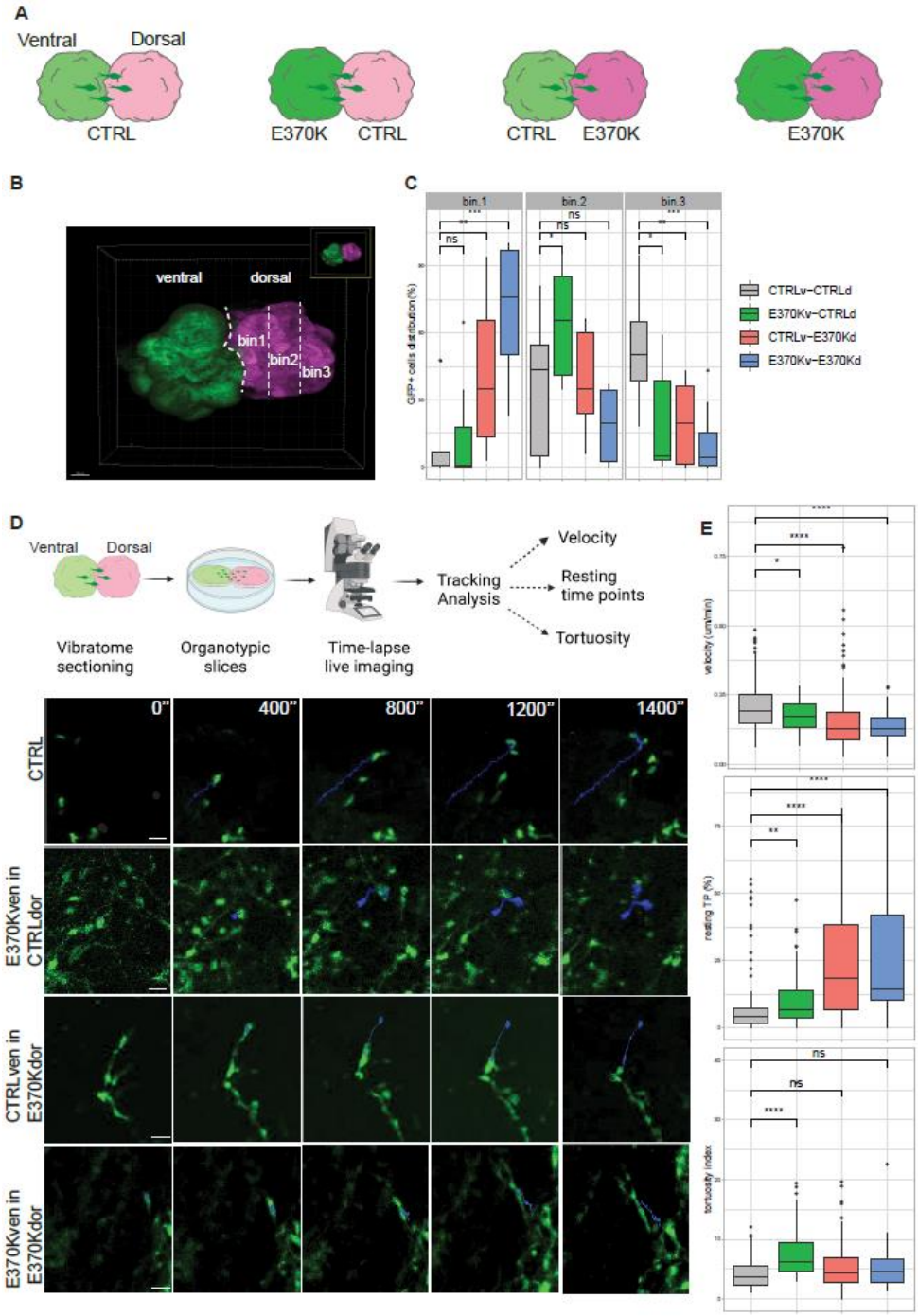

Figure 4-1: LGALS3BP variation affects interneuron distribution and migratory dynamics

A. Experimental set-up of the four different combinations of dvCAs generated for binning analysis and time-lapse live imaging.
B. Cleared dvCAs, with the dorsal area divided in 3 equally distributed bins for binning analysis. Scale bar: 200 µm.
C. Quantification of localization of GFP+ventral cells migrated in the three bins in the dorsal region of dvCAs. Box plots show median and interquartile range. Statistical significance was based on the Mann-Withney U test *p<0.05, **p<0.01, ***p<0.001. n of organoids: CTRLv-CTRLd=6, E370Kv-CTRLd=8, CTRLv-E370Kd=7, E370Kv-E370Kd=8, from at least 2 different batches.
D. Experimental set-up for time-lapse live imaging in dvCAs (top). Examples of the GFP+ ventral cells time-lapse migration in dorsal area of dvCAs for each condition are shown (bottom). Scale bar: 80 µm. Created with BioRender.com.
E. Analysis of migratory parameters: velocity (top), number of resting time points (middle), and tortuosity index (bottom) of migrating GFP+ventral cells within the dorsal area. Box plots show median and interquartile range. Statistical significance was based on the Mann-Withney U test *p<0.05, **p<0.01, ****p<0.0001. Figure and figure legend adapted from Pipicelli et al., 2022.

4.2 E370K-vCOs have altered cell identity

To analyze the intrinsically altered migration of mutant INs, we generated ventral forebrain organoids (vCOs) from isogenic control and E370K iPSC lines (Bagley Joshua A , Reumann Daniel , Bian Shan, 2017). The vCOs are a valuable system to look at differentiation of ventral progenitors into INs. The ganglionic emincences (GEs) are the regions where INs are generated. The ventral germinal zones of MGE and CGE generate different subpopulations of INs, while LGE gives rise to medium-spiny neurons (MSNs) that reach the striatum (Miura and Pașca, 2019; Peyre et al., 2015).

We observed a significant decrease of LGALS3BP expression in mutant vCOs (Figure 4-2, A). Moreover, we also found differences in GEs marker expression. Specifically, E370K-vCOs are characterized by a decrease of MGE NKX2-1+ cells, and a increase of CGE PAX6+ and LGE MEIS2+ cells (Figure 4-2, B). This data show that E370K vCOs produce more CGE and LGE regions. However, PAX6 is also a expressed in the dorsal cortex.

We then, aimed to understand the regional identity of the increased PAX6+ cells, we looked for dorsal markers, such as EOMES (marker of cortical intermediate progenitors-IP), TBR1 (marker of deep layer cortical neurons) and SATB2 (marker of upper layer cortical neurons). The immunohistochemistry analysis revealed that mutant vCOs express EOMES, TBR1, and SATB2. Specifically, EOMES was expressed in 50% of analyzed ventricles, TBR1 in circa 60%, and SATB2 in circa 90%. These results show that E370K vCOs express ectopic dorsal cortical markers (Figure 4-2, C and D).

Next, we assessed if E370K ventral cells (vCAs) migrated into CTRL-dCAs expressed TBR1 and SATB2, analyzing the proportions of ventral E370K GFP+ cells expressind the dorsal markers. Interestingly, 30% of the total E370K GFP+ migrated cells expressed TBR1, while 10% expressed SATB2. On the contrary, as expected. CTRL GFP+ ventral cells expressing TBR1 and/or SATB2 were absent in CTRL-dCAs.

Our findings suggest that LGALS3BP could be involved in regional patterning, regulating progenitor differentiation in the ventral forebrain. This alteration may, in turn, bring changes in migratory behavior.

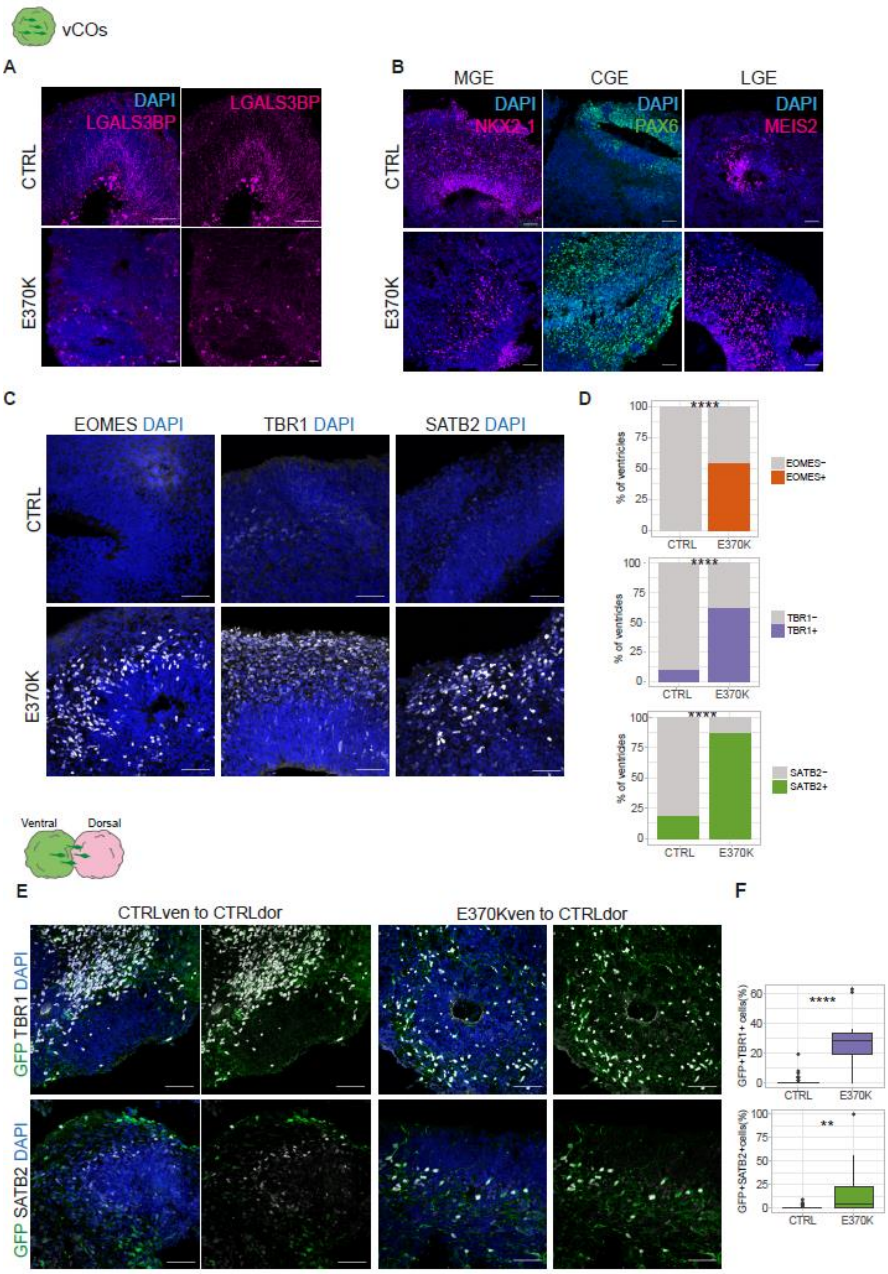

Figure 4-2: E370K-vCOs have altered cell identity

A. Representative pictures of 60-days old CTRL and E370K vCO immunostained for LGALS3BP (magenta). Scale bar: 50 µm.
B. Representative pictures of 60-days CTRL and E370K vCO immunostained for NKX2-1, PAX6 and MEIS2. Scale bar: 50 µm.
C. Representative pictures of 60-days CTRL and E370K vCO immunostained for cortical markers EOMES, TBR1 and SATB2. Scale bar: 50 µm.
D. Quantification of ventricles (%) expressing EOMES+cells (top), TBR1+cells (middle) and SATB2+cells (bottom) in 60-days CTRL and E370K vCOs. Statistical significance was based on the exact binomial test ****p<0.0001. n of observations: for EOMES, CTRL=96, E30K=53; for TBR1, CTRL=100, E30K =107; for SATB2, CTRL=48, E30K =76; from 3 different batches.
E. Representative pictures of dorsal regions of 60-days dvCAs showing ventral migrated cells (GFP+) and dorsal neurons (TBR1 and SATB2, white). Scale bar: 50 µm.
F. Quantification of migrated GFP ventral cells expressing TBR1 and SATB2 in the dorsal area of dvCAs. Box plots show median and interquartile range. Significance was based on the Mann-Withney U test **p<0.01, ****p<0.0001. n of ventricles: for GFP+TBR1+, CTRL=58, E370K=26; for GFP+SATB2+, CTRL=29, E370K =20; from at least 2 different batches. Figure and figure legend adapted from Pipicelli et al., 2022.

Moreover, considering that the E370K variant is heterozygous, it still has the functional allele. For this reason, we also generated iPSCs line carrying the Y366Lfs variation in *LGALS3BP* in homozygosity (Kyrousi et al., 2021), from which we generated Y366Lfs-vCOs.

Interestingly, also Y366Lfs-vCOs showed decreased expression of LGALS3BP and expressed EOMES, TBR1, and SATB2, recapitulating the phenotype observed in the E370K vCOs (Figure 4-3, A, B and C).

Altogether, we showed that functional *LGALS3BP* is important for the correct specification of interneurons.

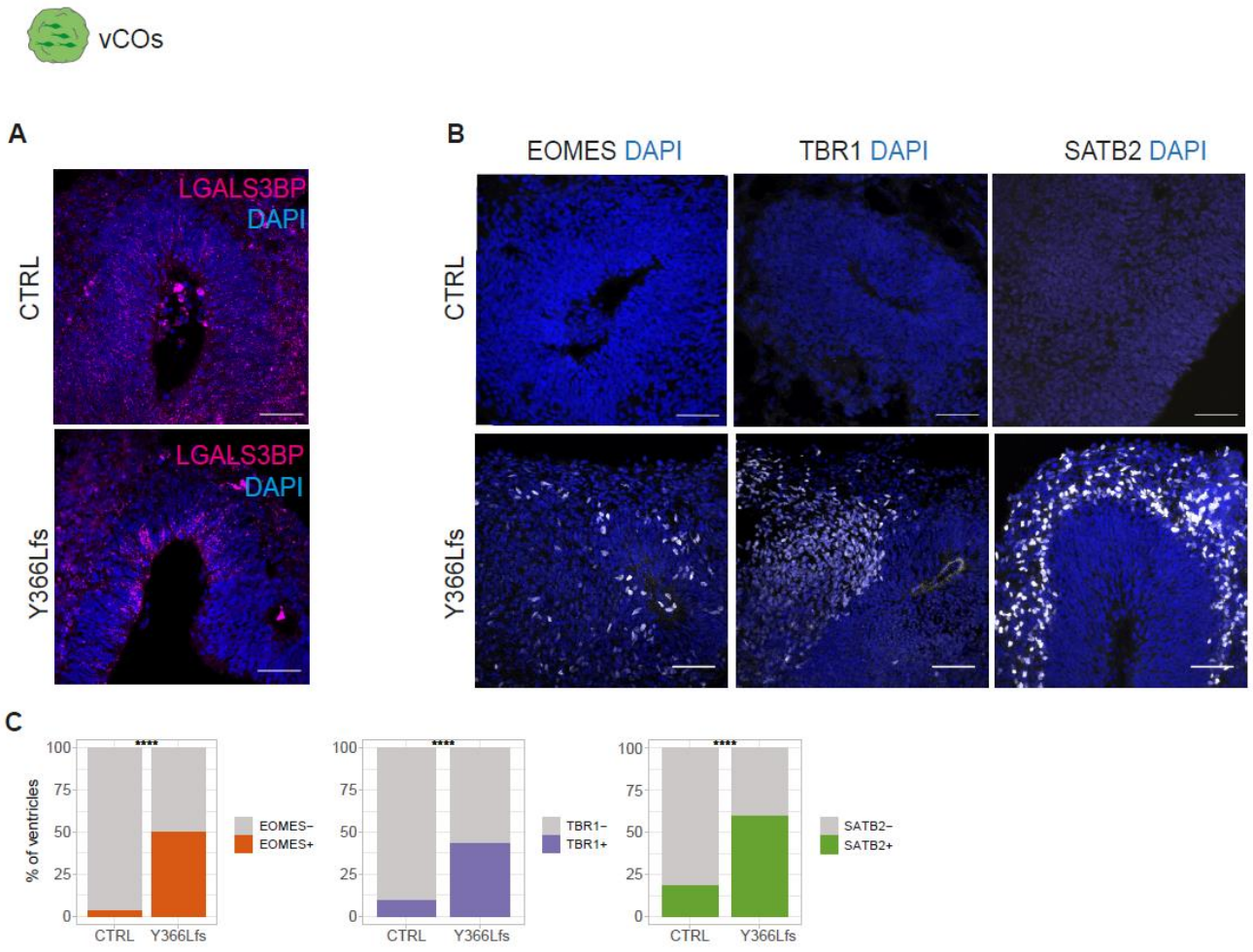

Figure 4-3: E370K-vCOs show alteration in cell identity (II)

A. Representative pictures of 60-days CTRL and Y366Lfs d60 vCOs immunostained for LGALS3BP (magenta). Scale bar: 50 µm.
B. Representative pictures of 60-days CTRL and Y366Lfs d60 vCOs immunostained for cortical markers EOMES, TBR1, SATB2. Scale bar: 50 µm.
C. Quantification of ventricles (%) expressing EOMES (top), TBR1 (middle) and SATB2 (bottom) in 60-days old vCOs. Statistical significance was based on exact binomial test ****p<0.0001. n of ventricles: for EOMES, CTRL=96, Y366Lfs =80; for TBR1, CTRL=100, Y366Lfs = 119; for SATB2, CTRL=48, Y366Lfs =119; from 2 different batches. Figure and figure legend adapted from Pipicelli et al., 2022.

4.3 Molecular changes in cells derived from E370K-vCOs

Intrigued by the altered migratory dynamics of E370K ventral cells, we dissected the transcriptional features of mutant vCOs. To this end, we performed single-cell RNA-sequencing (scRNA-seq) analysis CTRL-vCOs and E370K-vCOs (60-days old). We identified 5369 cells that clustered into eight groups. We identified progenitor cells, characterized by the expression of *TOP2A*, IP expressing *TTYH1*, *ASCL1* and *NKX2-1*, and interneurons expressing *MAP2* and *DLX5* (Figure 4-4, A, B and C). Interestingly, we noticed that E370K-vCOs presented different cell proportions compared to control. Specifically, the MGE IP cluster which comprise only 10% of mutant cells (Figure 4-4, D).

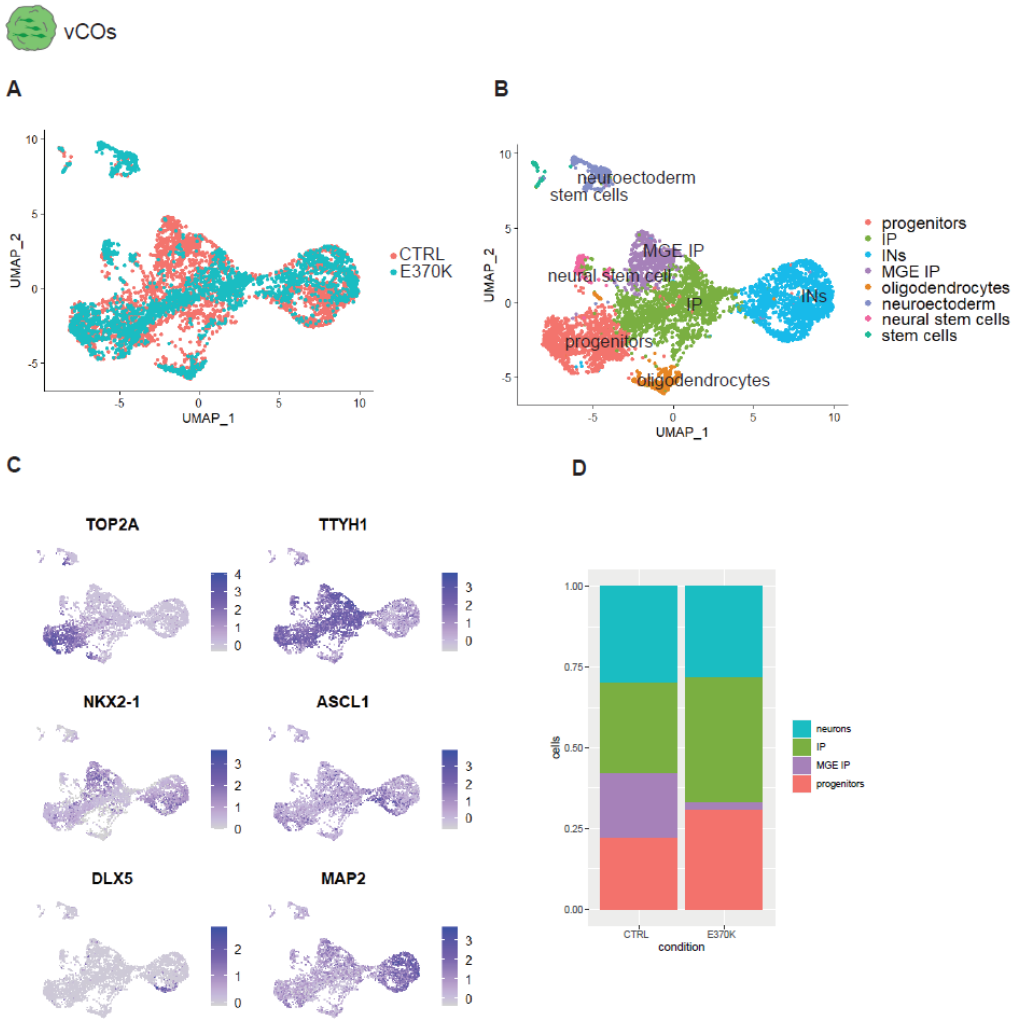

Figure 4-4: Molecular changes in cells derived from E370K-vCOs

A,B. Uniform Manifold Approximation and Projection for Dimension Reduction (UMAP) visualization showing clusters of scRNA-seq data from 60-days old control and E370K vCOs .
C. Feature plot showing the expression of progenitor markers (TOP2A), IPs markers (TTYH1, NKX2-1, ASCL1) and interneurons (DLX5, MAP2) in 60-days old control and E370K vCOs.
D. Bar plot showing cell proportion in CTRL and E370K vCOs. Figure and figure legend adapted from Pipicelli et al., 2022.

Next, we identified a pseudo-differentiation trajectory from progenitors to interneurons, using Monocle3(Trapnell et al., 2014), (https://cole-trapnell-lab.github.io/monocle3/). As expected from the immunohistochemistry analysis and from the difference in cell proportion in the E370K-vCOs, the mutant vCOs were lacking on the IP-MGE IP trajectory (Figure 4-5, A and B).

Then, we performed differential expression (DE) analysis in the three main cell populations (progenitors, IP and MGE-IP, and INs) (Figure 4-5, C, D and E). All three populations of E370K-vCOs show downregulation of ventral genes (*NKX2-1*, *NKX6-2*, *SIX3*, *DLK1*, *OCIAD2*, and *SHH).*

As expected, they upregulate genes associated with dorsal identity, such as *PAX6*, *PTN*, *POU3F2*, *GLI3*, and *NEUROG2*. These results confirmed that E370K ventral cells gain dorsal identity.

Interestingly, also genes associated with axon guidance were differentially expressed in mutant vCOs (*EFNA5*, *EPHB2*, *SEMA5B*, and *SLIT2),* which could explain the alterations in IN migration and recruitment observed in the assembloids.

Moreover, genes associated with periventricular heterotopia (PH), *FAT4*, *DLL1*, *ROBO3* and *RND2*, (Klaus et al.), were dysregulated in E370K-vCOs. The DE analysis confirmed that, in E370K-vCOs genes associated with pattern specification, regionalization, differentiation, neurogenesis, are dysregulated (Figure 4-5, F, G and H).

These findings suggested a key role of LGALS3BP in human ventral forebrain pattern and development.

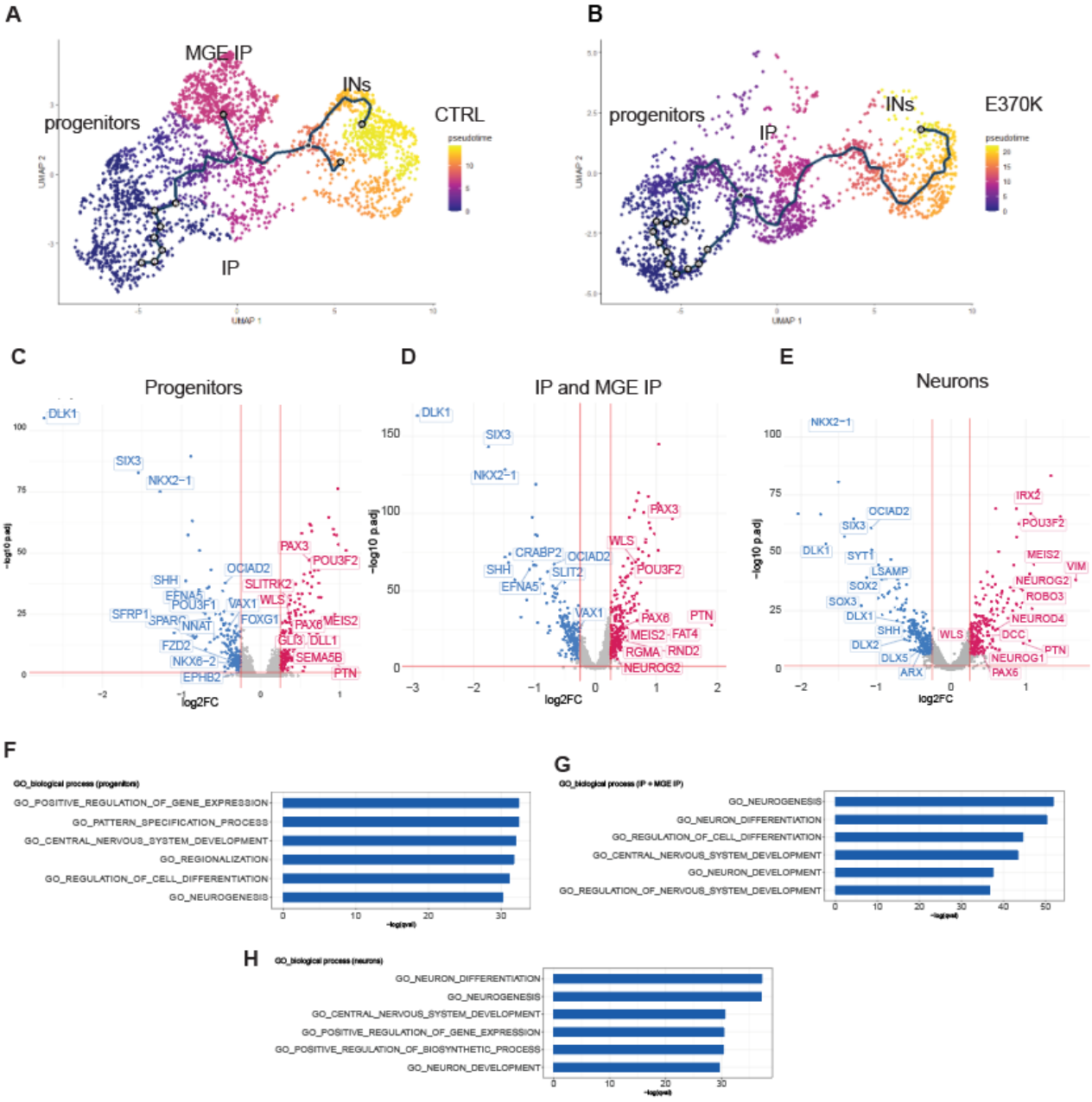

Figure 4-5: Molecular changes in cells derived from E370K-vCOs

A, B. Uniform Manifold Approximation and Projection for Dimension Reduction (UMAP) visualization of pseudo-time trajectories in control vCOs and in E370K from progenitors to interneurons.
C, D, E. Volcano plot showing the fold change (CTRL vs E370K) of gene expression in progenitors, IP and MGE IP, and in INs in control vCOs and in E370K.
F, G, H. GO enrichment for DE genes in progenitors, IP and MGE IP and INs. GO for biological process are reported. Figure and figure legend adapted from Pipicelli et al., 2022.

4.4 LGALS3BP has a short-distance effect in ventral cell fate decision and in specification of neurons

LGALS3BP is a secreted glycoprotein and its functions have been mainly characterized in cancer, being LGALS3BP a cancer biomarker (Capone et al., 2020, 2021a; Escrevente et al., 2013; Fogeron et al., 2013; Gomes et al., 2015; Luo et al., 2021; Song et al., 2020; Zhang et al., 2019).

For this reason, together with our data, we hypothesized that LGALS3BP might have a non-cell autonomous function. We assessed if the dorsal identity gained by mutant vCOs can be rescued by generating a more physiological environment. To address this issue, we established two approaches: (i) we treated E370K-vCOs with media from CTRL-vCOs; (ii) we generated ventral mosaic organoids (vMOs) by mixing, in a ratio of 1:1, control iPSCs (isogenic control) and E370K IPCs labeled with GFP (Figure 4-6, A and B)

Interestingly, a rescue of the phenotype in both cases was obtained. Specifically, upon exposure to control medium or cell to cell contact with control cells, a significant reduction of the expression of the dorsal markers (EOMES for IP, TBR1 for deep layer neurons and SATB2 for upper layer neurons) compared to E370K-vCOs (Figure 4-6, C, D, E and F) was observed.

To get more insight on the transcriptomic features of vMOs, we performed scRNA-seq (, A). The 4898 identified cells clustered into six main clusters. We identified progenitor cells expressing *TOP2A*, IP expressing *TTYH1* and *ASCL1*, MGE IP expressing *NKX2-1*, INs expressing *DLX5* and *MAP2*, and LGE-derived medium-spiny neurons (MSNs) expressing *ZFHX3* (Figure 4-7,B, C and D).

Interestingly, vMOs have increased progenitors, IP, and MGE IP cell proportions compared to E370K-vCOs (Figure 4-7, E). These results indicate that a more physiological environment could change cell proportions of mutant cells. Next, we looked at the trajectory from progenitors to INs, as seen in vCOs. To identify trajectories of cortical INs, we excluded LGE-derived MSN (Fig.S4A). Using Monocle3 (Trapnell et al., 2014), (https://cole-trapnell-lab.github.io/monocle3/), the pseudo-time trajectories in vMOs were identified. The trajectories included both CTRL and E370K cells. Interestingly we noticed that the trajectories of vMOs resembled the ones found in CTRL-vCOs (Figure 4-7, F and G). These findings suggested that E370K cells in vMOs have partially rescued the phenotype after exposure to CTRL cells.

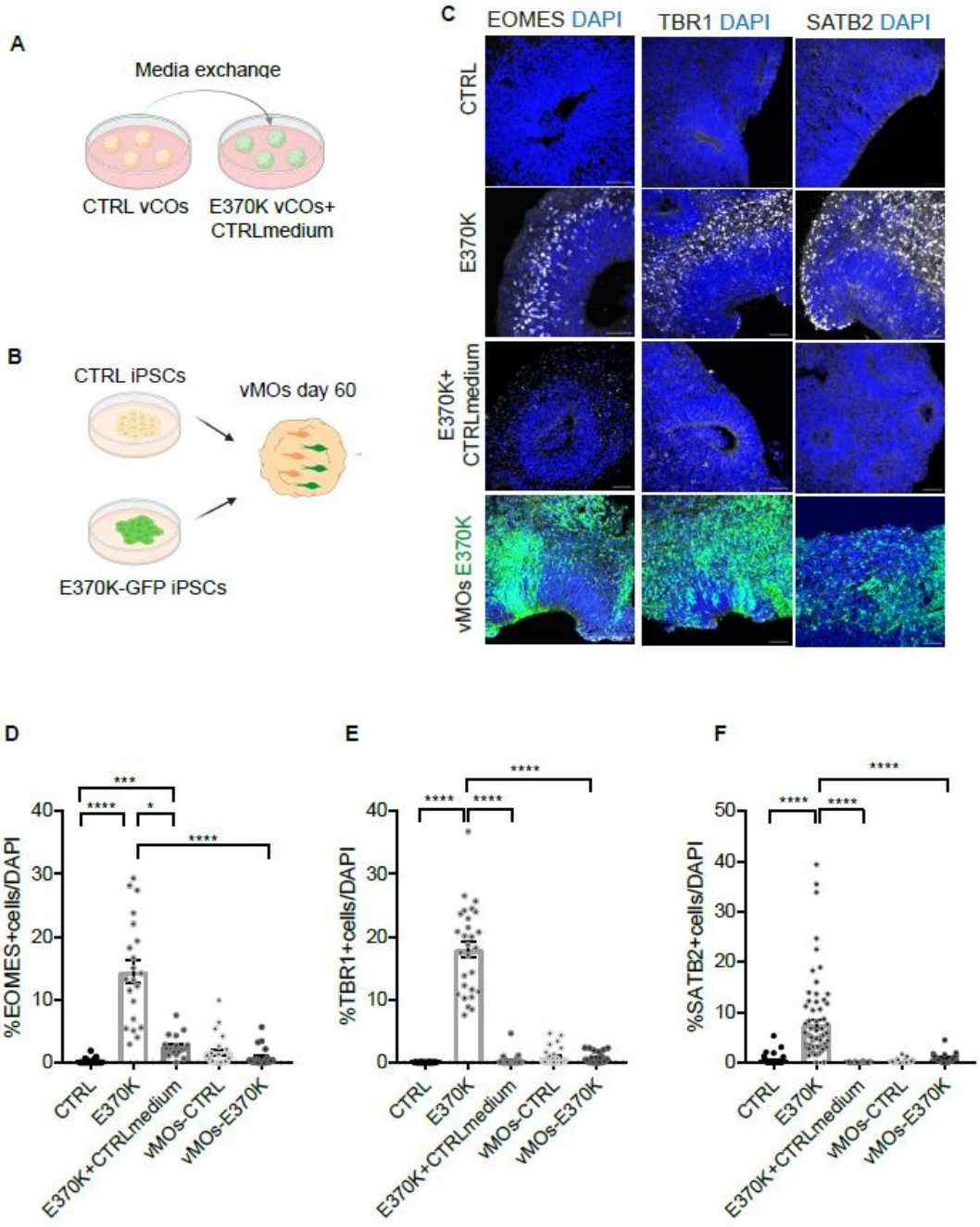

Figure 4-6: Short-distance effect of LGALS3BP in ventral cell fate decision and in specification of neurons

A. Experimental setup for media exchange in vCOs. E370K vCOs are treated with control culture media from day 12 of culture until day 60.
B. Experimental setup for generation of vMOs. . Created with BioRender.com.
C. Representative immunostaining of vCOs and vMOs showing the IP marker EOMES (grey), the deep layer neuronal marker (TBR1, grey) and upper layer neuronal marker (SATB2, grey). Scale bar: 50 µm..Created with BioRender.com.
D. Quantification of the percentage of EOMES+cells in vCOs and vMOs normalized by DAPI in the analyzed GE unit. Significance was based on the Kruskal-Wallis multiple comparison test *p=0.029, ***p=0.0004, ****p<0.001. Every dot in the plots refers to analyzed ventricles per vCO from at least 3 different vCOs generated in at least 2 independent batches.
E. Quantification of the percentage of TBR1+cells in vCOs and vMOs normalized by DAPI in the analyzed GE unit. Significance was based on the Kruskal-Wallis multiple comparison test ****p<0.001. Every dot in the plots refers to analyzed ventricles per vCO from at least 3 different vCOs generated in at least 2 independent batches.
F. Quantification of the percentage of SATB2+cells in vCOs and vMOs normalized by DAPI in the analyzed GE unit. Significance was based on the Kruskal-Wallis multiple comparison test ****p<0.001. Every dot in the plots refers to analyzed ventricles per vCO from at least 3 different vCOs generated in at least 2 independent batches. Figure adapted from Pipicelli et al., 2022.

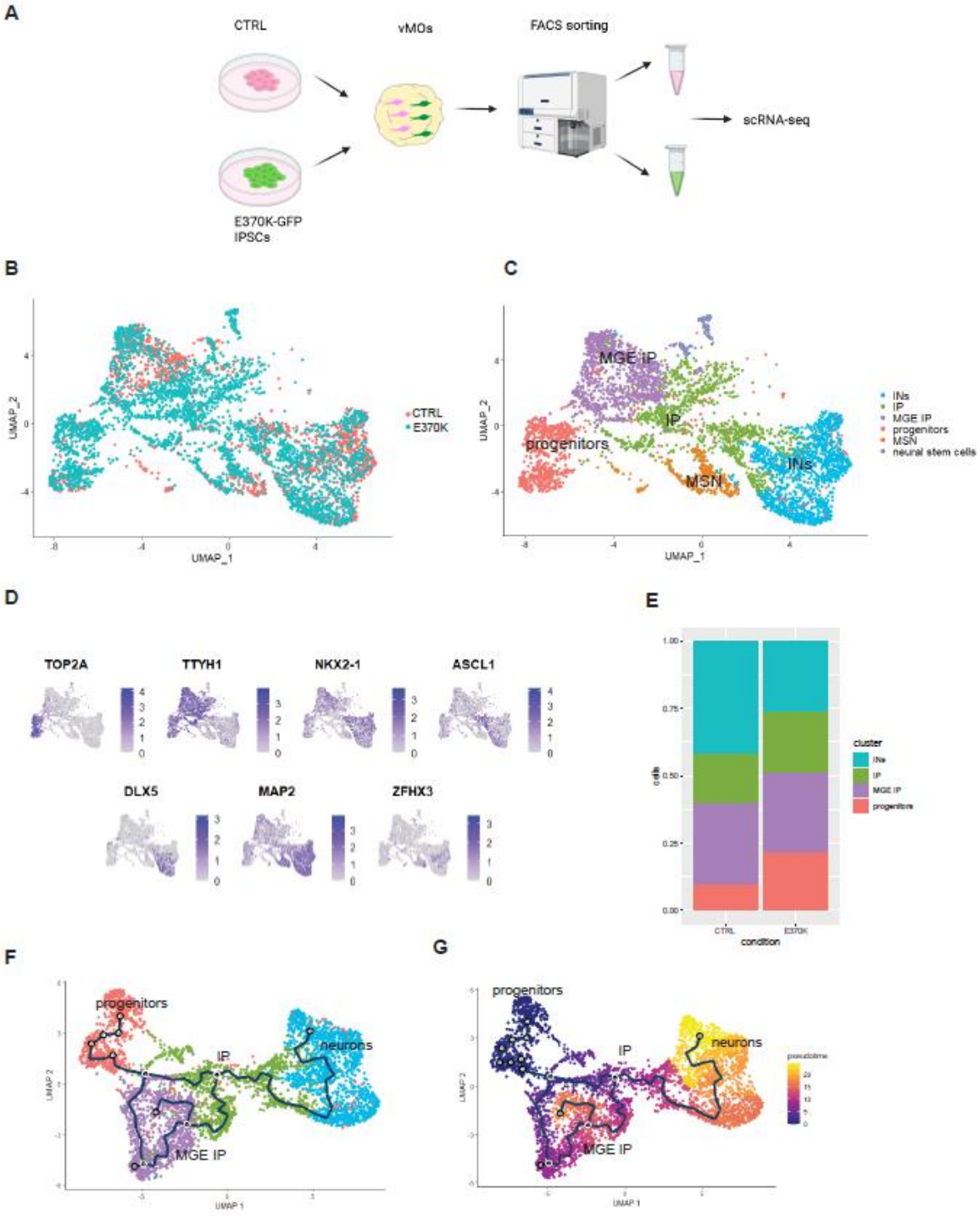

Figure 4-7: Short-distance effect of LGALS3BP ventral cell fate decision and in specification of neurons (II)

A. Experimental set-up showing generation and processing of vMOs . Created with BioRender.com.
B,C. Uniform Manifold Approximation and Projection for Dimension Reduction(UMAP) visualization showing clusters of scRNA-seq data from 60-days old vMOs.
D. Feature plot showing the expression of progenitor markers (TOP2A), IPs markers (TTYH1, NKX2-1, ASCL1), INs (DLX5, MAP2) and MSNs (ZFHX3) in 60-days old vMOs.
E. Bar plot showing cell proportion in 60-days old vMOs.
F,G. UMAP visualization of pseudo-time trajectories in vMOs from progenitors to neurons. Figure and figure legend adapted from Pipicelli et al., 2022.

4.5 LGALS3BP role in reverting ventral progenitor and interneuron molecular identity

By taking advantage of a dorso-ventral model, we better analyzed the molecular identity acquired by E370K vCOs and vMOs. This model allows the prediction of the molecular identity (dorsal and/or ventral) of cells according to their transcriptome, defining a dorso-ventral score (DV). To this end, we collected scRNA-seq data from CTRL-dCOs and CTRL-vCOs, E370K-vCOs, and CTRL/E370K-vMOs and cluster them all together. (Figure 4-8, A). We identified three main clusters, including progenitors, expressing *TOP2A*, IP, expressing *TTYH1*, and neurons, expressing *MAP2* (Figure 4-8, B, C and D).

As expected, the model predicted the highest score (more dorsal identity) in CTRL-dCOs and the lowest in control CTRL-vCOs (more ventral identity), as expected. The other conditions showed an "in between" dorso-ventral identity. The predicted identity of E370K-vCOs were intermediate through the dorso-ventral score, while the predicted identity of cells from vMOs (both control and mutant) was similar. In particular, the molecular identity of CTRL cells from vMOs was closer to the identity of CTRL cells from vCOs. E370K cells from vMOs revealed an identity which was similar to the one of E370K-vCOs (Figure 4-8, E).

These results strongly confirmed that E370K cells gain a dorsal molecular identity, showing a high DV score compare to CTRL-vCOs. The dorsal identity of mutant cells can be partially rescued by exposure to CTRL cells (Figure 4-8, E).

We also looked if gene expression might be affected in vMOs. We, then, looked at the ventral genes *NKX2-1* and *DLX5*. These genes are almost not expressed or are expressed at very low levels in E370K-vCOs. However, *NKX2-1* and *DLX5* are expressed along the pseudo-differentiation trajectory in E370K cells from vMOs.

On the other hand, the dorsal genes *GLI3* and *POU3F2* are enriched in CTRL-dCOs. They are also highly expressed in E370K-vCOs. However, the expression levels of *GLI3* and *POU3F2* are still lower in E370K-vMOs compared to E370K-vCOs (Figure 4-8, F).

Next, we looked at the in-situ hybridization data from the "Allen Developing Mouse Brain Atlas"(Thompson et al., 2014) and, using VoxHunt (Fleck et al., 2021) (https://quadbiolab.github.io/VoxHunt/), we plotted our CO single-cell RNAseq data on the developing mouse brain.

As expected, data from CTRL dCOs plot to the mouse dorsal forebrain (pallium), while data from vCOs map to the and ventral forebrain (subpallium). Interestingly, data from E370K-vCOs, map to the mouse ventral forebrain but also to the dorsal forebrain, confirming their dorsal cortical identity. Both CTRL and E370K cells from vMOs, mostly map to the mouse ventral forebrain; however, E370K cells still correlate with the mouse ventral forebrain (Figure 4-8, G).

Overall, our results reveal that the molecular identity of ventral progenitors, IP, and neurons can be influenced by extrinsic factors released in the extracellular space.

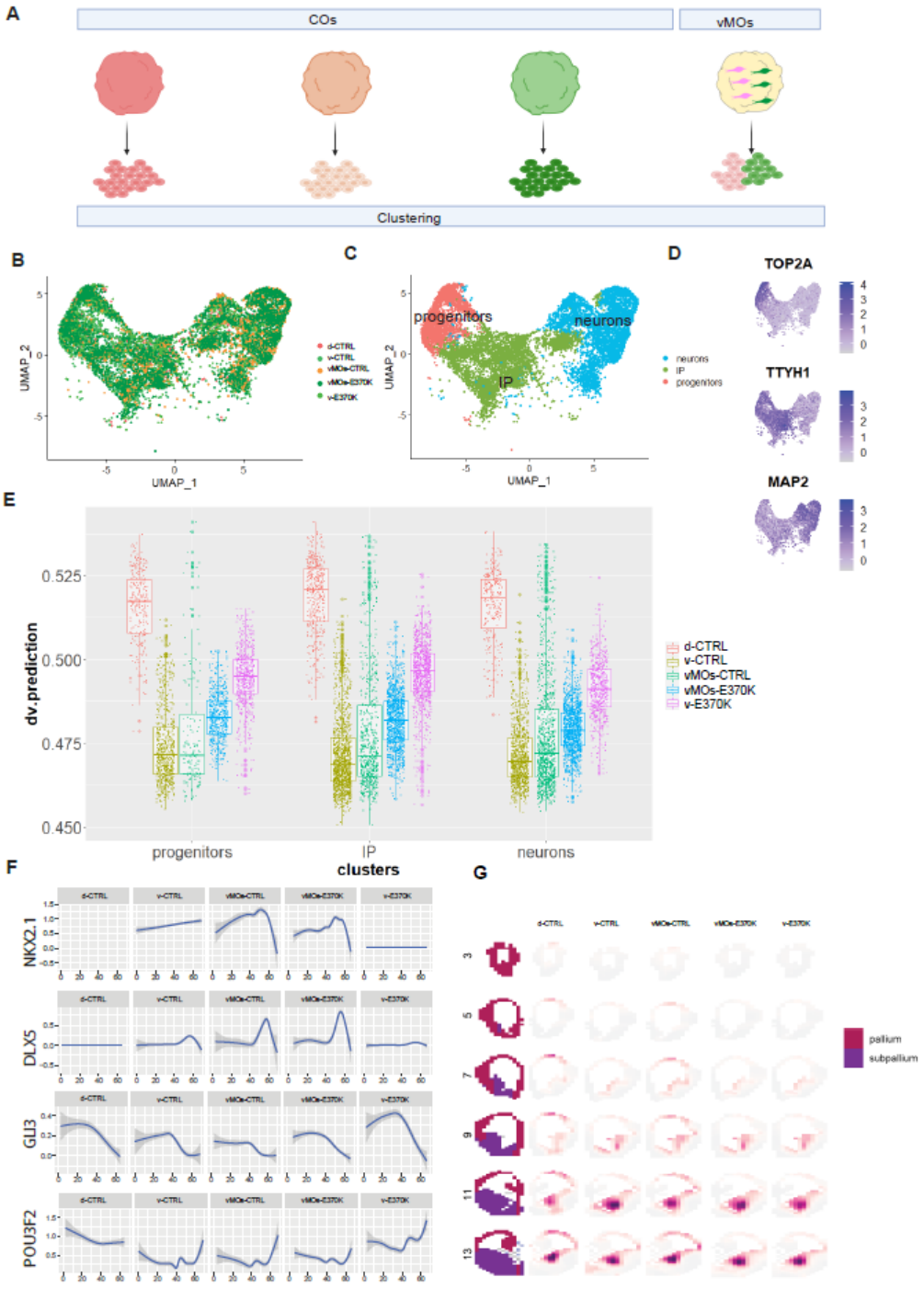

Figure 4-8: LGALS3BP role in reverting ventral progenitor and interneuron molecular identity

A. Experimental set-up showing cluster analysis of 60-days old CTRL dCOs (d-CTRL), CTRL vCOs (v-CTRL), E370K vCOs (v-E370K) and vMOs (vMOs-CTRL and -E370K). Created with BioRender.com.
B,C. Uniform Manifold Approximation and Projection for Dimension Reduction(UMAP) visualization of scRNA-seq data from CTRL dCOs, CTRL vCOs, E370K vCOs and vMOs.
D. Feature plot showing the expression of progenitor marker (TOP2A), IPs marker (TTYH1,), neuronal marker (MAP2).
E. Boxplot showing the dorso-ventral (DV) prediction score of progenitors, IP, and neurons in all conditions. Box plots show median and interquartile range.
F. Expression level of ventral (NKX2.1 and DLX5) and dorsal (GLI3 and POU3F2) genes along the pseudo-time axis in each condition.
G. VoxHunt spatial brain mapping of the scRNA-seq from all conditions onto data from E13.5 mouse brains from the Allen Brain Institute.
Figure and figure legend adapted from Pipicelli et al., 2022."

4.6 Different cellular composition in E370K dCOs might affect interneuron recruitment

We showed that E370K ventral cells have an altered molecular identity, namely they acquire dorsal identity rather than ventral. This cell fate switch could result in the altered migratory dynamics observed in vE370K-dCTRL assembloids, described in chapter 4.1. Moreover, we showed that localization of control ventral cells is altered when migrating into the E370K dorsal region, suggesting a long-distance role of LGALS3BP in the recruitment of interneurons.

We, therefore, sought to understand the mechanisms underlying the recruitment of INs in assembloids. Recruitment of INs is a highly regulated and complex process (already described in the introduction), and it is influenced by extrinsic cues that attract them to the cortex (Marín, 2013; Peyre et al., 2015; Silva et al., 2018). We hypothesized that changes in cellular composition could lead to alteration in interneuron migration and, specifically, to the cortex.

To this end we performed single-cell RNA-sequencing (scRNA-seq) analysis in 60-day old dorsal CTRL-dCOs and E370K-dCOs. The 6951 identified cells clustered into eleven main groups (Figure 4-9, A and B), including progenitors expressing *TOP2A*, *PAX6, SOX2*, RGCs expressing *FABP7* and *HOPX*, neurons expressing *STMN2, SYT1, NEUROD6, POU3F2* and *EMX1* and neuroectoderm and neuroepithelium expressing *LUM* and *VCAN* (Figure 4-9, C).

Interestingly, E370K dCOs show different cell proportions compared to control. Specifically, they present more neuroectoderm (39%), neuroepithelium (10%), proliferating cells (15%) compared to CTRL dCOs where neuroectoderm, neuroepithelium represent the 2% and 1% of total cells, respectively; and proliferating cells represent the 17% of total cells (Figure 4-9, D).

Then, the cells were aligned on a developmental pseudo-differentiation axis. Clearly, E370K cells exhibit difference in the pseudo-differentiation, showing earlier developmental stages (Figure 4-9, E and F). The different cell composition observed in E370K dCOs might alter the extracellular environment, resulting in changes in the attractive cues which could explain the alteration in interneuron localization when migrating in the mutant dorsal part of assembloids.

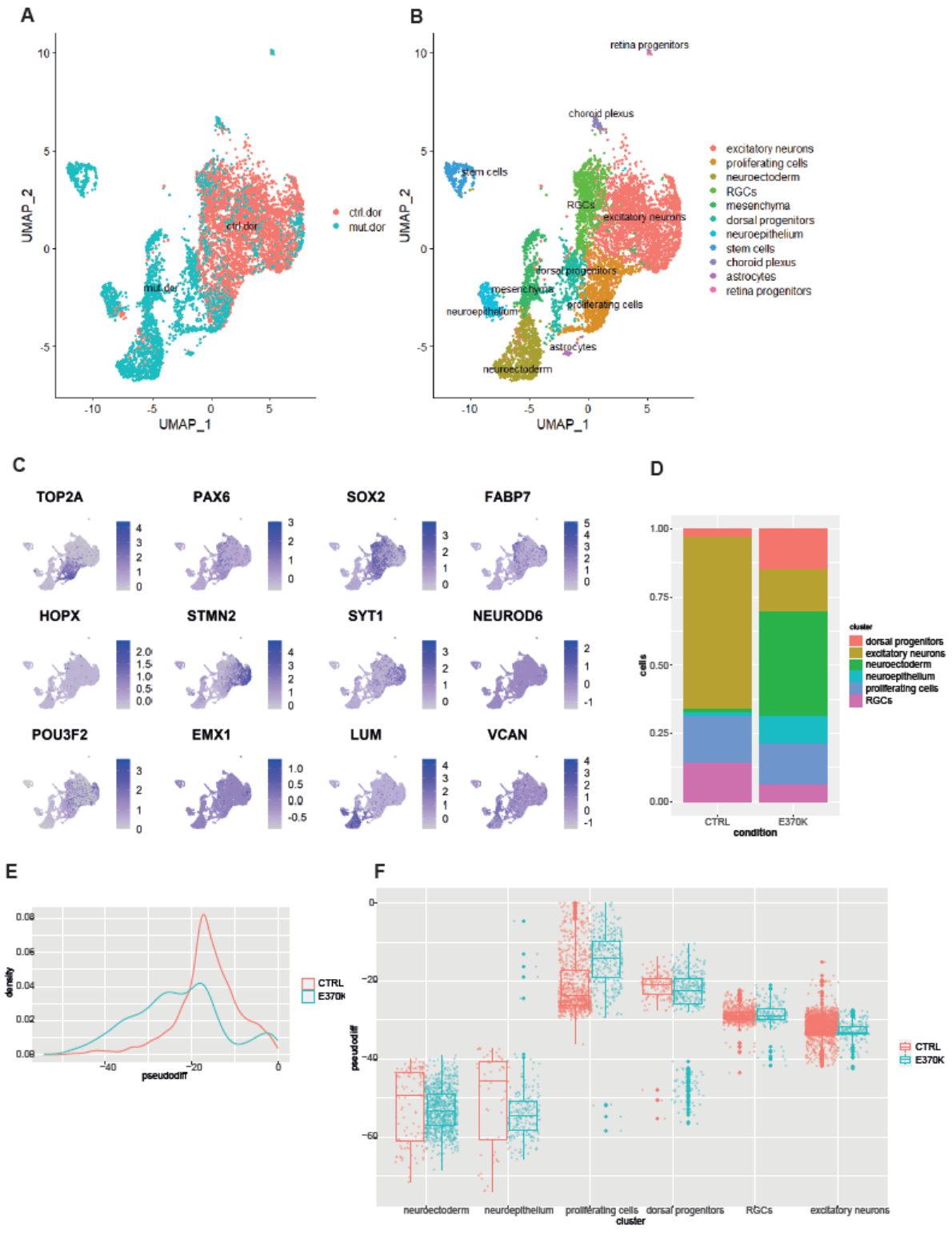

Figure 4-9: Different cellular composition in E370K dCOs might affect interneuron recruitment

A,B. Uniform Manifold Approximation and Projection for Dimension Reduction(UMAP) visualization of scRNA-seq clusters of 60-days old control and E370K dCOs (n= 6951 cells from a pool of 5 organoids each condition).
C. Feature plot showing the expression of progenitor markers (TOP2A, PAX6, SOX2), RGs markers (FABP7, HOPX), excitatory neurons (STMN2, SYT1, NEUROD6, POU3F2 and EMX1), neuroectoderm (LUM) and neuroepithelium (VCAN) in 60-days old dCOs.
D. Bar plot showing cell proportion in 60-days old CTRL and E370K dCOs.
F. Density plot showing cell distribution along pseudo-differentiation axis in 60-days old CTRL and E370K dCOs.
G. Box plot showing cell distribution along pseudo-differentiation axis in 60-days old CTRL and E370K dCOs per each cluster.

Therefore, we performed DE analysis in proliferating cells, dorsal progenitors, and excitatory neurons. Interestingly, we found many genes associated with cell proliferation and differentiation, such as *HES4*, *EMX2*, *GLI3* and cerebral cortex regionalization including *WNT5A*, *HES1*, *RHOA* to be differentially expressed in E370K proliferating cells and progenitors. Moreover, mutant neurons dysregulate genes associated with axon guidance and chemotaxis, such as *ROBO3*, *RELN*, *SEMA6A*, *CXCL12*, *CXCR4*. Specifically, *CXCL12* and *CXCR4* are chemokines that guide INs in their migration to the cortex (López-Bendito et al., 2004; Marín, 2013).

Interestingly, in all the three cell populations, genes involved in extracellular matrix composition and assembly, extracellular vesicle were differentially regulated, suggesting that the ECM might play a crucial role in all these processes, especially in the migration and recruitment of INs (Figure 4-10, A, B and C).

These results showed that mutant dCOs have increased neuroepithelium and proliferating cells compared to CTRL dCOs. This difference in cell composition might lead to a different extracellular environment and ECM composition which could result in different attractive/repulsive cues that will ultimately affect interneuron recruitment in the cortex.

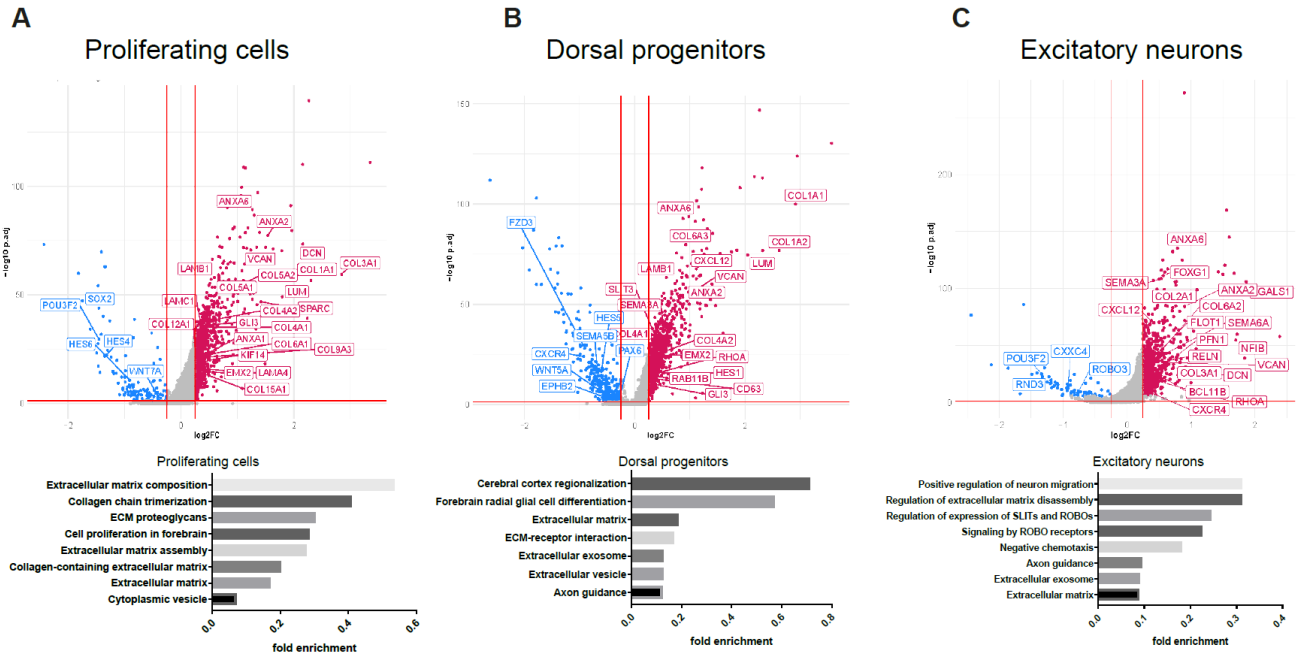

Figure 4-10: Different cellular composition in E370K dCOs might affect interneuron recruitment (II)

A, B, C. Volcano plots (top) showing the fold change (CTRL vs E370K) of gene expression in proliferating cells, dorsal progenitors, and excitatory neurons in 60-days old dCOs; and enrichment for DE genes (bottom) in proliferating cells, dorsal progenitors and excitatory neurons in dCOs. GO for biological process are reported."

4.7 Short- and long- distance effect of LGALS3BP is mediated via extracellular vesicles

In Chapter 3.9, I showed the importance of extracellular vesicles (EV) during neurodevelopment, in both physiological and pathological condition. Indeed, factors released in the ECM by EVs can impact on neurogenesis and cell migration (Peruzzotti-Jametti et al., 2021; Sharma et al., 2019; Taverna and Huttner, 2010). Moreover, our previous work showed that, in COs, LGALS3BP, has critical extrinsic functions in modeling the extracellular environment, mediated by its secretion via EVs (Kyrousi et al., 2021).

We then investigated the long-distance effect of extrinsic mechanisms underlying the altered interneuron distribution in the vCTRL-dE370K assembloid.

To this end, we looked, first at the role of EVs collected from ventral and dorsal E370K COs (E370K-vEVs and E370K-dEVs, respectively) on neuronal progenitor cells (NPCs) at the transcriptional level. NPCs were acutely treated with EVs isolated from control and E370K vCOs and dCOs (Figure 4-11, A). The RNA-seq analysis performed on NPCs revealed changes in the transcriptome after EV exposure. Interestingly, E370K-vEVs showed changes in DNA metabolic process, WNT and NOTCH pathways and axon guidance (Figure 4-11, B). On the otheR hand, NPCs treated with E370K-dEVs altered the expression of genes associated with cell cycle and interkinetic nuclear migration (INM) (Figure 4-11, C). Moreover, upon treatment with E370K-dEVs, NPCs upregulated genes associated with cell migration, including the chemokines CXCL10, CXCL11 or semaphoring SEMA6D (Figure 4-11, C).

Altogether, these results propose a role of EVs in cell fate decision, migration and recruitment of INs during brain development.

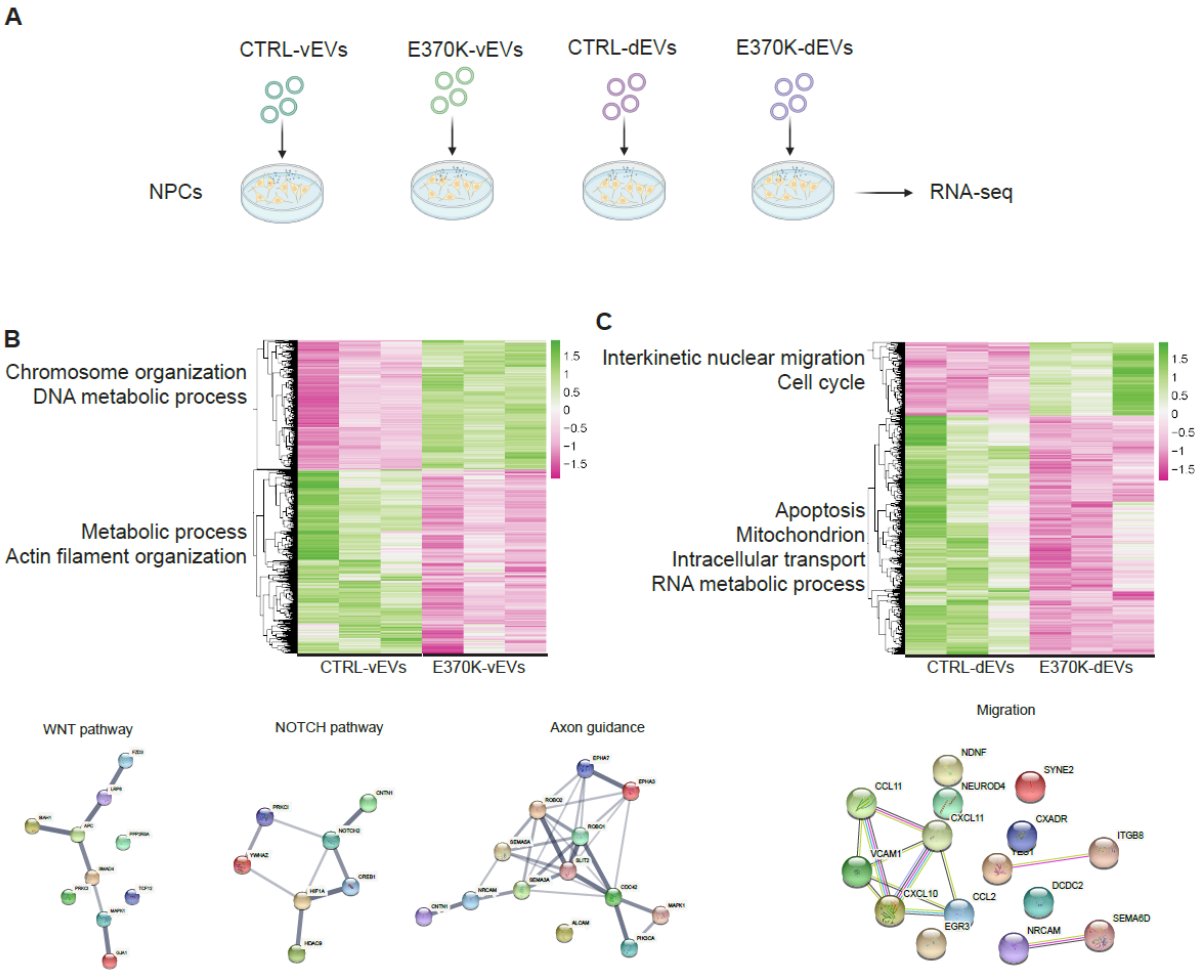

Figure 4-11: Short- and long-distance effect of LGALS3BP is mediated via extracellular vesicles

A. Schematic of acute treatment (12 h) of NPCs with vEVs and dEVs collected from CTRL and E370K vCOs and dCOs. Created with BioRender.com.
B. Heatmap showing differentially regulated genes in NPCs after treatment with E370K-vEVs (top), up-regulated genes In NPCs after E370K-vEVs associated with WNT and NOTCH pathways, and axon guidance (bottom).
C. Heatmap showing differentially regulated genes in NPCs after treatment with E370K-dEVs (top), up-regulated genes In NPCs after E370K-vEVs associated with neuronal migration (bottom). Figure and figure legend adapted from Pipicelli et al, 2022.

In **Chapter 5**, I will show the results of the project:

Extracellular vesicles are crucial mediators in orchestrating brain development and disease

The work presented in this project contains all original work done by me. All the proteomic data presented in this work were analyzed by me.

The samples analyzed in this project were collected and pre-processed by Rossella Di Giaimo, Giuseppina Maccarrone, from the Max Planck Institute of Psychiatry, and Pavel Kielkowski, from LMU in Munich. Experiments in NPCs, neurons, and astrocytes in 2D and all imaging and confocal pictures were performed by Andrea Forero Echeverry, from the Max Planck Institute of Psychiatry.

5 Extracellular vesicles are crucial mediators in orchestrating brain development and disease

This study focused on the role of extracellular vehicles (EVs) during brain development.

In the previous chapters of this thesis, I showed how extrinsic signals are important for neurodevelopment and during brain diseases. Since, extracellular signals regulate neurogenesis, neuronal migration, cell-cell communication, adhesion, and morphology, here I will focus on EVs, secreted vesicles by all cells which carry ECM components that regulates cell growth and differentiation.

The knowledge regarding EVs in brain development is very little, therefore, in this project, we analyzed the role of EVs in neurodevelopment in both physiological and pathological conditions. We characterized EV content, release, and uptake in 3D human cerebral organoids at different time points and in 2D cell cultures (neuronal progenitor cells-NPCs -, neurons and astrocytes).

We found that EVs collected from COs and NPCs, neurons, and astrocytes, showed changes in protein contents according to their developmental stage and cell types.

Moreover, we characterized EVs proteome and function of COs generated from EPM1 patients (refers to chapter 4), and in COs carrying a mutation of LGAL3BP described in individual with neurological disesase (see chapter 5). We found a decrease in number of proteins and alteration of proteins associated with cell-cell communication, cell fate decision, axon guidance and extracellular matrix composition.

This work shed new light in non-cell autonomous mechanisms in brain development and neurodevelopmental disorders.

5.1 Developmental characterization of vesicles in COs

In this work, we characterized vesicle composition using a 3D model of human brain development: cerebral organoids (COs). We isolated intracellular vesicles (IVs) from the cellular fraction and extracellular vesicles (EVs) from the secreted fraction by ultracentrifugation (Ferrara et al., 2009) and immuno-electron microscopy with transmembrane (CD81) and intraluminal (LGALS3) markers (Figure 5-1, A).

We, therefore, performed a systematic proteomic analysis of IVs and EVs at different developmental stages, from 15 to 360 days in culture. We detected a total of 7266 proteins, with varying complexity in IVs (7088) and EVs (3791).

At early stages of development, EVs originated mostly from neural progenitor cells (NPCs) while later they derived from a mixed population of NPCs, neurons, and glial cells.

Interestingly, the unique protein content for each developmental stage (37.72%) showed enrichment of GO terms associated to cell-cycle and RNA-splicing (d15), intracellular transport and mitochondrial membrane (d40), ribosome biogenesis and mitochondrion (d200) and locomotion, secretion, neuron part and cell motility (d360) (Figure 5-1, B and C).

We identified that 6.8% of EV proteins was shared across all developmental stages, including those involved in cell junctions and secretory functions (Figure 5-1, D).

This pronounced difference across development suggests unique EV signatures and complexity. Development-associated EV proteins were identified but did not follow their cellular expression strictly.

Markers for apical radial glia, like VIM and FABP7, differed in abundance, with a peak of expression at d100 (VIM) and d200 (FABP7). Typical markers for basal radial glia, were enriched at different stages in EVs with PTPRZ1 peaking at d100 and GNG5 at d200. Early neuronal markers were detected in EVs and while DCX peaked at d15, RELN was strongly enriched at d40. Mature neuronal markers also exhibited distinctive patterns; TUBB3 was persistently secreted in EVs while MAP2 only after 200 days (Figure 5-1, E).

We next examined typical EV markers and identified unique developmental expression trajectories suggesting EV heterogeneity (Figure 5-1, F).

As EVs modulate extracellular matrix (ECM) composition, we investigated the presence of ECM components. While some components (COL3A, COL4A and LGALS3BP) were

constantly detected, other ECM proteins changed (VCAN) or were absent in EVs at early stages (HAPLN1, LGALS3 and COL4A1) but expressed in IVs, suggesting a regulated secretion and an increased complexity of the ECM at late stages (Figure 5-1, G).

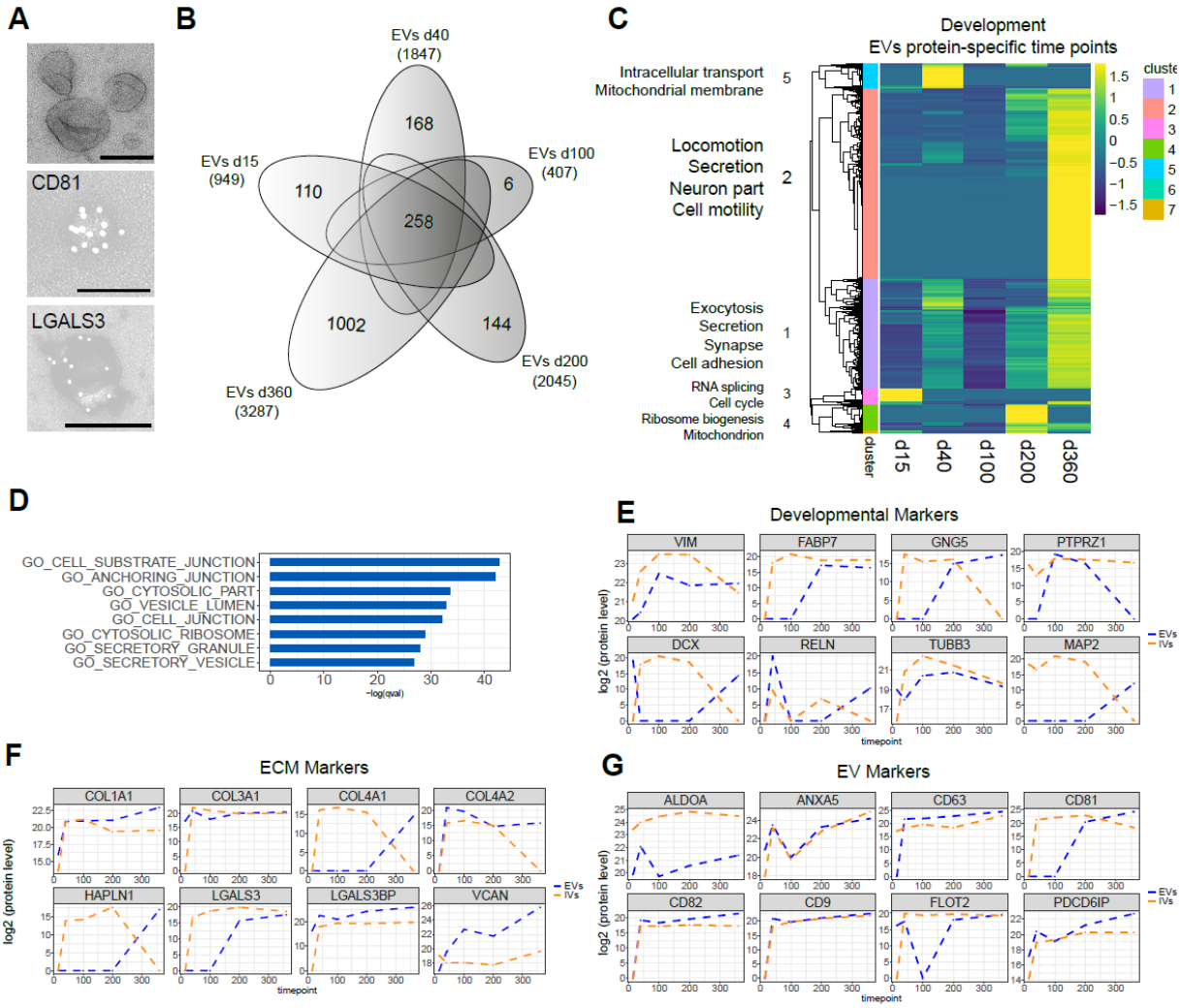

Figure 5-1: Developmental, cell-type-specific characterization of vesicles

A. Transmembrane (CD81) and intraluminal (LGALS3) marker immuno-electron micrographs in EVs collected from COs conditioned media. Scale bar:100nm.

B. Venn diagram of EV proteins at all timepoints.

C. Heatmap showing hierarchical clusters of EV proteins at different timepoints. GO enrichments of clusters are displayed.

E,F,G. Temporal trajectories of developmental, EV and ECM markers (as indicated in the panel) in IVs (orange) and EVs (blue).

5.2 Regional characterization of EVs in COs

Next, we characterized EVs collected from dorsally- and ventrally-patterned forebrain COs (dCOs and vCOs) (Bagley et al., 2017b; Birey et al., 2017) to investigate region specific difference in EV content. With this model, we aimed to address difference in EV content that could regulate crosstalk between cortical cell types (including RGs, IP and excitatory neurons); and between ventral cell types (including ventral progenitors and interneuron precursors).

Interestingly, we noticed that EVs from dorsal (dEVs) and ventral COs (vEVs) shared 62,5% of the total proteins. Moreover, vEVs only had a small fraction of unique proteins (2.5%) while dEVs contained 35% of unique proteins (Figure 5-2, A).

These results suggest a greater complexity in dorsal EVs and perhaps that dorsal cells make a more extensive use of EV-mediated communication.

We identified proteins involved in cell adhesion and motility proteins enriched in dEVs; while RNA, miRNA and chromatin binding were the main functions for vEV proteins, suggesting that in the cortex EVs mediate mostly adhesion and motility, while in the ventral forebrain they regulate gene expression (Figure 5-2, B, C, D and E).

Amongst the unique proteins, typical patterning-related proteins were expressed either in dEVs (WNT3) or vEVs (SHH). Moreover, we identified an essential molecular motor (KIF1A) and other proteins associated to neurodevelopmental disorders that were specific or enriched in dEVs or vEVs. Specifically, TUBB6 and KIF1A were detected only in vEVs; while CHD8 and WNT3 were present only in vEVs. RELN is detected in both dorsal and ventral EV, with a higher level in dEVs, probably due to its role in interneuron recruitment in the cerebral cortex (Thom et al., 2004) (Figure 5-2, C).

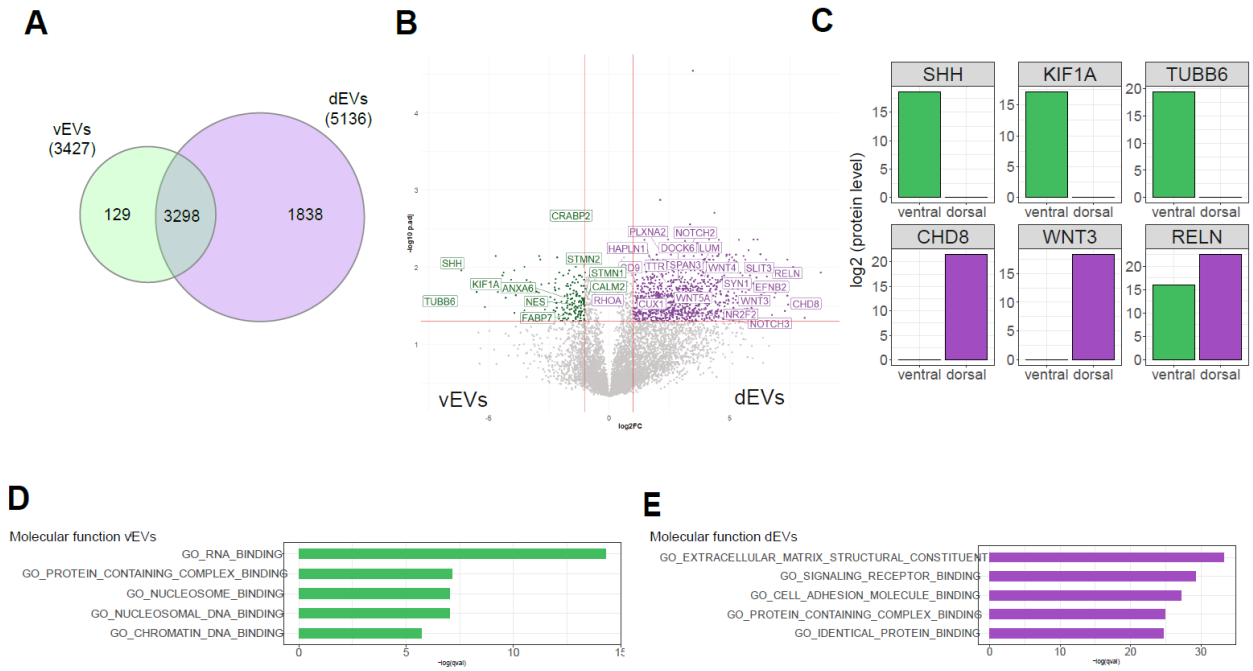

Figure 5-2 Regional characterization of EVs in COs

A. Venn diagram of vCO and dCO EV proteins (common proteins in bold).
B. Volcano plot of protein level of vCO and dCO EVs, plotting the negative log10 q-values (FDR) of all proteins against their log2 fold change (dCOs vs vCOs). Significantly expressed proteins (q-value < 0.05) are labelled (dCOs, purple and vCOs, green). GO enrichments are shown.
C. Brain-region-specific marker expression in vCO and dCO EVs.
D, E. GO enrichments for proteins significantly expressed in EVs secreted by vCOs (green) and by dCOs (purple).

5.3 Neurological disorders-associated proteins are secreted via EVs

Recent proofs suggest that changes in the extracellular environment might lead to brain disorders (Amin and Borrell, 2020; Mazurskyy and Howitt, 2021).

To prove this point, we looked at proteins associated with neurological disorders, particularly cortical malformation (CM), epilepsy, Autism Spectrum Disorders (ASD) and Schizophrenia (SCZ) obtained from DisGenet (https://www.disgenet.org/) if they were expressed in IV and EV. Interestingly, we found that ca 45% of ASD-, epilepsy- and schizophrenia-associated proteins were detected in vesicles collected from control organoids, while CM-associated proteins showed higher percentage (50%) (Figure 5-3, A).

We then looked at the percentage of proteins associated with ASD, epilepsy, CM and SCZ expressed in EVs at each time point. Overall, they show similar trajectories, with pics of higher enrichment of proteins at 40 and 360 days, suggested a neuron/late-enrichment in disease secreted proteins (Figure 5-3, B, C, D and E).

Moreover, we identified proteins specific for each disease with different expression in EVs along the developmental trajectory, suggesting that their secretion is regulating over time. These results showed that proteins associated with brain disease are secreted via EVs, which could suggest an important role of vesicles in the biology of neurological disorders.

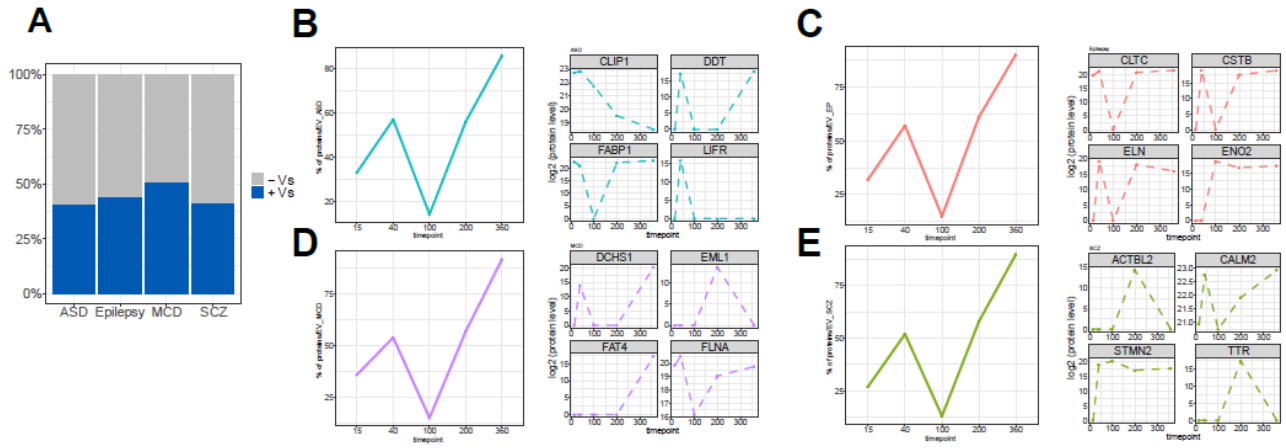

Figure 5-3: Impact of EVs in neurodevelopmental disorders

A. Bar plot indicating the proportion of proteins found in CO EVs associated with neurodevelopmental disorders (DisGeNET). B,C,D,E. Proportion of disease-associated proteins found in CO EVs during development and developmental trajectory of selected proteins associated with ASD (B), epilepsy (C), CM (D) and schizophrenia (E) (as shown in the panel).

5.3.1 Different EV content in EPM1 COs

In chapter 3, I showed that one of the molecular mechanisms associated with EPM1 epilepsy is mediated by the secretion of CSTB, moreover we identified that EVs collected from EPM1 COs can alter the gene expression of neuronal progenitor cells, dysregulating genes associating with neurogenesis and cell proliferation.

First, we confirmed that CSTB is secreted in control COs over time, then, we characterized the content of EVs derived from EPM1 vCOs and dCOs (Figure 5-4, A).

To this end, we collected EPM1-vCOs-EVs and EPM1-dCO-EVs and confirmed the strong decrease of proteins in both EPM1-vEVs and EPM1-dEVs (~50%) (Figure 5-4, B and C).

Interestingly, while vEVs and dEVs shared 62.5% of the proteins and only 2.5% was unique for vEVs and 35% for dEVs, EPM1-EVs showed the opposite trend, with 65.5% shared content, 31.5% unique for EPM1-vEVs and only 3% unique for EPM1-dEVs. Particularly, we found proteins associated with RNA metabolic process or cell adhesion dysregulated in EPM1-vEVs, suggesting a role in CSTB in these processes in ventral forebrain crosstalk. In EPM1-dEVs, instead, signaling by ROBO receptor or metabolism of lipid were differentially regulated, indicating a function of CSTB in lipogenesis and axon guidance in dorsal forebrain. Interestingly, both ventral and dorsal EPM1 EVs differentially expressed proteins involved in ECM organization, suggesting a common process altered in both dorsal and ventral forebrain in EPM1(Figure 5-4, D and E). Moreover, we identified 226 proteins, whose genes' mutations are associated to epilepsy, that were altered in the EPM1-EVs, confirming the role of EVs in neurological disorders, specifically in epilepsy (Figure 5-4, F).

Altogether, these data suggest that less proteins were loaded into EPM1-EVs, and while vEVs acquired a stronger signaling function (maybe pathological), dEVs were less rich in content (maybe less functional). These results propose a role of CSTB as signaling molecule regulating the ECM composition and mediating proper packaging of EVs during development.

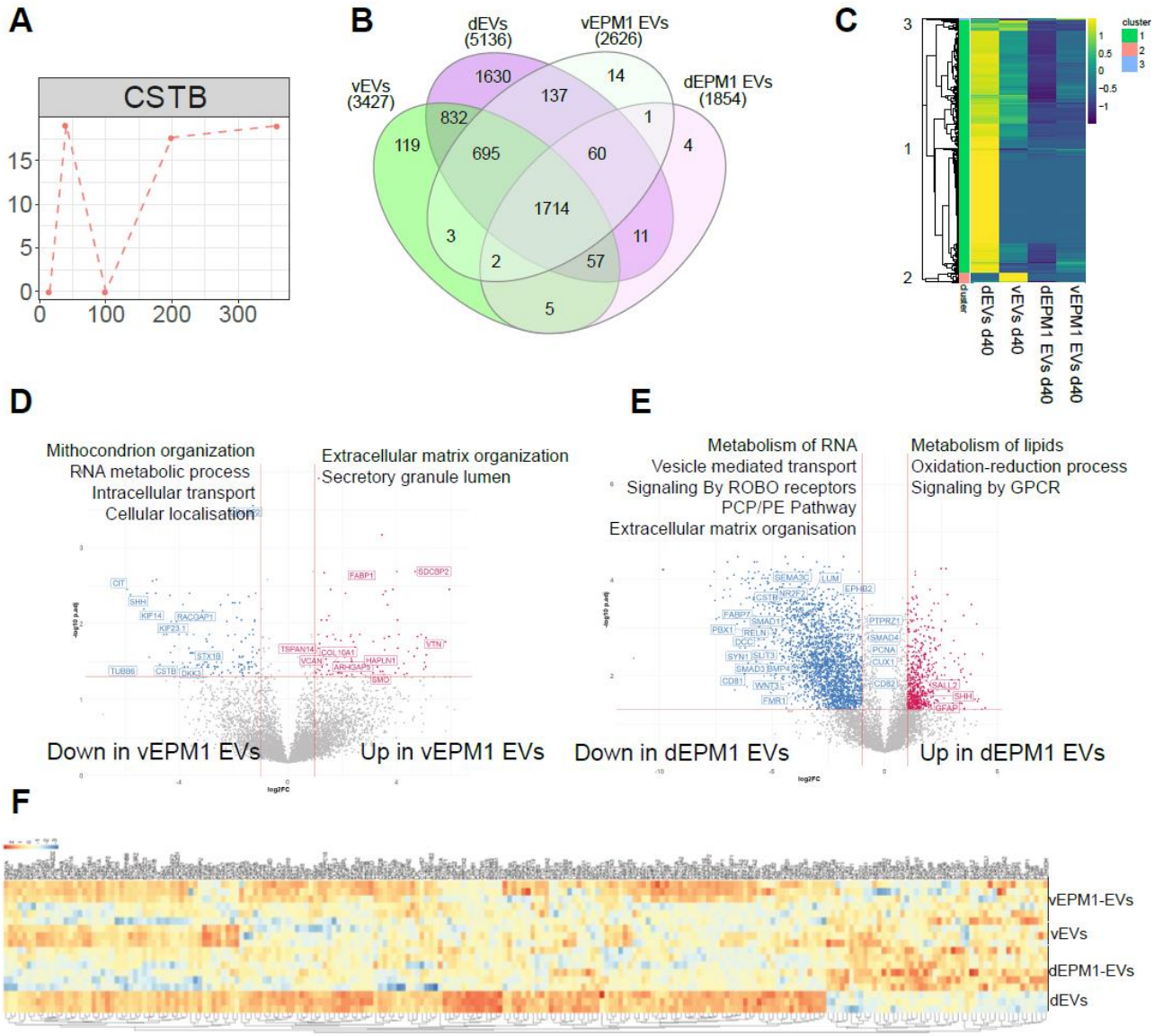

Figure 5-4: Different EV content in EPM1 COs

A. Developmental trajectory of CSTB in EVs.
B. Venn diagram of vCO, dCO, EPM1-vCO and EPM1-dCO EV proteins.
C. Heatmap showing hierarchical clusters of vCO, dCO, EPM1-vCO and EPM1-dCO EV proteins.
D. Volcano plot of protein level of vCO and EPM1-vCO EVs, plotting the negative log10 q-values (FDR) of all proteins against their log2 fold change (EPM1-vCO EVs vs vCOs EVs). Significantly expressed proteins (q-value < 0.05) are labelled. GO enrichments are shown.
E. Volcano plot of protein level of dCO and EPM1-dCO EVs, plotting the negative log10 q-values (FDR) of all proteins against their log2 fold change (EPM1-dCO EVs vs vCOs EVs).
F. Heatmap showing the 226 vCO, dCO, EPM1-vCO and EPM1-dCO EV proteins associated with epilepsy.

5.3.2 Different EV content in E370K COs

In chapter 5, I focused on a variation in the gene LGALS3BP (E370K) characterized in individual with cortical malformation and psychiatric disorders in interneuron recruitment, migration and specification. Moreover, we showed that LGALS3BP has short as well as long distance regulation in cell fate decision and axon guidance mediated via EVs.

To get more insight in the EV-mediated function of LGALS3BP, we characterized the EV content from ventral and dorsal E370K-EVs (E370K-vEVs and E370K-dEVs).

We identified more than 5000 proteins (Figure 5-5, A, B and C), and found a lower number of proteins in both ventral and dorsal E370K-EVs.

Moreover, we confirmed that LGALS3BP is secreted in both dorsal and ventral EVs, however its level of expression is lower in mutant EVs (Figure 5-5, D).

We then performed DE analysis in EVs from dCOs and vCOs. We found that proteins involved in axon guidance and neuronal migration, such as RELN, EPHB4, EPHB2, EIF4B are dysregulated in mutant dEVs. This dysregulation could be responsible for the altered migration and recruitment of INs found in dvCAs. We also found alterations in proteins of the ECM - COL4A3BP, COL1A1, LGALS3, VCAN- and transcription factors – TTYH1, CUX1, PTPRZ1- that indicate a role of EVs in ECM composition and activation/repression of gene expression mediated by E370K-dEVs (Figure 5-5, E).

Moreover, in EVs secreted by E370K-vCOs proteins associated with cell migration and motility –SEMA3G, EPHA2, EPHB2, PLXNA1 SLIT1, KIF1A - are differentially regulated. E370K-vCOs also dysregulate protein of the ECM, including HAPLN1, LUM, VCAN. Interestingly, proteins of NOTCH, SHH, and WNT pathways -SHH, DVL2, NOTCH2-, known as essential for the proper establishment of the dorso-ventral patterning, are altered in vEVs (Figure 5-5, F).

Altogether, these findings suggest that E370K dCOs and vCOs might have alteration in the secretion of proteins associated cellular migration, differentiation, regionalization, acting as short- and long-distance extrinsic factors.

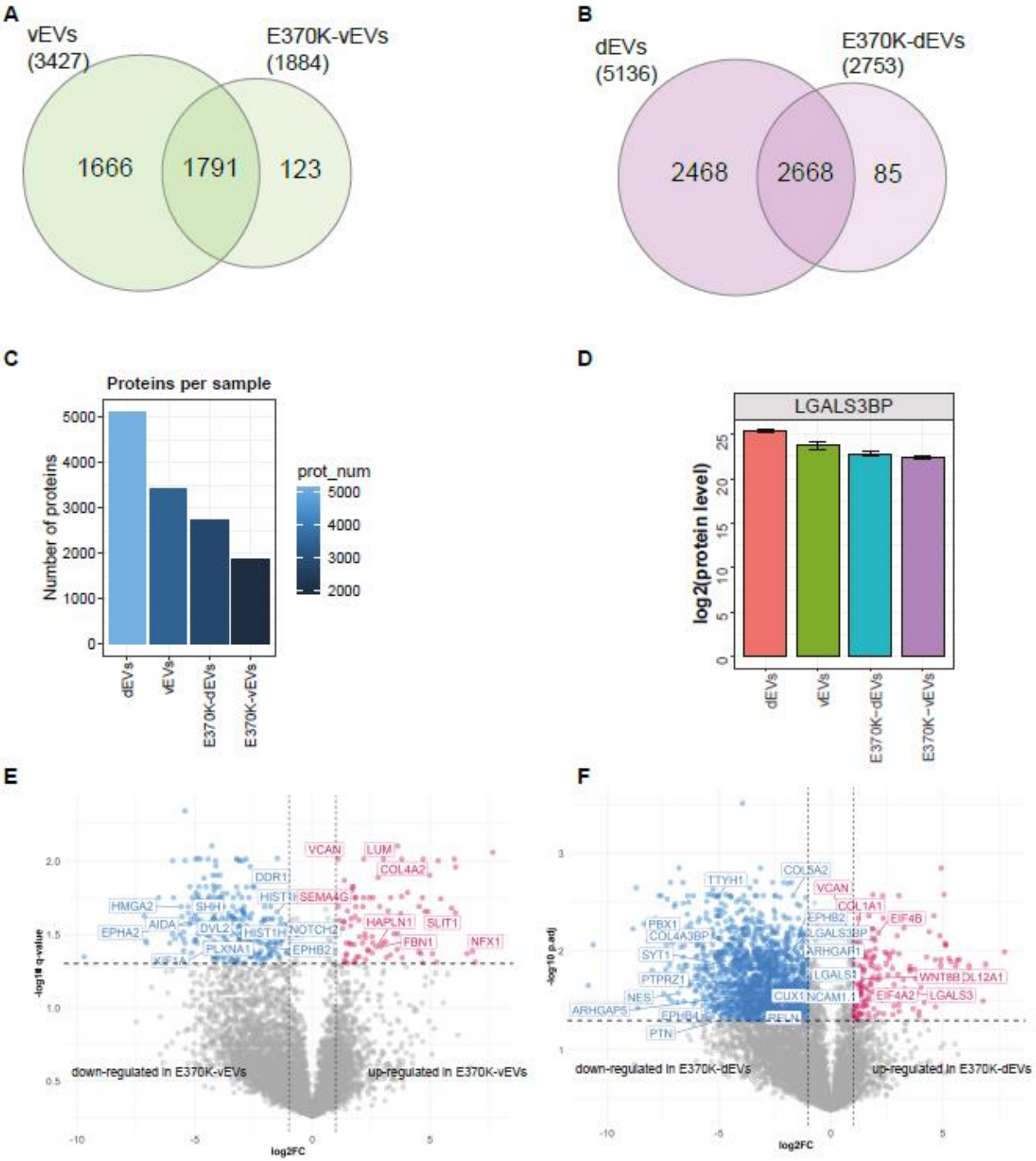

Figure 5-5: Different EV content in E370K COs

A,B. Venn diagram showing number of proteins detected in vCO (green), E370K-vCO (green), dCO (purple) E370K-dCO EVs (purple).
C. Bar plot showing the number of proteins detected in dEVs, vEVs, E370K-dEVs and E370K-vEVs.
D. Bar plot of LGALS3BP protein level detected in dEVs, vEVs, E370K-dEVs and E370K-vEVs.
E. Volcano plot of protein level of dCO and E370K-dCO IVs, plotting the negative log10 q-values (FDR) of all proteins against their log2 fold change (E370K-dCO vs vCOs). Significantly expressed proteins (q-value < 0.05) are labelled. GO enrichments are shown.
F. Volcano plot of protein level of vCO and E370K-vCO EVs, plotting the negative log10 q-values (FDR) of all proteins against their log2 fold change (E370K-vCO EVs vs vCOs). Significantly expressed proteins (q-value < 0.05) are labelled. GO enrichments are shown. Figure and figure legend adapted from Pipicelli et al., 2022"

Moreover, it is known that changes in the ECM composition can lead to neurological disorders. For example, altered composition of collagens mediated by EVs in the extracellular space might alter ECM structure (Amin and Borrell, 2020).

Since we identified proteins associated with neurological disorders in EVs, we sought to analyze the correlation between E370K-EVs and brain disease. To this end, we looked at proteins whose genes are associated with epilepsy (EP), autism spectrum disorder (ASD), and cortical malformations (CMs) and identified several proteins that were altered in E370K-EVs, suggesting a role of EVs in these pathologies (Figure 5-6, A, B and C).

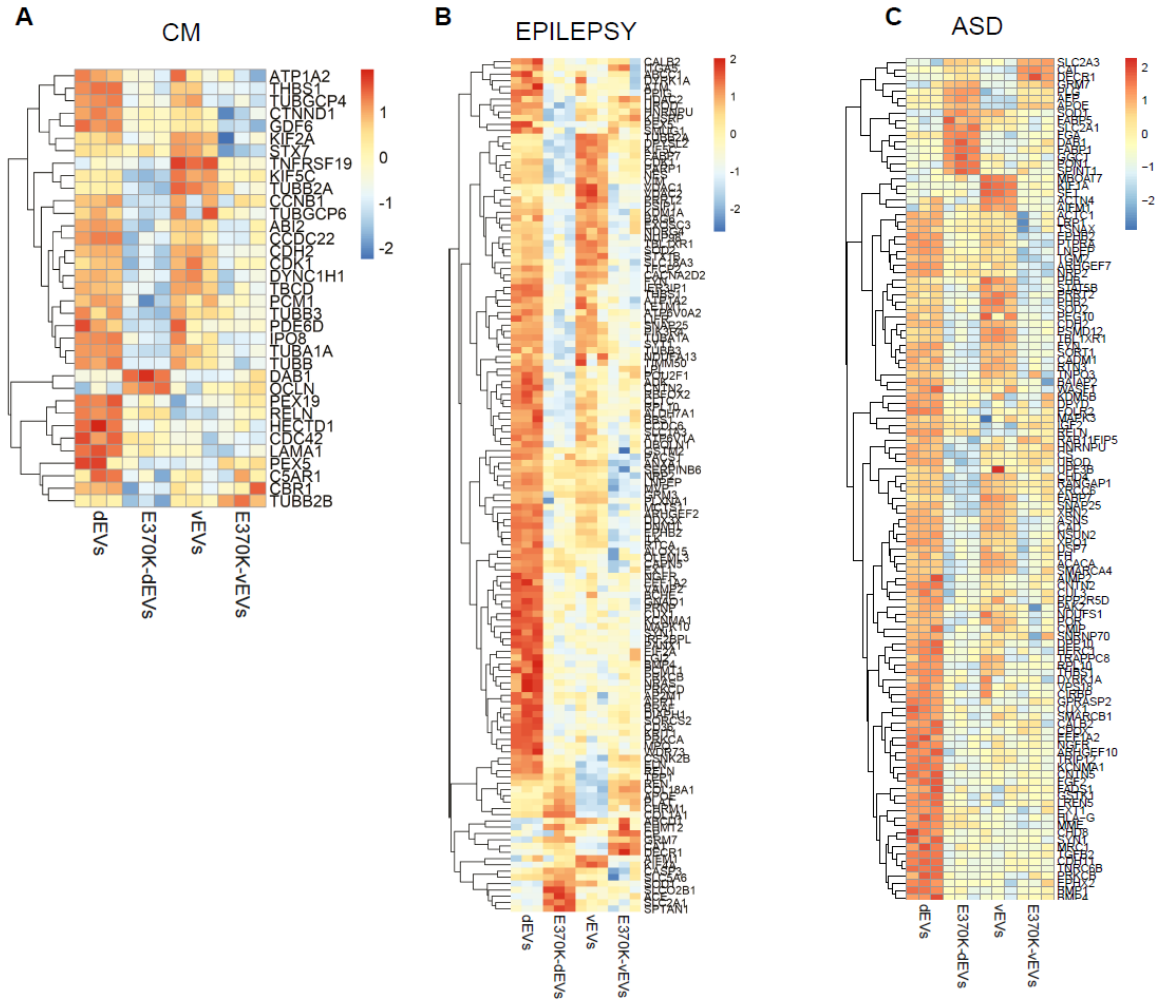

Figure 5-6 Different EV content in E370K COs (II)

A, B, C. Heatmaps of DE protein in E370K-dEVs and E370K-vEVs associated with CM (A), epilepsy (B) and ASD (C). Figure adapted from Pipicelli et al., 2022

5.4 Cell-type-specific characterization and uptake of EVs

We characterized EV content for COs (cerebral, ventral and dorsal), a 3D in vitro model that resemble the human ventral and dorsal forebrain development and we identified differences in EV content during development and in different brain regions. Since organoids are characterized by the presence of many cell types which could contribute to the heterogeneity observe in EV, we analyzed EV content in NPCs, neurons and astrocytes in a 2D monolayer in order to dissect cell-type specificity in EVs (Figure 5-7 , A).

The three populations of cells grown in 2D share less than 8% of the total proteins. EVs from NPCs (pEVs) were the least complex (in total protein number) and less than 1% of the proteins was unique for NPCs (cluster 8) (Figure 5-7, B and C).

The three populations of cells grown in 2D share less than 8% of the total proteins. Interestingly, EVs from NPCs (pEVs) were the least complex (in total protein number) and less than 1% of the proteins was unique for NPCs (cluster 8). On the contrary, neurons exhibited the most unique proteins in EVs (nEVs, >50% of total proteins found in 2D) suggesting that neurons make extensive use of EVs for cellular crosstalk, as showed previously (Ferrara et al., 2009). We found that the 17% of the unique proteins found in astrocytes (aEVs) are associate with RNA catabolic process and ribonucleoprotein complex (cluster 4) (Figure 5-7, C).

We confirmed that EVs collected from 2D cultures express standard positive EV markers, such as CD63, CD81, CD82, CD9, TSG101 and PDCD6IP, while negative (CYC1 and GOLGA2) markers were undetectable (Figure 5-7, D). Moreover, in line with the hypothesis of cell-type-specific EVs, EV marker expression varied among cell-types; pEVs lacked CD9, CD81 and CD82 (Figure 5-7, D).

Therefore, we performed immunohistochemical analysis of EV markers in NPCs, young neurons (4 weeks in culture), mature neurons (10 weeks in culture) and astrocytes in 2D. The analysis confirmed the ubiquitous expression of CD63 and PDCD6IP. CD81 was found in NPCs even though less immunoreactivity was observed compared to nEVs and aEVs. Interestingly, CD82+ and CD9+ EVs were the least abundant overall, limited to a small number of NPCs and astrocytes while absent in neurons (Figure 5-7, E).

Together, our data show that varying combinations and numbers of EV markers are present in different cell-types suggesting cell-specific types of EVs. Moreover, cell-to-cell contact increases EV heterogeneity.

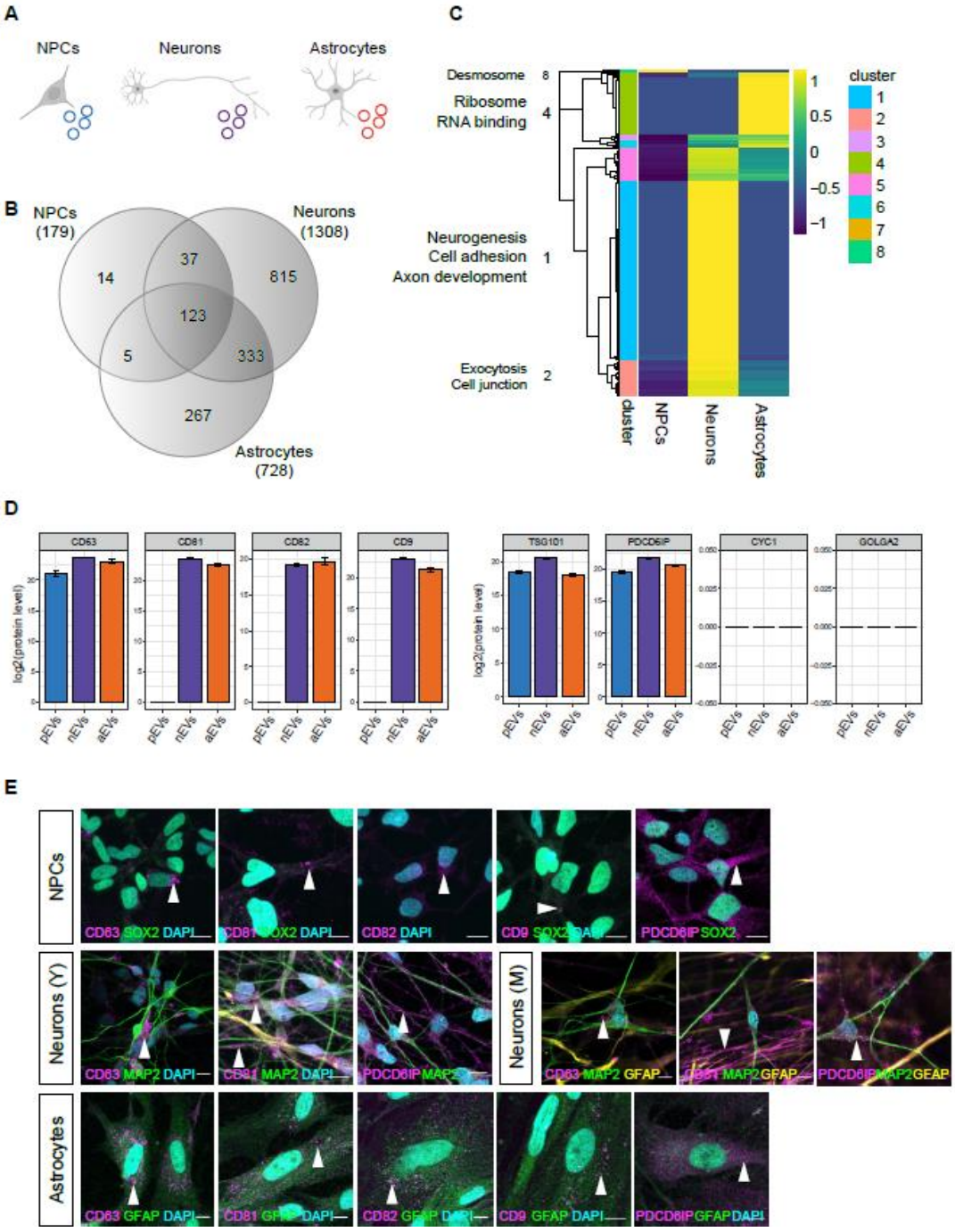

Figure 5-7: Cell-type-specific characterization and uptake of EVs

A. Schematic of EVs secreted by 2D cell populations: NPCs (neural progenitor cells, blue), neurons (purple) and astrocytes (orange). Created with BioRender.com.
B. Venn diagram of proteins in NPC, neuron, and astrocyte EVs.
C. Heatmap showing hierarchical clusters of proteins in NPC, neuron, and astrocyte EVs. GO enrichments of clusters are displayed.
D. Bar plots showing positive and negative EV markers' expression in NPC, neuron, and astrocyte EVs. Data are represented as mean ± SD of technical replicates.
E. CD63, CD81, CD9, PDCD6IP immunostaining in NPCs (SOX2+, green), young neurons (MAP2+, green), mature neurons (MAP2+, green and GFAP+, yellow) and astrocytes (GFAP+, green) (arrow heads). DAPI, cyan. Scale bar: 10 µm. Courtesy of Andrea Forero Echeverry.

We next looked at how specific cell types uptake EVs from NPCs, neurons and astrocytes to assess if the crosstalk between different cell types is regulated. To this end, we labeled EVs from three different cell populations with RFP (NPCs, neurons and astrocytes).

We showed that, using a microfluidic chamber, RFP-labeled NPCs released RFP+EVs travelled to MAP2+ neurons. Based on this observation, we applied RFP+pEVs directly to NPCs, neurons (young and mature) and astrocytes, and observed that the uptake varies between cell-types.

Surprisingly, not all NPCs were positive for RFP+pEVs, suggesting that pEVs were selectively taken up by recipient cells. Nevertheless, EVs reached cytoplasm and nucleus of NPCs. On the contrary, all astrocytes appeared to internalize both pEVs and nEVs and distribute them uniformly in the cytoplasm.We noticed that in neurons, RFP+pEVs and aEVs remained primarily docked on the cell membrane of the soma and dendrites, suggesting receptor-mediated signaling.

These data indicate that EVs instruct receiving cells, which, in turn, specifically determine the localization in different cellular compartments.

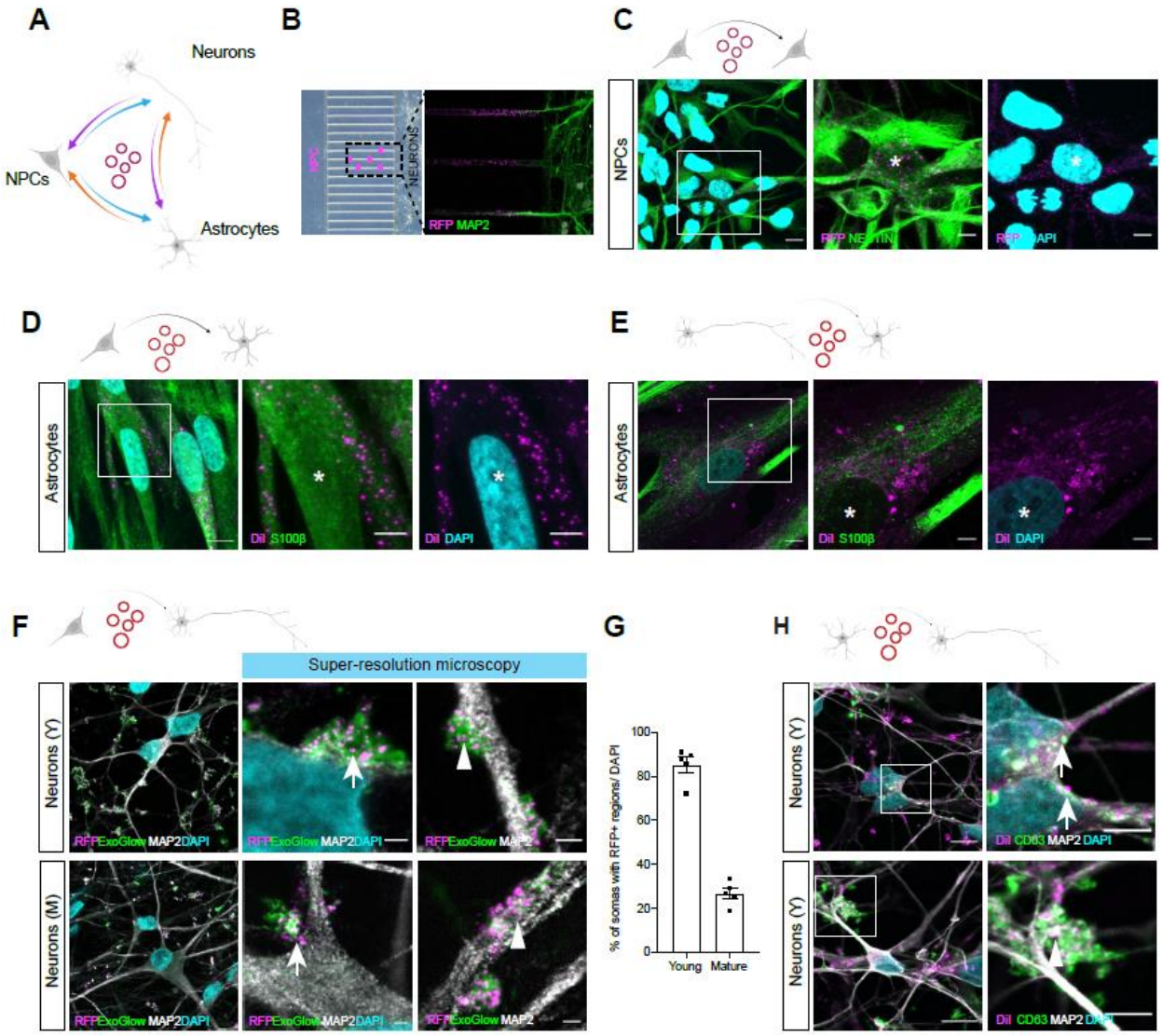

Figure 5-8 Cell-type-specific characterization and uptake of EVs (II)

A. Schematic of the experimental setup of EV exchange between different cell-types.
B. Microfluidic chamber showing the stream of EVs (RFP+) secreted by NPCs traveling to neurons (MAP2+).
C, D, E. Immunostaining indicating uptake of NPC EVs (RFP+) by NPCs (Nestin+) (C) and astrocytes (S100b+) (D), and uptake of neuron EVs (DiI+) € by astrocytes (S100b+). Asterisks indicate EV receiving cells. DAPI, cyan. Scale bars: full image, 10 µm; close-up 5 µm.
D. Immunostaining indicating uptake of NPCs-derived EVs (RFP+, ExoGlow, green) by young (Y, top) and mature (M, bottom) neurons (MAP2+). Super-resolution microscopy images (right) show EV localization on cell soma (arrows) and dendrites (arrow heads). DAPI, cyan. Scale bars: full image, 10 µm; close-up 1 µm.
E. Quantification of somas with RFP+ regions in young and mature neurons in (F). Data are represented as mean and ± SEM. Every dot refers to a field of view.
F. Immunostaining indicating uptake of astrocyte EVs (DiI+) by neurons (MAP2+). Scale bars: full image, 10 µm; close-up 5 µm. Courtesy of Andrea Forero Echeverry. Illustrations in A, C, D, E,F,H were created with BioRender.com.

5.5 Cell-type specific EVs are less heterogenous than COs EVs

To better dissect the protein content of EVs from NPCs, neurons and astrocytes, we compared the number of detected proteins in 2D culture with the one detected in 3D COs (Figure 5-9, A, B and C). Specifically, since young COs (15 days old) mostly present NPCs, we compared EV proteome from 15 days old COs with EV proteome from NPCs. Also, since mature neurons and astrocytes are present in older organoids, we compared EV proteome of neurons and astrocytes with EV proteome from 360 days old COs.

As expected, the total number of EV proteins from 2D cultures was strongly decreased compared to 3D COs suggesting a lower complexity in 2D. Moreover, when comparing EVs from NPCs in 2D and 3D (d15 COs) or mature neurons/astrocytes and 3D (d360 COs), the number of proteins varied greatly suggesting that cell-cell contact contributes to EV secretion as indicated from the enriched GO terms (Figure 5-9, A, B and C).

Interestingly, processes such as exocytosis, neuron projection and anchoring junctions were shared between different cell types and CO EV, suggesting common mechanisms regulated by EVs.

Since we demonstrated the relation between proteins associated with neurological disorders and vesicles in COs, we also compared the same proteins (chapter 5.3) with protein secreted by intracellular and extracellular vesicles collected from NPCs, neurons and astrocytes. Interestingly we found that circa %25 of proteins associated with ASD, epilepsy and SCZ, and 30% of protein associated with CM are present in vesicle from NPCs. Vesicles from neurons present the highest % of protein associated with brain disease (between 40% and 60%), while only about 10% of proteins associated with ASD, epilepsy, CM and SCZ were found in astrocytes (Figure 5-9, D, E and F). This data suggests an enrichment of secreted protein associated with neurological disorders in neurons.

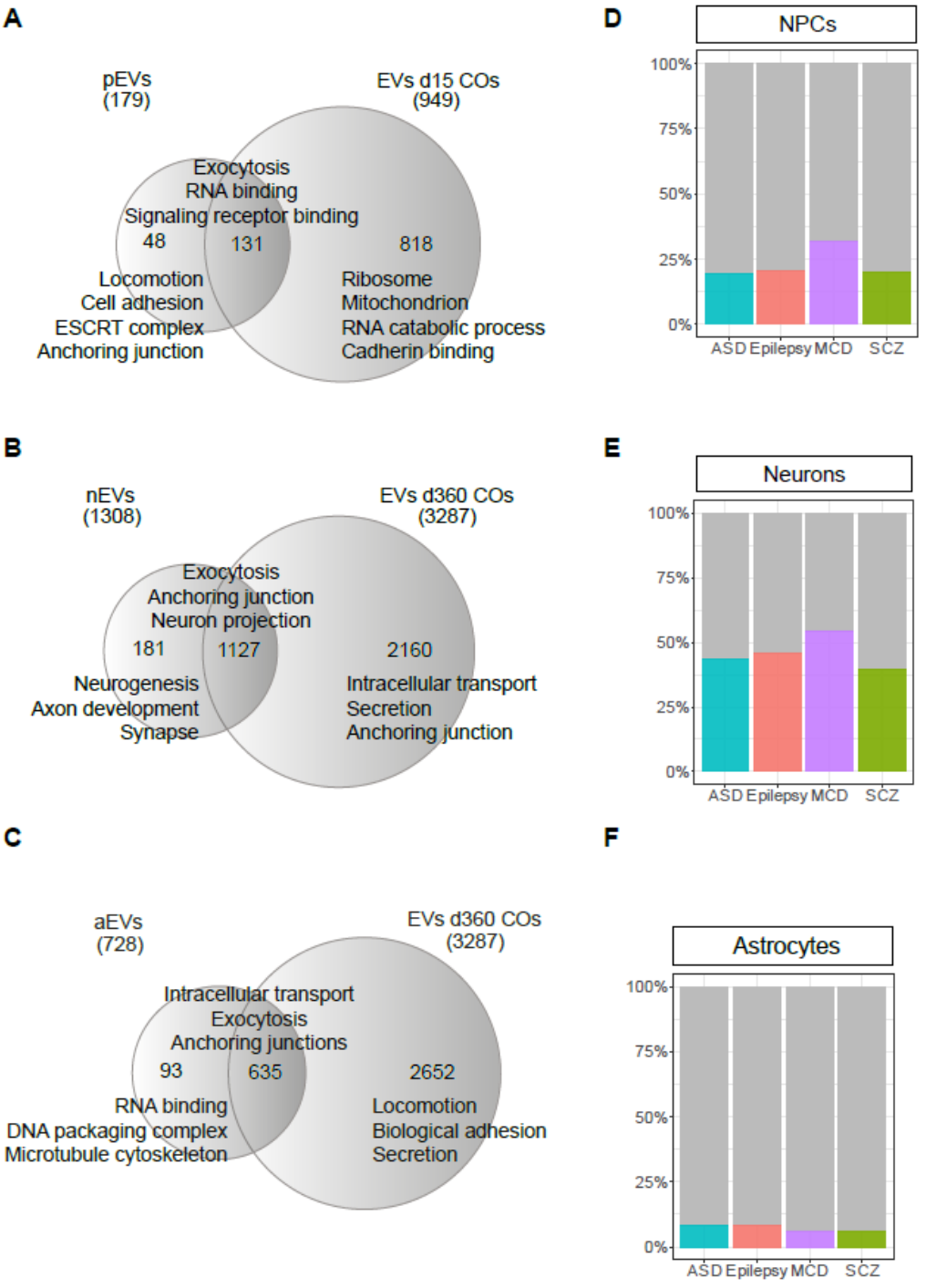

Figure 5-9: Cell-type specific EVs are less heterogenous than COs EVs

A,B,C: Venn diagrams indicating the number of unique and common proteins secreted by NPCs and 15d COs, (A) neurons and 360d COs and (B) astrocytes and 360d COs (C). Functional annotations of GO enrichments of each protein group are shown.
D,E,F: Bar plot indicating the proportion of proteins associated with neurodevelopmental disorders found in CO EVs with proteins secreted in EVs from NPCs (D), neurons (E) and astrocytes (F) (DisGeneNet).

6 Discussion

6.1 Extrinsic factors in brain development and disease

The study of the development of the human brain is extremely complex. Many mechanisms and processes are involved, and the limited availability of human tissue makes the research even harder. In this thesis, I proposed new mechanisms that shed light in the understanding of neurodevelopment, reporting three research studies performed in both animal and human model systems.

Particularly, I demonstrated the importance of extracellular, extrinsic regulation in neurodevelopment and in neurological disorders. I showed how two secreted proteins mutated in epilepsy (CSTB and LGALS3BP) share some common non-cell autonomous regulatory mechanisms in cell proliferation, neurogenesis, cell fate decision and neuronal migration.

As already described in the introduction, neurological disorders have an extremely high degree of complexity. This thesis shed new light on the biology of neurological disorders, proposing non-cell autonomous regulation at the basis of epilepsy. I showed that 2 proteins (CSTB and LGALS3BP) of the extracellular matrix (ECM) are involved in neurological disorders, confirming the fact that the composition and organization of the ECM is crucial for brain development.

6.1.1 ECM: a key factor in neurodevelopment and disease

The ECM functions as a support for brain cells by regulating tissue shape, and, therefore, neocortex morphogenesis, during development. Defects in morphogenesis can lead to cortical malformations, including lissencephaly or changes in the gyrification pattern of the brain (Amin and Borrell, 2020; Long and Huttner, 2019; Long et al., 2018).

However, the ECM is also involved in proliferation, differentiation, cell adhesion and motility, neuronal plasticity and gyrification. Specifically, in early brain development ECM regulates proliferation. The ECM components known to have functions in proliferation are proteoglycans, laminins, and integrins. Proteoglycans are important for the maintenance of the basement membrane in the neuroepithelium of the mouse cortex. Laminins are also implicated in regulating the basement membrane; however, it has been shown that they can regulate neural proliferation and differentiation, interacting with their receptors, the integrins. Integrins,

expressed on the cell surface, are involved in cell-matrix adhesion and they link extracellular and intracellular space by activating different pathways, including proliferation and differentiation (Long and Huttner, 2019; Wojcik-Stanaszek et al., 2011).

The ECM is also crucial in regulating neuronal migration, both radial and tangential. One of the ECM components regulating neuronal migration is Reelin. This glycoprotein is secreted by Cajal-Retzius cells in the marginal zone of the cortex, and it is associated with migratory regulation via activating cellular integrins or apolipoproteins.

However, the role of the ECM is important also because of the proteins and molecules that are released in it. Many molecules, including morphogens and growth factors, regulate cell differentiation, proliferation, and migration during brain development and they are transported by extracellular vesicles.

6.1.2 Extracellular vesicles have a role in neurodevelopment and disease

In this thesis, I propose a novel role of another type of extrinsic factors – extracellular vesicles, EVs – in neurodevelopment and disease. EVs are involved in intercellular communication, and they are secreted by all cells. They have been identified in many body fluids, including plasma and cerebrospinal fluid (CSF). However, their role in neurodevelopment is still poorly understood. It has been shown that EVs can regulate proliferation and development of neural circuits in vitro and in vivo (Sharma et al., 2019).

In this thesis, I showed that many ECM components implicated in neuronal migration and in interneuron recruitment (Long and Huttner, 2019; Miyata and Kitagawa, 2017) are transported by EVs, including Reelin (RELN) or versican (VCAN). Interestingly, they showed different protein levels over time and in intracellular and extracellular vesicles. Specifically, RELN showed peak of secretion in EVs at 40 days, while its level in IVs is lower compared to EVs, suggesting an active secretion of this protein. Interestingly, RELN, secreted by Cajal-Retzius cells in the cortex, is not detected in EVs collected from ventral COs, but only from cerebral/dorsal organoids, suggesting a regional and developmental regulation of the secretion of RELN. Moreover, VCAN showed high proteomic level in EVs compared to IVs, with a peak at 100 days and it has been detected in both ventral and dorsal EVs, suggesting a more general function in the developing brain.

Many semaphorins, plexins and Ephrin/Eph were also identified in regionally patterned EVs, indicating a regulation of neuronal migration also via attractive/repulsive cues mediated by EVs. Semaphorins interact with ECM proteoglycans or with their receptors, the plexins,

regulating axonal growth during development. They can act both as attractants and repellents for interneuron migration (Lepiemme et al., 2022; Soleman et al., 2013; Villar-Cerviño et al., 2013). Generally, Ephrin/Eph signaling is known to required cell-cell contact, however, we found that these proteins are also transferred by EVs, suggesting a role of EVs in long distance signaling. Interestingly it has been shown that EVs carrying EphB2 lead to neuronal axon repulsion activating EphrinB1 signaling (Gong et al., 2016; Zhao et al., 2018).Furthermore, the Ephrin/ Eph receptors signaling is involved in guiding neuronal migration, specifically tangential migration of interneurons (Steinecke et al., 2014; Villar-Cerviño et al., 2013; Zimmer et al., 2008). These findings propose a novel mechanism of regulation of interneuron migration via EVs during brain development.

As it was already mentioned, ECM not only has a role in regulating cell motility, but also in morphogenesis and, therefore, in gyrification. Interestingly, the ECM components LUM, HAPLN1 and collagenase 1 (COL1A) are also secreted by EVs. These three proteins together induce local changes in tissue stiffness and folding of the cortical plate in human fetal brain tissue (Long et al., 2018). We found that COL1A1 and COL2A2 started to be secreted by EVs from day 40, while HAPLN1 from day 200 and LUM is expressed at day 15 and 360 in whole-brain /unpattern organoids. These data showed that, in whole-brain organoids, these proteins are expressed together at later time points, suggesting a regulation in morphogenesis in older organoids, and therefore at a later stage of development (Figure 6-1).

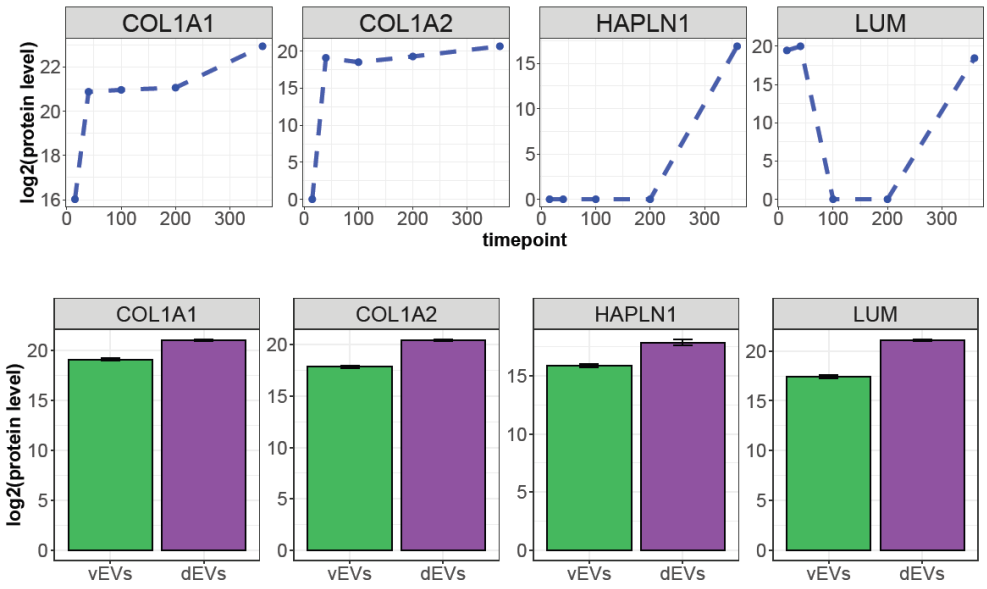

Figure 6-1: Collagen type I, HAPLN1 and LUM detection in EVs

Developmental trajectory (top) and barplot (bottom) showing the protein level of the ECM components COL1A1, COL1A2, HAPLN1 and LUM in EVs collected from unpattern and dorsal and ventral COs. dEVs: dorsal EVs; vEVs: ventral EVs.

However, they are all secreted by 40 days regionalized organoids and they are enriched in dorsal EVs, suggesting (i) that regionalized organoids might have more specific regulation of secretion and (ii), since these proteins are required for the folding of the neocortex, they show a higher protein level in dorsal EVs, probably acting locally (Figure 6-1).

Moreover, many developmental markers are secreted via EVs at different time points, suggesting that they can modulate developmental processes. Interestingly, the development-associated proteins identified in EVs did not match their cellular expression strictly and their trajectories did not always follow gene expression and cellular compartmentalization in intracellular vesicles, suggesting a regulation of their EV-associated secretion.

Interestingly, also transcription factors (TFs) are transported by EVs. Specifically, we identified 84 TFs in EVs collected from dCOs and 50 TFs in EVs collected from vCOs. Among these TFs, CUX1 and YAP1 were identified (Figure 6-2), suggesting a regulation of neurogenesis and proliferation mediated by EVs (Cubelos et al., 2010; Kodaka and Hata, 2015). Specifically, CUX1 was identified only in dEVs, indicating a role in the dorsal region, maybe with a short-distance effect. Indeed, CUX1 regulates branching, spine morphology and synapses of cortical upper layer neurons (Cubelos et al., 2010); while YAP1, involved in proliferation, is secreted by both dorsal and ventral COs.

EVs isolated from mouse retinal stem cells contain TFs such as Pax6, Hes1 and Sox2, suggesting that EVs play a role in retinal development (Zhou et al., 2021). Interestingly, these TFs are not present in EVs collected from human cerebral organoids, suggesting a region-, and probably also specie-, specific regulation of transport of TFs via EVs during development.

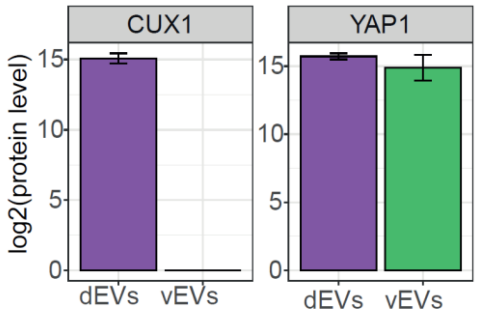

Figure 6-2: CUX1 and YAP1 detection in dorsal and ventral EVs

Barplot showing the protein level of TFs CUX1 and YAP1 in EVs collected from dorsal and ventral COs. dEVs: dorsal EVs; vEVs: ventral EVs.

We tested the function of EVs on neural progenitor cells, finding that the transcriptomic profile of the receiving cells changed after EV exposure, specifically of genes involved in cell fate decision and in extracellular space organization.

Furthermore, EVs carry a modest number of proteins associated with cortical malformations, such as FAT4, DCHS1 and FLNA, associated with periventricular heterotopia (Klaus et al.; Parrini et al., 2016) or EML1, associated with subcortical heterotopia (Hakanen et al., 2019). Moreover, proteins described to be mutated in neurological disorders, including ASD or epilepsy, have been detected in EVs. These findings open new perspectives for studying and understanding mechanisms underlying the biology of neurological diseases.

6.2 Non-cell autonomous function of CSTB in neurogenesis

6.2.1 CSTB and neurodevelopment

EPM1 patients present mutation in the *CSTB* gene. The pathology has been associated with neuronal apoptosis, activated by the activity of cathepsins, which is inhibited by CSTB. However, the role of CSTB in brain development is still poorly understood. Studies performed in the murine model of epilepsy revealed an increase of Cstb expression (D'Amato et al., 2000) and it has been shown that the *Cstb*-KO mouse model presents neuronal atrophy in the cortex, suggesting a role of Cstb in regulation of neuronal structures.

Other studies demonstrated that lack of Cstb results in oxidative damage and thus contributing to the phenotype (Lehtinen et al., 2009; Shannon et al., 2002; Žerovnik, 2019). EPM1 patients also show atrophic changes in the cerebral cortex and cerebellum, indicating that absence of CSTB affects brain cortical regions (Nigri et al., 2017). Considering the early clinical manifestation of the disease, we have hypothesized that CSTB might play an important role in early cortical development.

We demonstrated that, *in vivo*, the overexpression of *Cstb* in the developing cortex affects cell proliferation during cortical development, suggesting an explanation of the cellular mechanisms underlying the reduction in cortical thickness observed in EPM1 patients and in *Cstb*-KO mice (Danner et al., 2013; Koskenkorva et al., 2009). On the contrary overexpressing the pathological variant of CSTB, leads to reduction in cell proliferation. As a matter of fact, patients with low levels of CSTB present reduced brain size and volume; and patients homozugous for the non-functional pathological variant (R68X) present microcephaly (Mancini et al., 2016).

6.2.2 Non-cell autonomous function of secreted CSTB in regulating neurogenesis and interneuron migration

We showed that Cstb is secreted into the CSF and that it impairs cell proliferation and recruitment of interneurons. We demonstrated the non-cell autonomous role of CSTB in proliferation by exchanging media between control and EPM1 COs, which resulted in a rescue of the phenotype observe in the patients' COs. Moreover, the recruitment of control interneurons was decreased when migrating in EPM1 dorsal region in cerebral assembloids, compared to control. These finding could suggest that the latent hyperexcitability, that favors seizures, is given by the decrease of CSTB. Moreover, alteration in interneurons migration and maturation could lead to an unbalance of excitatory/inhibitory neurons. This disruption can

bring to neuropsychiatric disorders, including epilepsy and autism spectrum disorders (ASD) (Marín, 2012; Rubenstein and Merzenich, 2003).

As a matter of fact, proteomic analysis of EPM1 COs, showed that cell secretion is one of the dysregulated biological processes. Also, proteins important for the organization and regulation of the extracellular matrix were altered, including collagens, vitronectin, and tetraspanins. Interestingly, recent studies suggest that neuropsychiatric disorders are associated with modification in the ECM (Amin and Borrell, 2020) and that many proteins associated with brain diseases are secreted via EVs including CSTB. We showed that EPM1 EVs carry less proteins, suggesting a potential role of CSTB in EV biogenesis and/or in protein docking. As expected, we found CSTB being significantly downregulated in both ventral and dorsal EPM1 EVs, confirming that the loss of function of the protein, in this case also in the secretion, is causative of the pathology.

Interestingly, we found many proteins involved in ROBO/SLIT signaling as well as in the Eph/Ephrin dysregulated in EPM1 dEVs. These data could explain that the altered recruitment of interneurons observed in EPM1 assembloids is given by an alteration of secretion of attractive/repulsive cues. We showed that neuronal progenitor cells alter their transcriptome profile after exposure with EVs secreted from EPM1 COs, specifically, neurogenesis and extracellular space organization are dysregulated.

Our findings propose novel mechanisms for defects in neurogenesis and neuronal migration due to low levels of CSTB and by secretion mediated via EVs.

6.2.3 Common genes in EPM1 and epilepsies

It has been reported that patients with mutations in *PRICKLE1* (Prickle planar cell polarity protein 1) and *SCARB2* (Scavenger receptor class B member 2) present symptoms like EPM1 patients (Bassuk et al., 2008; Dibbens et al., 2009); and it is poorly understood how different types of PMEs can share similar mechanisms.

PRICKLE1 is involved in cellular morphogenesis, specifically neurons whit a role in axonal and dendritic extension during neurodevelopment in mouse model (Liu et al., 2013). PRICKLE1 is localized at the level of focal adhesion promoting cell migration (Lim et al., 2016), process affected in EPM1 COs (result evicted from proteomic analysis). One of the functions of focal adhesions is to attach the cytoskeleton to the extracellular matrix (Parsons et

al., 2010), suggesting that the altered mechanisms in EPM1 could be shared with other mutated genes.

SCARB2 contributes to membrane transport and reorganization of the endosomal/lysosomal compartment (Reczek et al., 2007). Indeed, proteomic analysis of EPM1 COs revealed alteration of secretory mechanisms, indicating other possible common mechanisms.

Interestingly, the majority of the proteins that are differentially regulated in EPM1 COs are enriched in radial glia cells and involved in different types of epilepsies, including collagen COL11A1 COL2A1 or COL11A1, IFITM3, GLUD1, RRAS, MGST1 (Aka et al., 2016; Cava et al., 2018; Ercegovac et al., 2015; Guo et al., 2017; Savasta et al., 2015; Shang et al., 2008; Zhou et al., 2018) Altogether, the proteomic results support a novel mechanism that remodeling of extracellular matrix and contacts between cells are critical processes for epileptogenesis (Dityatev, 2010).

This work proposes a novel role of CSTB in regulating early human neurogenesis and the extracellular environment during brain development. Moreover, this suggests a function of CSTB as a long-distance molecule important for the recruitment of interneurons.

6.3 Non-cell autonomous function of LGALS3BP in interneuron migration and specification

6.3.1 LGALS3BP and evolution

As mentioned in the introduction of this thesis, *LGALS3BP* is enriched in human progenitor cells, while it is almost not detected in the mouse developing cortex.

A previous study performed in our lab (Kyrousi et al., 2021) confirmed the expression of LGALS3BP in cerebral organoids, showing an higher expression in RGs compared to IPs and neurons. The fact that LGALS3BP is enriched in human progenitor cells suggested its importance in an evolutionary point of view. Interestingly, the overexpression of the wild-type form of LGALS3BP induces ectopic HOPX+ RGs cells in the mouse cortex which results in the generation of folds. The pathological mutation (E370K) described in this work is one of the few variations between human and macaque (Lodermeyer et al, 2018), reinforcing the possible role of LGALS3BP in evolution. Moreover, the individual with the E370K mutation also presents gyrification index changes, strongly suggesting a role of LGALS3BP in gyrification.

In Kyrousi et al., 2021, whole-brain organoids or unpatterned organoids (Lancaster et al., 2013b) were used as a model to study the role of LGALS3BP in cortical development.

However, in this thesis, I assessed the function of LGALS3BP in specification and migration of interneurons. To this end, we used ventral regionalized organoids and dorso-ventral assembloids (Bagley Joshua A , Reumann Daniel , Bian Shan, 2017). Differences between protocols of organoids have been described in chapter 1.5.3.

In ventral organoids, LGALS3BP is also enriched in progenitors, with higher expression level in MGE-derived IP compared to progenitor and IP cells. Recent evidence showed the high heterogeneity of interneurons in humans (Delgado et al., 2021; Krienen et al., 2020), as LGALS3BP is enriched also in ventral progenitors, it is a candidate protein that could contribute to the diversity of human neural progenitors and neurons, dorsal and ventral.

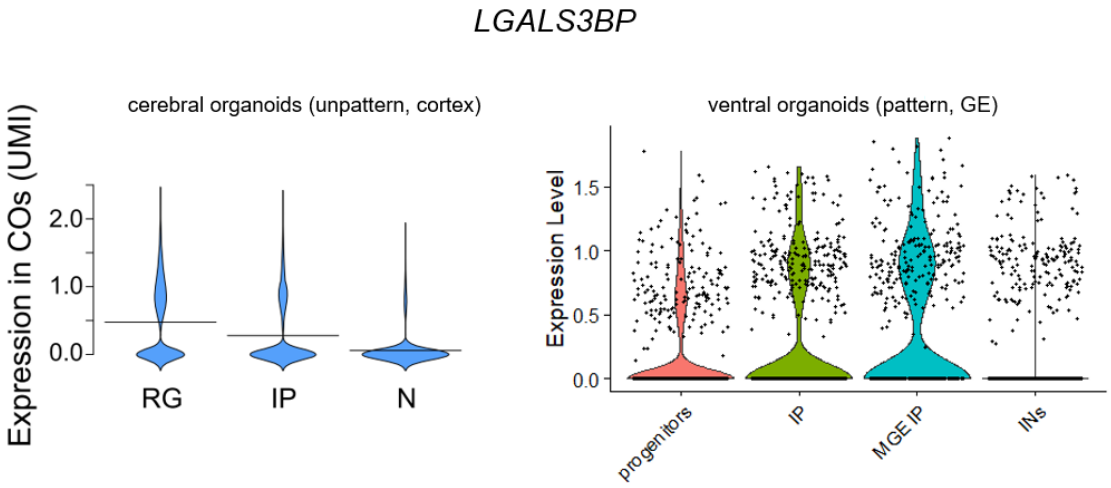

Figure 6-3: LGALS3BP expression in human organoids

Single-cell RNA-seq data showing expression level on LGALS3BP in unpattern-cortical cerebral organoids (left, data from Kyrousi et al., 2021) and in ventral cerebral organoids (right). RG: radial glia; IP: intermediate progenitors, N: neurons, MGE: medial ganglionic eminence; INs: interneurons.

6.3.2 Alteration in ECM composition of dorsal region of assembloids affects recruitment of interneuron

Neurological disorders, including epilepsy and ASD, are characterized by an excitatory/inhibitory imbalance in neuronal circuits, caused by defects in interneuron specification, migration, and/or recruitment. For example, individuals affected with EPM1 (Progressive Myoclonus Epilepsy type1) show loss of GABA synaptic terminals (Buzzi et al., 2012b) and the recruitment of INs is altered in EPM1-hCAs (as described in chapter 3) (Di Matteo et al., 2020). Moreover, it has been shown that ASD patients have reduced GABAergic neurons in their cerebral cortex (Ariza et al., 2018; Puts et al., 2016), and organoids derived from individuals with ASD dysregulate genes associated with GABAergic interneuron differentiation and migration (Wang et al.).

In the project here presented, we showed that LGALS3BP modulates IN migration with a short- and long-distance regulation. Specifically, INs migrating into E370K dorsal region of hCAs are slower and rest more compared to control INs.

We hypothesized that the altered migration of mutant interneurons may also be caused by different cell composition in E370K dCOs. Indeed, single cell RNA sequencing revealed that mutant dCOs have more neuroectoderm and proliferating cells and less RGs and excitatory neurons, compared to control dCOs. Particularly, the reduced RG cells, observed in the E370K

mutant dCOs, could explain the difference in control interneuron distribution once they migrated into the E370K mutant dorsal side of the assembloids. Neurons and interneurons migrating radially through the cortex, use the basal processes of RGs as a scaffold. Different cellular proportions, including less RGs could lead to defects in neuronal migration and distribution within the cortex (Florio and Huttner, 2014).

Moreover, the different cell proportion observed could lead to a different composition of the ECM that might result in an unfavorable environment for cell migration. As a matter of fact, many genes associated with extracellular matrix assembly and composition are differentially expressed in E370K dCOs, including *VCAN*, *LUM*, *COL1A1*, *COL3A1*.

Knowing that LGALS3BP is secreted by EVs in cerebral organoids (Kyrousi et al., 2021), the altered migration may be caused also by changes in EV proteomic content from E370K dorsal region. EVs might play a role in the tangential migration of INs by secreting molecules that attract them to the cortex (Agnati and Fuxe, 2014; Janas et al., 2016).

Notably, E370K dorsal EVs are loaded with different ECM components, such as RELN, collagenases, and VCAN. RELN, a secreted glycoprotein that guides neuronal migration (Pfennig et al., 2011), is associated with lissencephaly (Hong et al., 2000), epilepsy, schizophrenia, and Alzheimer's disease (Herz and Chen, 2006). Since RELN guides the formation and positioning of cortical layers (Caviness, 1982), a lower level of secreted RELN from the dorsal region of hCAs could lead to the altered distribution of migrating INs.

VCAN, an ECM chondroitin sulfate proteoglycan, is also involved in cell migration and adhesion (Wight, 2002). VCAN is also one of the components of the perineuronal nets (PNNs), assemblies that surround mature PV+ INs regulating their inhibiting function. Disruption of PNNs is associated with schizophrenia and epilepsy, leading to altered cortical excitability (Luca and Papa, 2016; Wen et al., 2018).

Moreover, NPCs treated with E370K-dEVs present altered INM associated genes which could result in changes in aRGs\bRGs proportion and, therefore, in alterations in cortical attractive cues that recruit INs to the cortex (Peyre et al., 2015).

6.3.3 Common features of migrating neurons with different mutations associated with PH

We showed that neuronal migration is also regulated by short-distance extrinsic factors. We looked at the migratory behavior of E370K cells, finding an alteration in their trajectory. These cells have a more tortuous, 'exploratory' migratory behavior. We have previously shown that

migrating neurons from an individual with PH (with a mutation in *DCHS1* and *FAT4*) also have increased tortuosity (Klaus et al.), suggesting that directional changes are guided locally.

Since the E370K *LGALS3BP* variation was identified in an individual with PH, it is not surprising that *LGALS3BP* mutant neurons share some molecular signatures with *DCHS1* and *FAT4* mutant neurons. However, LGALS3BP mutant neurons are of ventral origin. Interestingly, some patients with PH showed the presence of GABAergic inhibitory neurons in ectopic nodules (Ferland et al., 2009), suggesting a contribution of interneurons in PH.

DCHS1, *FAT4* and *LGALS3BP* mutant neurons all dysregulate genes associated with axon guidance. Interestingly, we assessed the effect of E370K-vEVs on NPCs and found that genes associated with actin filament organization were dysregulated. These findings confirmed that PH is due to defects in axon guidance resulting by disruption in the cytoskeleton assembly.

6.3.4 EVs can determine cell fate decision

The defective cell migration observed in E370K neurons can also be caused by the altered identity of these cells. We showed that E370K INs acquire a dorsal identity, which could result in a different response to extrinsic attractive/repulsive stimuli. E370K INs dysregulate genes associated with migratory behavior in PH (like *FAT4*, *RND3,* and *DLL1*) and down-regulate the *EPHB2* receptor, which regulates tangential migration (Zimmer et al., 2011). It has been shown that deletion of *EphrinB* receptors leads to reduced INs in the mouse neocortex causing cortical hyperexcitability and seizures in a cell-autonomous way (Talebian et al., 2017). We suggest that migratory directional changes, down-regulation of *EPHB2,* and an altered molecular identity can regulate IN migration.

However, the mechanism by which LGALS3BP regulates neuronal migration and recruitment are still unclear. One possible hypothesis would be that LGALS3BP is involved in EV biogenesis, speculating that the LGALS3BP variation might influence EV biogenesis. It has been shown that the glycosylation pattern of EV-associated proteins regulates the recruitment of specific proteins in the vesicles (Batista et al., 2011; Liang et al., 2014). The different protein content of mutant vesicles could affect the extracellular environment since we identified many ECM proteins and attractive/repulsive molecules being differentially regulated. Further studies will be focused on detailed investigation in the glycosylation pattern of EVs-associated LGALS3BP to understand its role in EV biogenesis.

6.3.5 Wnt pathway regulating dorso-ventral patterning and LGALS3BP

The alteration in migratory dynamics of mutant interneuron is probably due to their altered cell identity. We found that E370K vCO have a dorsal identity, upregulating *PAX6*, *GLI3*, *NEUROD6*, and other dorsal genes. Our data showed that LGALS3BP might be involved in the dorso-ventral patterning and that the mutation of LGALS3BP leads to a cell fate change, failing in the activation of the ventral pattern.

Previous studies in mice showed that *Pax6*, *Gli3*, *Shh*, regulate the dorso-ventral patterning during neurodevelopment (Fuccillo et al., 2006; Theil et al., 1999; Tole et al., 2000). Specifically, *Gli3* and *Pax6* mutant mice present dorsal pallial tissue with ventral identity (DLX2+) (Theil et al., 1999; Tole et al., 2000). Moreover, mice carrying a deletion in the *Gli3* gene have ectopic ventral forebrain identity in the dorsal forebrain, maybe associated with defects of the *Wn*t pathway (Tole et al., 2000).

We propose that LGALS3BP has an extrinsic short-distance regulation in the specification of ventral progenitors. Studies on cancer showed that, in the ECM, LGALS3BP binds Galectin-3 (Gal-3), forming a complex that binds the membrane tetraspanins CD9 and CD82. This complex activates the Wnt/b-catenin signaling (Lee et al., 2010; Pikkarainen et al., 2017) which activate the gene expression of dorsal genes (Wnt target genes) (Chi et al., 2017).

One possible case in the mutant COs, is that the E370K mutation interferes with LGALS3BP-tretraspanins binding. We hypothesize that E370K mutant form might bind wildtype LGALS3BP preventing it to contact cell membrane CD9 and CD82. This will eventually result in the repression of the ventralization of mutant cells, activating the Wnt/b-catenin signaling in ventral COs and, therefore, leading to the ectopic expression of *PAX6* and local repression of *NKX2-1*. These changes in the transcriptome profile result in the expression of *EOMES*, *TBR1*, and *SATB2* that determine the dorsal identity of E370K vCOs (Figure 6-4).

In another possible scenario, the reduced protein level of LGALS3BP observed in mutant vEVs might result in less LGALS3BP binding CD9 and CD82. We propose that the activation of the Wnt/b-catenin singaling through membrane tetraspanins, might function in a dose-response manner, meaning that in the mutant cells the lower level of EV-LGALS3BP is not sufficient to repress the dorsalization (Figure 6-4).

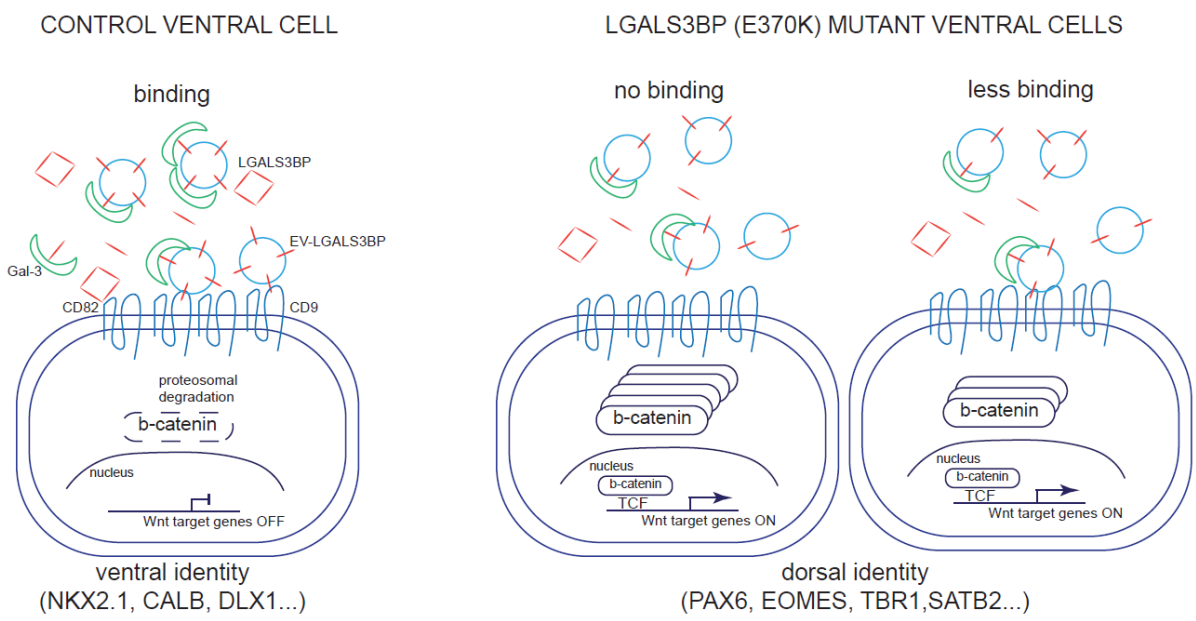

Figure 6-4: Model of activation of Wnt/b-catenin pathway by LGALS3BP

Schematic representation of regulation of the Wnt/b-catenin pathway in control and E370K mutant cells in vCOs.

The dose-response effect might also explain the partial rescue of the dorsal phenotype observed in mutant vCOs. The two approaches used were: culturing E370K vCOs with conditioned media (CM) from CTRL vCOs; and generating ventral mosaic organoids (vMOs) mixing control and mutant iPSCs. In both experimental setups, the mutant cells were able to revert their dorsal identity. The E370K mutation is heterozygous, which means that the wildtype form of LGALS3BP is still present in the mutant organoids. However, when adding CM from CTRL organoids or generating a more physiological environment in vMOs, the additional LGALS3BP wild type form can overcome the mutant form, restoring the ventral identity.

We, therefore, showed that changes in the extracellular environment influence cellular identity and IN specification in a non-cell autonomous manner. Particularly, in vMOs, CTRL and E370K progenitors present resembling transcriptomic features; however, after the transition to IPs, they explicate their intrinsic program identity. “Interneuron identity is refined at later stages, after interaction with the local extracellular environment”(Kepecs and Fishell, 2014; Wamsley and Fishell, 2017). Indeed, we showed that the presence of control cells could partially rescued the ventral identity of E370K cells.

6.4 Conclusions and future perspectives

This thesis combines three studies aimed at the understanding of non-cell autonomous mechanisms during neurodevelopment and disease. This work successfully identified common signatures in two disease candidate genes: CSTB, associated with EPM1, and LGALS3BP, mutated in individuals with neurological diseases.

Interestingly, both 3D human models of EPM1 and E370K (LGALS3BP variation identified in individual with cortical malformations and epilepsy) used in this thesis, revealed alteration and disruption in distribution and recruitment of interneurons. The observed defects in these processes could lead to disruption in cortical circuits, leading to the unbalance between excitation and inhibition found in epileptic patients. The two models also share alteration in EV protein content, including many proteins of the ECM, suggesting that their non-cell autonomous function is mediated by EVs. The common phenotype observed in the EPM1 and E370K models represents one of the complex pictures of neurological diseases, where genes and phenotype have a convergent relationship (Klingler et al., 2021). In other words, mutations in different genes can lead to the same phenotype.

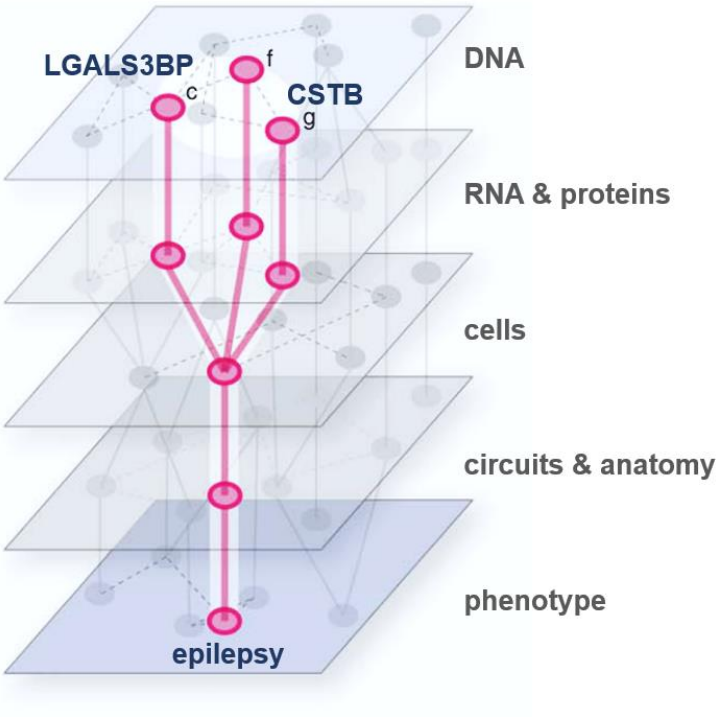

Figure 6-5: Convergent relationship between CSTB and LGALS3BP mutations and phenotype

Schematic representation of divergent relationship between mutations and phenotype at different level. Individuals with mutations in different genes (*CSTB* and *LGALS3BP*) have the same phenotype (epilepsy). Figure adapted from Klinger et al., 2021.

However, in this thesis, I also identified mechanisms specific to each gene. I demonstrated the non-cell autonomous function of CSTB in cell proliferation and neurogenesis and of LGALS3BP in cell-fate decision, dorso-ventral patterning, and migratory dynamics (Figure 6-6).

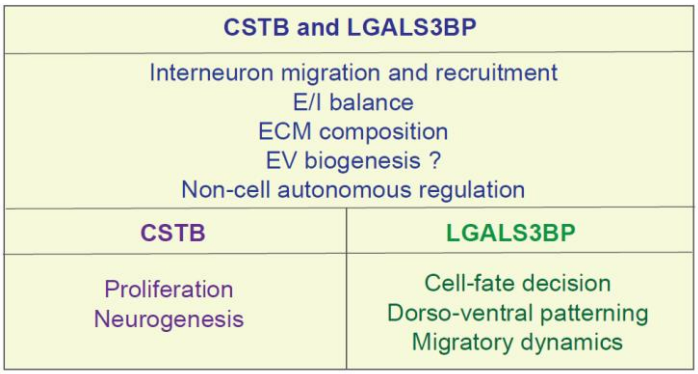

Figure 6-6: Summary of CSTB and LGALS3BP functions

Table illustrating the main functions of CSTB and LGALS3BP found in this thesis.

In conclusion, this thesis confirms a key role of extracellular factors in brain development and in neurological disorders.

Further studies will be focused on suggesting possible therapeutic strategies based on extracellular vesicles (already widely used in cancer therapy) to neutralize the progression of neuropsychiatric disorders.

7 Materials and Methods

7.1 General techniques

IPSC culture, splitting and freezing.

IPSC lines used in Chapter 3 derived from PBMCS, extracted from human blood samples, according to the manufacturer's recommendations using SepMate-50 tubes (StemCell, 15450). PBMCs were taken from a female control sample of 39-year-old; a female patient sample of 35-year-olds with EPM1, and female patient sample of 13-year-olds with EPM1 (UL4). The Ludwig Maximilian University of Munich's Ethical Commission gave its approval for the creation of iPSCs (Project 19-635). The detailed steps of the reprogramming procedures are published in Di Matteo et al., 2020.

IPSC lines used in Chapter 4 and 5 were reprogrammed from NuFF3-RQ human new-born foreskin feeder fibroblasts (GSC-3404, GlobalStem) (Cárdenas et al., 2018).

We cultured iPSCs on Matrigel Basement Membrane Matrix (Corning) coated plates (Thermo Fisher, Waltham, MA, USA). Matrigel was diluted 1:100 in DMEM-F12+Glutamax. iPSCs were fed with mTesR1 basic medium supplemented with 1x mTesR1 supplement (Stem Cell Technologies, Vancouver, Canada). Media was changed every day. IPSCs were kept at 37°C, 5% CO2 and ambient oxygen level. Passaging was done when cells reached 80% of confluence. After a wash in DPBS, colonier were detached from the plate using Accutase diluted 1:4 (Stem Cell Technologies). We added DMEM-F12+Glutamax to the detached cell to stop the accutase treatment, and centrifuged the colonies for 4 minutes at 300g. The pellet containing IPSC colonies was resuspended in 1ml of mTeSR1 basic medium supplemented with 1x mTesR1 supplement and Rock inhibitory (Y-27632) in a final dilution of 1:1000. IPSCs were diluted according to the experiment. IPSCs were frozen when they reached 80% confluence. The steps for freezing cells are the same of their splitting, except that the pellet is resuspended in Freezing media (50%FBS, 40%DMEM-F12+Glutamax, 10%DMSO) and stores in cryovials and kept at -80°C for 24 hours, and then, transferred into liquid nitrogen tank.

Generation of labeled iPSC line

We generated GFP and RFP-labeled iPSC lines by nucleofection of piggyBac transposase (1 ug) and PB-GFP (1 ug), as described previously and in (Di Matteo et al., 2020), or PB-RFP (1 ug) (Chen and LoTurco, 2012; Pipicelli et al., 2022). Single cells suspension was transfected with Amaxa Nucleofector 2b (using the program B-016). We, then picked GFP and RFP

positive colonies and cultured on Matrigel (Corning/VWR International, 354234). GFP and RFP-labeled iPSC lines were cultured as described above.

Generation of unpatterned COs

In Chapter 3 and 4, COs were generated and cultured according to (Lancaster and Knoblich, 2015).

Briefly, when iPSCs were 70-80% confluent, we dissociated them into single cells using pure Accutase (Sigma-Aldrich, A6964), and incubate for 5 minutes at 37°C. We, then, added DMEM-F12+Glutamax to stop the reaction and centrifugated the cells at 300g for 4 minutes. We then counted the cells in order to obtain 90'000 cells per one Ultra-low attachment U bottom 96-well plate. Therefore, we plated 9'000 cells per well of the plate and fed them with hES medium (DMEM-F12+Glutamax supplemented with 20% KnockOut™ Serum Replacement, 3% hESC-quality FBS, 0.1 mM 2-Mercaptoethanol (50 mM), 1% MEM Non-Essential Amino Acids Solution (100X)) with FGF2 (4 ng/ml) and Rock inhibitor (50 μM). After 1 day, Embryoid bodies (EBs) are generated. EBs are cultured for 5 days in hES medium changing medium at day 3. At day 5, we induced the neuronal differentiation, feeding them with NIM medium (DMEM-F12+Glutamax supplemented with 1:100 N2™-Supplement (100X), 1% MEM Non-Essential Amino Acids Solution (100X) and 5 μg/ml Heparin) for 7 days, changing the medium every second day.

At day 12, each EB was placed on a single mold of a parafilm sheet, the excess of media was removed and a drop of Matrigel was added to each mold containing the EBs. EBs embedded in Matrigel were transferred to the incubator for at least 30 minutes to let the Matrigel to solidify. Afterwars, EBs were washed off the parafilm by adding 25 ml of NDM-A medium (DMEM-F12+Glutamax and Neurobasal™ Medium in a 1:1 ratio, 1:200 N2™-Supplement (100X), 1:100 B-27™ Supplement (50X) minus vitamin A, 0.5% MEM Non-Essential Amino Acids Solution (100X), 0.5% GlutaMAX™ Supplement, 50 μM 2-Mercaptoethanol (50 mM), 1:100 Antibiotic Antimycotic Solution (100X) and 2.5 μg/ml Insulin). to each 10 cm plate, containing approximatively 30 EBs. At day 16, COs were fed with NDM+A medium (DMEM-F12+Glutamax and Neurobasal™ Medium in a 1:1 ratio, 1:200 N2™-Supplement (100X), 1:100 B-27™ Supplement (50X), 0.5% MEM Non-Essential Amino Acids Solution (100X), 0.5% GlutaMAX™ Supplement, 50 μM 2-Mercaptoethanol (50 mM), Antibiotic Antimycotic Solution (100X) and 2.5 μg/ml Insulin) and kept on an orbital shaker (55 rpm) inside an incubator (37°C, 5% CO2 and ambient oxygen level). Media exchange was performed every 4-5 days.

Generation of patterned COs and dorsal-ventral assembloids

Assembloids and patterned COs were generated as described in (Bagley et al., 2017a).

The formation of EBs follows the same steps described above. For the patterning, EBs are treated with SAG (1:10000) (Millipore, 566660) + IWP-2 (1:2000) (Sigma-Aldrich, I0536) for ventral identity and with cyclopamine A (1:500) (Calbiochem, 239803) for dorsal identity. The patterning molecules are added during the neuronal induction phase and added to the NIM medium. For dorsal and ventral COs (dCOs, vCOs), EBs were embedded individually in each Matrigel droplet, while for the assembloids, one ventral EB was embedded together with a dorsal EB in the same Matrigel droplet. From this point on, the patterned COs and assembloids are cultured as described above.

Immunohistochemistry and confocal imaging

Mouse brain and organoid sections were first cool down for 20 minutes at room temperature and washed once with PBS.

Treatment for antigen retrieval was done for nuclear markers. We incubated the section in a 10 mM citric buffer (pH6). Sections were put in a microwave for 1 min at 720 Watt and then, for 10 mins at 120 Watt. We then left the slides to cool down for 20 mins at room temperature.

Then, sections were permeabilized with 0.3% Triton incubation for 5 mins. We then blocked the sections with Blocking Solution (0.1% TWEEN, 10% Normal Goat Serum (Biozol, VEC-S-1000).

Sections were then incubated with primary antibodies overnight at 4 °C; and with secondary antibodies for 1 h at room temperature. Both primary and secondary antibody solutions were diluted in Blocking Solutions. Nuclei were visualized using 0.5 mg/ml 4,6-diamidino-2-phenylindole (DAPI) (Sigma-Aldrich, D9542). Immunostained sections were analyzed using a Leica laser-scanning microscope.

For to BrdU immunostaining, we previously denaturated the DNA by 30 min incubation in 4 M HCl followed by neutralization for 10 min in 0.1 M sodium borate at pH 8.5. Two 5-min washing steps were performed before continuing with the IHC procedure.

Immunostained sections were visualized with a Leica SP8 confocal laser-scanning microscope (25x and 40x objectives were used).

Table 1: Immunostaining antibodies

Antibody	Host	Company	Catalogue No.	Dilution
CSTB	Mouse	Santa Cruz Biotechnology	sc-166561	1:500
ACETYLATED TUBULIN	Mouse	Sigma- Aldrich	T7451	1:6000
PH3	Rabbit	Millipore	06-570	1:500
GAPDH	Mouse	Millipore	CB1001	1:6000
GFP	Chicken	Aves Lab	GFP-1020	1:1000
RFP	Rabbit	Rockland	600-901-379	1:1000
DCX	Guinea pig	Millipore	AB2253	1:2000
TUBB3		Sigma Aldrich	T8660	1:500
KI67	Mouse	DAKO	M7248	1:500
KI67	Rabbit	ABCAM	AB15580	1:500
ACTIN (Actb)	Mouse	Merck Millipore	MAB1501	1:1000
BrdU	Rat	ABCAM	AB6326	1:200
PAX6	Rabbit	ABCAM	AB78545	1:500
Ccdn1	Rabbit	Thermo scientific	RM-9104-S0	1:100
TBR2	Rabbit	Merck Millipore	Ab2283	1:500
NKX2.1	Mouse IgG1	Merk Millipore	MAB5460	1:500
TBR1	Rabbit	Abcam	Ab31940	1:500
LGALS3BP	Mouse IgG1	eBioscience	BMS146	1:100
PAX6	Rabbit	Biolegend	PRB-278p	1:500
MEIS2	Mouse IgG1	Santa Cruz Biotechnology	SC 101850	1:300
EOMES	Rabbit	Abcam	ab23345	1:500
SATB2	Mouse IgG1	Abcam	Ab51502	1:500

CD63	Mouse	Santa Cruz	sc-5275	1:300
CD81	Mouse	Santa Cruz	sc-7637	1:1000
CD82	Rabbit	Santa Cruz	sc-1087	1:100
CD9	Mouse	Santa Cruz	sc-59140	1:100
PDCD6IP (ALIX)	Mouse	Santa Cruz	sc-53540	1:100
SOX2	Rabbit	Abcam	ab5603	1:500
MAP2	Chicken	Abcam	ab5392	1:500
GFAP	Rabbit	Agilent Dako	Z0334	1:500
RFP	Rabbit	Rockland	600-901-379S	1:500
NESTIN	Mouse	EMD Millipore	MAB5326	1:500
S100β	Mouse	Sigma	S2532	1:500
DCX	Guinea pig	EMD Millipore	AB2253	1:500

Data visualization, quantifications and statistical analysis of animal and CO experiments

Data visualization and statistical analysis were performed using GraphPad Prism® Version 7.04 (Chapter 3) and Version 8 (Chapter 4 and 6); and RStudio 4.1.1. For normally distributed data, T-test was used to analyzed significance, while for not-normally distributed data, not-parametric Mann–Whitney test was used for to analyzed significance. For animal experiments, at least three brains from at least two different pregnant mothers were analyzed. For experiments in organoids and assembloids, at least three organoids from at least two independent batches were analyzed.

EVs and IVs collection and analysis

We collected extracellular vesicles (EVs) from CMs obtained from COs (ventral and dorsal). The CMs was centrifugated several times: first at 300 g for 15 mins, then at 2000g for 10 mins. After that, the supernatant was centrifugated several times using an ultracentrifuge: first, at 10.000 g for 30 mins; then, 100.000 g for 120 mins. Afterwards, the pellet containing the EVs was washed one time in PBS and centrifugated at 100.000 g for 60 mins. As an alternative method, EVs have also been collected using, miRCURY Exosome Cell/Urine/CSF Kit (Qiagen, 76743) according to the manufacturer instructions.

IVs were isolated by subcellular fractionation. Briefly, the COs were homogenized and upon removal of nuclei, cell debris and mitochondrial fraction as previously reported (Ferrara et al., 2009), the supernatatant was ultracentrifuged at 100.000 g for 30 min to obtain the cellular fraction (IVs).

Nanoparticle tracking analysis (NTA) was performed according to (Kyrousi et al., 2021).

ZetaView Software 8.05.12 SP1 was used to analyzed particle size and concentration. For immune-electron microscopy, EV suspensions were analyzed by Dr Ilkka Miinalainen at Biocenter Oulu / EM laboratory, Finland (Deun et al., 2020), as described in (Kyrousi et al., 2021).

Bulk-RNA-sequencing of NPCs treated with EVs

For the projects in chapter 3 and 4, we extracted RNA from 3 independent wells of NPCs from a 24 well plate and used 10ng of RNA for sequencing.

For the NPCs treated with EVs, extracellular vesicles were isolated by ultracentrifugation from 20 ml of CM collected from 28-37 days old ventral and dorsal, control and mutant COs.

We lysed NPCs in 1ml Trizol(Qiagen) for each well and isolated the RNA following the RNA Clean & Concentrator kit (Zymo Research).

Next, cDNA synthesis was obtained using the SMART-Seq v4 Ultra Low Input RNA Kit (Clontech cat. 634888). We then gragmented the cDNA fragmented to a size of 200–500 bp using the Covaris S220 device (5 min; 4°C; PP 175; DF 10; CB 200).

Libraries were prepared from the fragmented cDNA using the MicroPlex Library Preparation Kit v2 (Diagenode, cat. C05010012). Qubit and Agilent DNA Bioanalyzer were used to control the quality of the libraries. Deep sequencing was performed on a HiSeq 1500 system following to the standard Illumina protocol for 50 bp paired-end reads with v3 sequencing reagents.

7.2 Techniques specific to chapter 3

The techniques in this chapter are adapted from the published manuscript (Di Matteo et al., 2020) and from the preprint manuscript (Pipicelli et al., 2022).

Electroporation of COs

For electroporation, 35 days old COs were kept in antibiotic-free conditions and placed in an electroporation chamber (Harvard Apparatus, Holliston, MA, USA). Using a glass microcapillary, we injected 1 µl of plasmid DNAs into CO ventricles. To see the site of electroporation, Fast Green (0.1%, Sigma) was injected together with the DNAs. The COs were electroporated with 5 pulses applied at 80 V for 50 ms each at intervals of 500 ms (ECM830, Harvard Apparatus). COs were, then, kept for additional 24 hrs in antibiotic-free media, and then changed into the NDM+A (Neuronal Differentiation Media + Vitamin A) until fixation. The COs were fixed using 4% PFA for 1 hr at 4°C, cryopreserved with 30% sucrose and stored at -20°C. For IHC, 16 um cryosections were prepared. The CSTB or R68X plasmid constructs used in the electroporation experiments are described in (Cipollini et al., 2008) and in (Di Matteo et al., 2020).

Animal experiments

All the mice used in this research were kept in the animal facility of the Max Planck Institute of Psychiatry, Munich. All the experiments were performed according the German and European Union guidelines. In this project, C57BL/6J mouse line, Tg (Gad2-EGFP)DJ31Gsat (GAD65-GFP) transgenic mouse strain (López-Bendito et al., 2004) and Gad1$^{tm1.1Tama}$ (GAD67-GFP) knock-in mouse strain (Tamamaki et al., 2003) were used. All mice used for in utero electroporation were pregnant females between 4 – 6 months.

In utero electroporation

In utero electroporation experiments were approved by the Government of Upper Bavaria (license number 55.2-1-54-2532-79-2016). Pregnant C57BL/6, GAD65-GFP, and GAD67-GFP animals were used. Saline solution containing fentanyl (0.05 mg per kg body weight), midazolam (5 mg per kg body weight) and medetomidine (0.5 mg per kg body weight) (Btm license number 4518395) were injected intraperitoneally. E14 embryos were electroporated (Saito, 2006). DNA plasmids (1 µg/µl.) were injected together with fast green (2.5 mg/µl; Sigma). Animals were injected with buprenorphine (0.1 mg per kg body weight), atipamezole (2.5 mg per kg body weight) and flumazenil (0.5 mg per kg body weight) to terminate the anesthesia. Fixation of brains was done 2 or 3 dpe in 4% PFA for 12-16 hrs. For IHC, 25 µm

sections were prepared using a cryostat. For each experiment, we used at least 3 different mouse brains per condition.

BrdU injections

Mice were injected intraperitoneally with BrdU (50 mg/kg bodyweight). Mice were sacrificed 30 min later. Tissue preparation and processing were performed as described above.

Primary cell cultures from mouse embryonic cerebral cortex

We isolated brains were isolated from E14 embryos from pregnant C57BL/6 wild-type mice (Stahl et al., 2013). We dissected the mouse cortices and pooled in HBSS buffer (10 mM HEPES) and we enzymatically dissociated the cells cells with 0.05% Trypsin/EDTA for 15 min at 37°C. We then resuspended the cells in DMEM with 10% fetal calf serum (FCS) to terminate the enzymatic reaction. Then, we used a fire polished Pasteur pipette to mechanically dissociate the cells. We transfected the cells with pEGFP-C1 plasmid as a control and pEGFP-Cstb (for CSTB overexpression) or pEGFP-R68X (for mutant CSTB form overexpression) plasmids using the Amaxa Nucleofector. After 4 days, we lysed the cells in RIPA buffer. The CM was recovered, and filtered on 0.22 µm membranes (Millipore). We used10% of the recovered CM for WB.

Collection of cerebral spinal fluid from mice

CSF were collected from the fourth ventricle of E14 embryos using microcapillary samplers (typically 1-2 µl) (Johansson et al., 2006). More details are found in (Di Matteo et al., 2020)

Western Blot

For WB, we lysed iPSCs and tissues from mouse cortices in RIPA buffer containing protease and phosphatase inhibitors (Roche, Basel, Switzerland). We used SDS-PAGE with a 12.5% Acrylamide gel. 50 mM DTT to separate the proteins and added 50 mM DTT to dissociate proteins and avoid protein aggregates. iPSCs and tissues from mouse cortices were lysed in RIPA buffer with protease and phosphatase inhibitors (Roche, Basel, Switzerland) and proteins were separated by SDS-PAGE The used loading controls were GAPDH (MW 37kDa) and Actb (MW 42 kDa).

The collected conditioned media from COs and cells were concentrated using Amicon® Ultra-15 Centrifugal Filter Units according to the instructions (Millipore, UFC901024). Same volume of CM from cells or COs plates (with comparable number of organoids or cells) was collected.Then the proteins were transferred to a nitrocellulose membrane (GE Healthcare, Chalfont St Giles, Buckinghamshire, Great Britain). Then, we colored the membranes with a

Ponceau Red solution (Serva, 33427.01) to verify the quality of the transfer. Next, we incubated the membranes with primary antibodies overnight in rotation at 4 °C. The membranes were washed three times with TBS-T for 10 minutes each, and incubated with secondary antibodies for 1h at room temperature. After three washes in TBS-T, we treated the membrane with ECL Western Blotting Detection solution (Millipore, Billerica, MA, USA) for protein detection. Bands were quantified using ImageJ software.

Proteomic analysis

We selected 20-30 CTRL or UL1 COs and lysed in in RIPA buffer (50 mM Tris-HCl pH 8.8, 150 mM NaCl, 0.1% SDS, 0.5% NP-40, 0.5% DOC; protease and phosphatase inhibitor cocktail, Sigma-Aldrich). We quantified protein concentration by Bradford assay (Biorad). For mass spectrometry analysis, we used 100ug of proteins. Next, we diluted the protein extracts in triethylammonium bicarbonate buffer (TEAB, 100 mM final concentration) containing 1% SDS. Using the Pierce BCA Protein assay kit (Thermo Scientific, Rockford, Illinois, USA), we determined protein concentration. Trypsin digestion of 80 µg of proteins (diluted in 100 µL of 100 mM TEAB) was performed. Proteins were then labeled with the TMT isobaric tags according to the procedure reportes in (Napolitano et al., 2019; Russo et al., 2019): For LC-MS/MS analyses, we mixed and diluted the TMT- labeled samples in 2% TFA (final concentration of 0.5 µg/µL).

2.5 µg of TMT-labeled peptides were analyzed by high-resolution nanoLC−tandem mass spectrometry. A Q-Exactive Orbitrap mass spectrometer with an EASY-Spray nanoelectrospray ion source (Thermo Scientific, Rockford, Illinois, USA), coupled to a Thermo Scientific Dionex UltiMate 3000RSLC nano system was used (Thermo Scientific, Rockford, Illinois, USA) as described in (Russo et al., 2019).

Protein Identification and Quantitation

We analyzed the data with the Thermo Scientific Proteome Discoverer 2.1 software (Thermo Scientific, Rockford, Illinois, USA), using the SEQUEST HT search engine. The HCD MS/MS spectra were searched against the Homo sapiens Uniprot_sprot database (release 2019_11, 20380 entries). The used parameters and downstream analysis are published in (Di Matteo et al., 2020).

Bioinformatic analysis

Proteins with Log2 fold change values (Log2FC) ≥0.3 and ≤-0.3 were considered as differentially expressed (DE). We used g:GOSt tool of the g:Profiler toolset

(https://biit.cs.ut.ee/gprofiler/gost) to identifies the Gene Ontology (GO) term for Biological processes for DE proteins (adjusted p-values <0.05). Visualization of selected GO categories was performed using the GOplot package v 1.0.2 of the RStudio v 1.2.1335. Data visualization of DE proteins was drawn in RStudio.

7.3 Techniques specific to chapter 4

The techniques in this chapter are adapted from the preprint manuscript (Pipicelli et al., 2022).

CRISPR genome editing for generation of mutant iPSC lines

Control iPSC line was genetically edited using CRISPR technology to generate isogenic control and E370K and Y366Lfs LGALS3BP lines. More details are reported in (Kyrousi et al., 2021).

Generation of vMOs

We generated ventral mosaic organoids (vMOs) as described above and in (Bagley et al., 2017b). We dissociated iPSCs as described above. We, then mixed together 4,500 cells of each line for a total of 90,000 cells, and transferred them to an ultra-low-attachment 96-well plate (9,000 cells in each well) (Corning). From this step, the protocol continues as described in "Generation of dvCAs and vCOs".

Time-lapse imaging of dvCAs

Dorso-ventral assembloids were prepared and imaged as previously described in (Klaus et al.; Pilz et al., 2018). DvCAs were sliced in sections of 300 um of thickness using a vibratome (Leica VT1200S). During the procedure, assembloids were kept in cold DMEM-F12 (Invitrogen) with sodium bicarbonate, glucose and 10% antibiotics; and oxygenated with O2. We, then, placed the sections on a cell culture membrane insert (Millicell) and added NDM+A. The slices were put on a cell culture insert (Millicell) and cultured in NDM+A organoid. Inserts were then, put in the incubator for at least 1h.

Live imaging was performed for 48 h using Leica TCS SP8 Confocal microscope (Leica, Germany). We took images every 20 minutes. We tracked cell movement ImageJ software and the Manual Tracking Plugin, and the movement parameters calculated and analyzed in RStudio.

Single-cell RNA-sequencing library preparation and data analysis

For single-cell RNAseq analysis, we collected 5 organoids from vCOs, vMOs and dCOs.

We dissociate the selected organoids into single cells using StemPro Accutase Cell Dissociation Reagent (Life Technologies).

The cells when filtered through 30 uM and 20 uM filters (Miltenyi Biotec) and they were cleaned of debris using a Percoll (Sigma, P1644) gradient. For vMOs, we sorted the cells with FACS and collected control and GFP-labeled E370K cells. We performed FACS analysis at a FACS Aria (BD) in BD FACS Flow TM medium, with a 100 um diameter nozzle. For each run, we anlyzed 10,000 cells.

The cell suspensions were then resuspended in ice-cold Phosphate-Buffered Saline (PBS) supplemented with 0.04% Bovine Serum Albumin. The final concentration of cells was 1000 cells per ul.

We then, loaded single cells onto a Chromium Next GEM Single Cell 3′ chip following the Chromium Next GEM Single Cell 3′ GEM, Library & Gel Bead Kit v3.1. We generated cDNA libraries using the Single Index Kit T Set A, 96 rxns (10xGenomics PN-1000213). Sequencing of libraries was performed using Illumina NovaSeq6000 in 28/8/91bp mode (SP flowcell), quality control and UMI counting were performed by the Max-Planck für molekulare Genetik (Germany).

Single-cell RNA-sequencing library preparation and data analysis

We analyzed single-cell RNA-seq data were analyzed using the R package Seurat (version 3.2). We excluded cells with more than 2,500 or less than 200 detected genes or with mitochondrial content higher that 10%. Moreover, we excluded genes that were not expressed in at least three cells. Clusters with "glycolysis" identity based on GO terms of cluster-specific markers genes were excluded, as described in (Bhaduri et al. 2020; Kanton at al., 2019).

Gene expression was normalized using a normalization method (“LogNormalize”, scale.factor = 10000) and we selected the 2000 most variable genes (selection method, “vst”) and scaled (mean = 0 and variance = 1 for each gene) before PCA. We used the FindNeighbors" and "FindClusters" functions for clustering. A resolution of 0.5 and UMAP for visualization was used.

We grouped clusters based of the expression of markers. Differentially expressed gene were identified using the "FindAllMarkers" function. We identified the pseudo-differentiation axis of telencephalic cells with PCA analysis. For pseudo-differentiation analysis, we used Monocle3 algorithm (Trapnell et al., 2014).

Dorso-ventral identity model

The dorso-ventral model was built as described previously in (Oberst et al., 2019) and implemented in the bmrm R package.

The model was trained on a subset of single cells datasets obtained from single-cell RNA seq analysis of dCOs and vCOs.The 30 most-weighted genes were used for fold cross validation of additional dorsal and ventral control cells and prediction of dorsal and ventral mutant cells. The same method was applied to build a model to classify control and mutant cells, selecting for 100 most-weighted genes.

Enrichment analysis

We used the FUMA algorithm (Watanabe et al., 2017) to identify GO term of DE genes in mutant vCOs. We inserted the lists of differentially express genes from all the cell populations (progenitors, intermediate progenitors, and neurons) into the GENE2FUNC software, accepting FDR<0.05.

7.4 Techniques specific to chapter 5

Some of the techniques in this chapter are adapted from the preprint manuscript (Pipicelli et al., 2022).

NPCs, neurons and astrocytes cultures

Neural progenitor cells (NPCs) were generated and cultured by following Basic Protocol 1 described in (Boyer et al., 2012), with the exception that FGF8 and SHH were replaced by FGF2 (Peprotech, 100-18b-50) in the neural progenitor medium (NPM). Neural differentiation was conducted as described in (Gunhanlar et al., 2017b). Astrocytes were obtained from 8-month-old organoids. Organoids were transferred to a 15 ml falcon tube and washed 1 time with 1xPBS. For dissociation, they were placed in Accutase® solution (A6964, Sigma Aldrich, St. Louis, MO, USA) pipetted up and down 5-10 times with a P1000 tip, and then placed in the incubator for 10 mins at 37°C, followed by 5 times pipetting for a second time. The dissociated cells were then centrifuged at 300 x g for 3 mins and resuspended in NDM+A media for 24 hours. The next day, the cells were transferred to Matrigel® Basement Membrane Matrix, LDEV-free (Corning®, 354234) coated plates. One day later the media was changed to Astrocyte media (89% DMEM/F12+Glutamax, 10% fetal bovine serum, 1% Antibiotic-Antimycotic (100x)) All the cells were kept in an incubator at 37°C, 5% CO2 and ambient oxygen level with medium changes every 2–3 days.

EVs and IVs collection and analysis

EVs were collected from conditioned media from COs and 2D cultured cells by the steps described in Chapter 7.1. “EVs collection”.

IVs were isolated by subcellular fractionation. Briefly, the COs were homogenized and upon removal of nuclei, cell debris and mitochondrial fraction as previously reported (Ferrara et al., 2009), the supernatatant was ultracentrifuged at 100.000 g for 30 min to obtain the cellular fraction (IVs).

Nanoparticle tracking analysis (NTA) was performed according to (Kyrousi et al., 2021).

ZetaView Software 8.05.12 SP1 was used to analyzed particle size and concentration. For immune-electron microscopy, EV suspensions were analyzed by Dr Ilkka Miinalainen at

Biocenter Oulu / EM laboratory, Finland (Deun et al., 2020), as described in (Kyrousi et al., 2021).

EV uptake

NPCs, astrocytes and neurons were cultured in 24-well plates. 10-12 ml of conditioned media from astrocytes and neurons were treated with 1 ul of DiI (1,1'-Dioctadecyl-3,3,3',3'-Tetramethylindocarbocyanine Perchlorate) before the final ultracentrifugation. The media of the recipient cells was changed just prior to the addition of the labeled EVs. The cells were fixed 12 hours after EV treatment with 4% paraformaldehyde for 20 mins at room temperature.

Imaging

Immunostainings were imaged with confocal microscopy or Stimulated Emission Depletion (STED) microscopy. Confocal stack images were obtained using a Leica DMi8 laser scanning confocal microscope (Leica Microsystems, Wetzlar, Germany), equipped with 20x/0.75 (oil), 40x/1.10 (water), and 63x/1.30 (glyc) objectives. Images were then processed using ImageJ (Schneider et al., 2012). STED imaging was performed with a TCS SP8 STED 3X FALCON confocal head (Leica Microsystems, Germany) mounted on an inverted microscope (DMi8; Leica Microsystems, Germany). For imaging, a 405 nm diode and a white light laser were used as excitation sources for DAPI, ExoGlow-RNA EV (SBI, USA), Alexa Flour 594 (ThermoFisher, USA), and ATTO 647N (ATTO-TEC GmbH, Germany) (405 nm, 488 nm, 575 nm, 644 nm lasers lines respectively). Single photons were collected through a 100×/1.4 NA oil-immersion objective and detected on Hybrid Detectors (HyD) (Leica Microsystems) with a 420 – 500 nm, 500 – 560 nm, 590 – 670 nm, 660 – 720 nm spectral detection window for DAPI, ExoGlow-RNA EV, Alexa Flour 594, and ATTO 647N detection, respectively. For depletion, a 775 nm pulsed laser was used for Alexa Fluor 594 and ATTO 647N, whereas a 660 continuous wave laser was used for depletion of ExoGlow-RNA EV. DAPI was not depleted and only imaged with confocal resolution. The image size was set to 1024 × 1024 pixels and a 5-fold zoom factor was applied, giving a pixel size of 0.023 μm and an image size of 23,25 × 23,25 μm. For FLIM, the white light laser delivered 80 MHz repetition rate. Arrival time of single photons was measured with the included FALCON module and 8 frames were acquired at a scanning speed of 200 Hz. Recordings were done sequentially for each dye to avoid cross-talk. Raw STED images were further processed with the τ-STED module of LAS X software (Leica

Microsystems, Germany) increasing further the resolution thanks to the lifetime information recorded.

Sample preparation for mass spectrometry, MS data acquisition and raw data analysis of MS measurement

We collected and purified extracellular and intracellular vesicles (EVs and IVs) from 2D and 3D cultures. The vesicles were lysed in RIPA buffer (150mM NaCl, 50mM Tris pH8, 0.1% DOC, 0.1% SDS, 0.1% NP40).We applied a modified version of FASP protocol (Wiśniewski et al., 2009). to 10 ug of protein extract. More details are reported in (Pipicelli et al., 2022).
We processed the raw data, obtained using TimsControl, with the MaxQuant software (version 1.6.17.0) (Tyanova et al., 2016), the used settings can be found in (Prianichnikov et al., 2020). Proteins were quantified across samples using the label-free quantification algorithm in MaxQuant generating label-free quantification (LFQ) intensities.

Proteomic bioinformatic analysis

We identified a total of 7876 proteins in IVs and EVs. We retained the proteins that consistently were detected in two of the three technical replicates, in each condition.The downstream analysis and data visualization were performed using R. We transformed the LFQs values in the log2-scale. The missing values were imputed using the R package DEP (version 1.15.0) and replaced by random values of a left-shifted Gaussian distribution (shift of 1.8 units of the standard deviation and a width of 0.3). We identified differentially expressed (DE) proteins on the imputed dataset, using Student's t-Test. We considered as DE, proteins with with log2 fold change values (log2FC) ≥ 1 and ≤ -1 and with an FDR-corrected q-value < 0.05. We analyzed genes associated to neurological disorders by consulting the DisGeNET website (https://www.disgenet.org/search) (Piñero et al., 2017).

Enrichment analysis

Enrichment analysis was performed as described in Chapter 7.3, "Enrichment analysis".

8 References

Agnati, L.F., and Fuxe, K. (2014). Extracellular-vesicle type of volume transmission and tunnelling-nanotube type of wiring transmission add a new dimension to brain neuro-glial networks. Philos. Trans. R. Soc. B Biol. Sci. *369*.

Aka, S., Alanay, Y., Boodhansingh, K.E., Stanley, C.A., and Semiz, S. (2016). Seizures and diagnostic difficulties in hyperinsulinism-hyperammonemia syndrome. Turk. J. Pediatr.

Albert, M., Kalebic, N., Florio, M., Lakshmanaperumal, N., Haffner, C., Brandl, H., Henry, I., and Huttner, W.B. (2017). Epigenome profiling and editing of neocortical progenitor cells during development. EMBO J. *36*, 2642–2658.

Alcantara, D., Timms, A.E., Gripp, K., Baker, L., Park, K., Collins, S., Cheng, C., Stewart, F., Mehta, S.G., Saggar, A., et al. (2017). Mutations of AKT3 are associated with a wide spectrum of developmental disorders including extreme megalencephaly. Brain *140*, 2610–2622.

Alvarez-buylla, A., and Nottebohm, F. CfJ ·'·. 353–354.

Amin, S., and Borrell, V. (2020). The Extracellular Matrix in the Evolution of Cortical Development and Folding. Front. Cell Dev. Biol. *8*.

Anthony, T.E., Klein, C., Fishell, G., and Heintz, N. (2004). Radial glia serve as neuronal progenitors in all regions of the central nervous system. Neuron *41*, 881–890.

Arai, Y., and Taverna, E. (2017). Neural progenitor cell polarity and cortical development. Front. Cell. Neurosci. *11*, 1–11.

Ariza, J., Rogers, H., Hashemi, E., Noctor, S.C., and Martínez-cerdeño, V. (2018). The Number of Chandelier and Basket Cells Are Differentially Decreased in Prefrontal Cortex in Autism. 411–420.

Bagley, J.A., Reumann, D., Bian, S., Lévi-Strauss, J., and Knoblich, J.A. (2017a). Fused dorsal-ventral cerebral organoids model complex interactions between diverse brain regions. Nat. Methods *14*, 743–751.

Bagley, J.A., Reumann, D., Bian, S., Lévi-Strauss, J., and Knoblich, J.A. (2017b). Fused cerebral organoids model interactions between brain regions. Nat. Methods.

Bagley Joshua A , Reumann Daniel , Bian Shan, J.A.K. (2017). Fused dorsal-ventral cerebral organoids model human cortical interneuron migration. BioRxiv.

Bahi-Buisson, N., Poirier, K., Boddaert, N., Saillour, Y., Castelnau, L., Philip, N., Buyse, G., Villard, L., Joriot, S., Marret, S., et al. (2008). Refinement of cortical dysgeneses spectrum associated with TUBA1A mutations. J. Med. Genet. *45*, 647–653.

Barkovich, A.J., and Kuzniecky, R.I. (2000). Gray matter heterotopia. Neurology *55*, 1603–1608.

Barkovich, A.J., Guerrini, R., Kuzniecky, R.I., Jackson, G.D., and Dobyns, W.B. (2012). A developmental and genetic classification for malformations of cortical development: Update 2012. Brain *135*, 1348–1369.

Bassuk, A.G., Wallace, R.H., Buhr, A., Buller, A.R., Afawi, Z., Shimojo, M., Miyata, S., Chen, S., Gonzalez-Alegre, P., Griesbach, H.L., et al. (2008). A Homozygous Mutation in Human PRICKLE1 Causes an Autosomal-Recessive Progressive Myoclonus Epilepsy-Ataxia Syndrome. Am. J. Hum. Genet.

Batista, B.S., Eng, W.S., Pilobello, K.T., Hendricks-Muñoz, K.D., and Mahal, L.K.

(2011). Identification of a conserved glycan signature for microvesicles. J. Proteome Res. *10*, 4624–4633.

Baudoin, J.P., Viou, L., Launay, P.S., Luccardini, C., Espeso Gil, S., Kiyasova, V., Irinopoulou, T., Alvarez, C., Rio, J.P., Boudier, T., et al. (2012). Tangentially Migrating Neurons Assemble a Primary Cilium that Promotes Their Reorientation to the Cortical Plate. Neuron *76*, 1108–1122.

Beattie, R., and Hippenmeyer, S. (2017). Mechanisms of radial glia progenitor cell lineage progression. FEBS Lett. *591*, 3993–4008.

Bellion, A., Baudoin, J.P., Alvarez, C., Bornens, M., and Métin, C. (2005). Nucleokinesis in tangentially migrating neurons comprises two alternating phases: Forward migration of the Golgi/centrosome associated with centrosome splitting and myosin contraction at the rear. J. Neurosci. *25*, 5691–5699.

Bershteyn, M., Nowakowski, T.J., Pollen, A.A., Di Lullo, E., Nene, A., Wynshaw-Boris, A., and Kriegstein, A.R. (2017). Human iPSC-Derived Cerebral Organoids Model Cellular Features of Lissencephaly and Reveal Prolonged Mitosis of Outer Radial Glia. Cell Stem Cell *20*, 435-449.e4.

Betizeau, M., Cortay, V., Patti, D., Pfister, S., Gautier, E., Bellemin-Ménard, A., Afanassieff, M., Huissoud, C., Douglas, R.J., Kennedy, H., et al. (2013). Precursor Diversity and Complexity of Lineage Relationships in the Outer Subventricular Zone of the Primate. Neuron *80*, 442–457.

Bielen, H., and Houart, C. (2014). The Wnt cries many: Wnt regulation of neurogenesis through tissue patterning, proliferation, and asymmetric cell division. Dev. Neurobiol. *74*, 772–780.

Birey, F., Andersen, J., Makinson, C.D., Islam, S., Wei, W., Huber, N., Fan, H.C., Metzler, K.R.C., Panagiotakos, G., Thom, N., et al. (2017). Assembly of functionally integrated human forebrain spheroids. Nature *545*, 54–59.

Bizzotto, S., and Francis, F. (2015). Morphological and functional aspects of progenitors perturbed in cortical malformations. Front. Cell. Neurosci. *9*, 1–10.

Bizzotto, S., Uzquiano, A., Dingli, F., Ershov, D., Houllier, A., Arras, G., Richards, M., Loew, D., Minc, N., Croquelois, A., et al. (2017). Eml1 loss impairs apical progenitor spindle length and soma shape in the developing cerebral cortex. Sci. Rep. *7*, 1–14.

Bond, J., Roberts, E., Mochida, G.H., Hampshire, D.J., Scott, S., Askham, J.M., Springell, K., Mahadevan, M., Crow, Y.J., Markham, A.F., et al. (2002). ASPM is a major determinant of cerebral cortical size. Nat. Genet. *32*, 316–320.

Borello, U., Cobos, I., Long, J.E., Murre, C., and Rubenstein, J.L.R. (2008). FGF15 promotes neurogenesis and opposes FGF8 function during neocortical development. Neural Dev. *3*.

Borrell, V., and Götz, M. (2014). Role of radial glial cells in cerebral cortex folding. Curr. Opin. Neurobiol. *27*, 39–46.

Boyer, L.F., Campbell, B., Larkin, S., Mu, Y., and Gage, F.H. (2012). Dopaminergic differentiation of human pluripotent cells. Curr. Protoc. Stem Cell Biol. *Chapter 1*, Unit1H.6.

Bozzi, Y., Casarosa, S., and Caleo, M. (2012). Epilepsy as a neurodevelopmental disorder. Front. Psychiatry *3*, 1–14.

Brennand, K.J., Simone, A., Jou, J., Gelboin-Burkhart, C., Tran, N., Sangar, S., Li, Y., Mu, Y., Chen, G., Yu, D., et al. (2011). Modelling schizophrenia using human induced pluripotent stem cells. Nature *473*, 221–225.

Briscoe, J., and Ericson, J. (2001). Specification of neuronal fates in the ventral neural tube. Curr. Opin. Neurobiol. *11*, 43–49.

Brown, K.N., Chen, S., Han, Z., Lu, C.H., Tan, X., Zhang, X.J., Ding, L., Lopez-Cruz,

A., Saur, D., Anderson, S.A., et al. (2011). Clonal production and organization of inhibitory interneurons in the neocortex. Science (80-.). *334*, 480–486.

Buchsbaum, I.Y., and Cappello, S. (2019a). Neuronal migration in the CNS during development and disease: insights from in vivo and in vitro models.

Buchsbaum, I.Y., and Cappello, S. (2019b). Neuronal migration in the CNS during development and disease: insights from in vivo and in vitro models.

Buchsbaum, I.Y., and Cappello, S. (2019c). Neuronal migration in the CNS during development and disease: Insights from in vivo and in vitro models. Dev. *146*.

Buchsbaum, I.Y., Kielkowski, P., Giorgio, G., O'Neill, A.C., Di Giaimo, R., Kyrousi, C., Khattak, S., Sieber, S.A., Robertson, S.P., and Cappello, S. (2020). ECE 2 regulates neurogenesis and neuronal migration during human cortical development . EMBO Rep. *21*, 1–24.

Butt, S.J.B., Fuccillo, M., Nery, S., Noctor, S., Kriegstein, A., Corbin, J.G., and Fishell, G. (2005). The temporal and spatial origins of cortical interneurons predict their physiological subtype. Neuron *48*, 591–604.

Buzzi, A., Chikhladze, M., Falcicchia, C., Paradiso, B., Lanza, G., Soukupova, M., Marti, M., Morari, M., Franceschetti, S., and Simonato, M. (2012a). Loss of cortical GABA terminals in Unverricht-Lundborg disease. Neurobiol. Dis.

Buzzi, A., Chikhladze, M., Falcicchia, C., Paradiso, B., Lanza, G., Soukupova, M., Marti, M., Morari, M., Franceschetti, S., and Simonato, M. (2012b). Neurobiology of Disease Loss of cortical GABA terminals in Unverricht – Lundborg disease. Neurobiol. Dis. *47*, 216–224.

Canafoglia, L., Gennaro, E., Capovilla, G., Gobbi, G., Boni, A., Beccaria, F., Viri, M., Michelucci, R., Agazzi, P., Assereto, S., et al. (2012). Electroclinical presentation and genotype-phenotype relationships in patients with Unverricht-Lundborg disease carrying compound heterozygous CSTB point and indel mutations. Epilepsia.

Capone, E., Lamolinara, A., Pastorino, F., Gentile, R., Ponziani, S., Di Vittorio, G., D'agostino, D., Bibbò, S., Rossi, C., Piccolo, E., et al. (2020). Targeting vesicular lgals3bp by an antibody-drug conjugate as novel therapeutic strategy for neuroblastoma. Cancers (Basel). *12*, 1–18.

Capone, E., Iacobelli, S., and Sala, G. (2021a). Role of galectin 3 binding protein in cancer progression: a potential novel therapeutic target. J. Transl. Med. *19*, 1–19.

Capone, E., Iacobelli, S., and Sala, G. (2021b). Role of galectin 3 binding protein in cancer progression: a potential novel therapeutic target. J. Transl. Med. *19*, 1–18.

Cappello, S., Böhringer, C.R.J., Bergami, M., Conzelmann, K.K., Ghanem, A., Tomassy, G.S., Arlotta, P., Mainardi, M., Allegra, M., Caleo, M., et al. (2012a). A Radial Glia-Specific Role of RhoA in Double Cortex Formation. Neuron *73*, 911–924.

Cappello, S., Bohringer, C.R., Bergami, M., Conzelmann, K.K., Ghanem, A., Tomassy, G.S., Arlotta, P., Mainardi, M., Allegra, M., Caleo, M., et al. (2012b). A radial glia-specific role of RhoA in double cortex formation. Neuron *73*, 911–924.

Cappello, S., Gray, M.J., Badouel, C., Lange, S., Einsiedler, M., Srour, M., Chitayat, D., Hamdan, F.F., Jenkins, Z.A., Morgan, T., et al. (2013). Mutations in genes encoding the cadherin receptor-ligand pair DCHS1 and FAT4 disrupt cerebral cortical development. Nat. Genet. *45*, 1300–1308.

Carabalona, A., Beguin, S., Pallesi-pocachard, E., Buhler, E., Pellegrino, C., Arnaud, K., Hubert, P., Oualha, M., Siffroi, J.P., Khantane, S., et al. (2012). A glial origin for periventricular nodular heterotopia caused by impaired expression of Filamin-A. Hum. Mol. Genet. *21*, 1004–

1017.

Cava, C., Manna, I., Gambardella, A., Bertoli, G., and Castiglioni, I. (2018). Potential Role of miRNAs as Theranostic Biomarkers of Epilepsy. Mol. Ther. - Nucleic Acids.

Caviness, V.S. (1982). Neocortical histogenesis in normal and reeler mice: A developmental study based upon [3H]thymidine autoradiography. Dev. Brain Res. *4*, 293–302.

Chambers, S.M., Fasano, C.A., Papapetrou, E.P., Tomishima, M., Sadelain, M., and Studer, L. (2009). Highly efficient neural conversion of human ES and iPS cells by dual inhibition of SMAD signaling. Nat. Biotechnol. *27*, 275–280.

Chen, F., and LoTurco, J. (2012). A method for stable transgenesis of radial glia lineage in rat neocortex by piggyBac mediated transposition. J. Neurosci. Methods *207*, 172–180.

Chen, I.H., Xue, L., Hsu, C.C., Paez, J.S.P., Panb, L., Andaluz, H., Wendt, M.K., Iliuk, A.B., Zhu, J.K., and Tao, W.A. (2017). Phosphoproteins in extracellular vesicles as candidate markers for breast cancer. Proc. Natl. Acad. Sci. U. S. A. *114*, 3175–3180.

Chi, L., Fan, B., Feng, D., Chen, Z., Liu, Z., Hui, Y., Xu, X., Ma, L., Fang, Y., Zhang, Q., et al. (2017). The Dorsoventral Patterning of Human Forebrain Follows an Activation/Transformation Model. Cereb. Cortex *27*, 2941–2954.

Chiang, C., Litingtung, Y., Lee, E., Youngt, K.E., Cordent, J.L., Westphal, H., and Beachyt, P.A. (1996). mice lacking Sonic hedgehog gene function. Nature *383*, 407–413.

Ciardiello, C., Cavallini, L., Spinelli, C., Yang, J., Reis-Sobreiro, M., Candia, P. De, Minciacchi, V.R., and Di Vizio, D. (2016). Focus on extracellular vesicles: New frontiers of cell-to-cell communication in cancer. Int. J. Mol. Sci. *17*, 1–17.

Cipollini, E., Riccio, M., Di Giaimo, R., Dal Piaz, F., Pulice, G., Catania, S., Caldarelli, I., Dembic, M., Santi, S., and Melli, M. (2008). Cystatin B and its EPM1 mutants are polymeric and aggregate prone in vivo. Biochim. Biophys. Acta - Mol. Cell Res. *1783*, 312–322.

Cobos, I., Calcagnotto, M.E., Vilaythong, A.J., Thwin, M.T., Noebels, J.L., Baraban, S.C., and Rubenstein, J.L.R. (2005). Mice lacking Dlx1 show subtype-specific loss of interneurons, reduced inhibition and epilepsy. Nat. Neurosci. *8*, 1059–1068.

Costa, J., Pronto-Laborinho, A., Pinto, S., Gromicho, M., Bonucci, S., Tranfield, E., Correia, C., Alexandre, B.M., and de Carvalho, M. (2020). Investigating LGALS3BP/90 K glycoprotein in the cerebrospinal fluid of patients with neurological diseases. Sci. Rep. *10*, 5649.

Cubelos, B., Sebastián-Serrano, A., Beccari, L., Calcagnotto, M.E., Cisneros, E., Kim, S., Dopazo, A., Alvarez-Dolado, M., Redondo, J.M., Bovolenta, P., et al. (2010). Cux1 and Cux2 regulate dendritic branching, spine morphology, and synapses of the upper layer neurons of the cortex. Neuron *66*, 523–535.

D'Acunzo, P., Pérez-González, R., Kim, Y., Hargash, T., Miller, C., Alldred, M.J., Erdjument-Bromage, H., Penikalapati, S.C., Pawlik, M., Saito, M., et al. (2021). Mitovesicles are a novel population of extracellular vesicles of mitochondrial origin altered in down syndrome. Sci. Adv. *7*, 1–19.

D'Amato, E., Kokaia, Z., Nanobashvili, A., Reeben, M., Lehesjoki, A.E., Saarma, M., and Lindvall, O. (2000). Seizures induce widespread upregulation of cystatin B, the gene mutated in progressive myoclonus epilepsy, in rat forebrain neurons. Eur. J. Neurosci.

D'Gama, A.M., Geng, Y., Couto, J.A., Martin, B., Boyle, E.A., LaCoursiere, C.M., Hossain, A., Hatem, N.E., Barry, B., Kwiatkowski, D.J., et al. (2015). mTOR pathway mutations cause

hemimegalencephaly and focal cortical dysplasia. Ann. Neurol. *77*, 720–725.

Danner, N., Julkunen, P., Hyppönen, J., Niskanen, E., Säisänen, L., Könönen, M., Koskenkorva, P., Vanninen, R., Kälviäinen, R., and Mervaala, E. (2013). Alterations of motor cortical excitability and anatomy in unverricht-lundborg disease. Mov. Disord.

DeMyer, W. (1986). Megalencephaly: Types, clinical syndromes, and management. Pediatr. Neurol. *2*, 321–328.

Desikan, R.S., and Barkovich, A.J. (2016). Malformations of cortical development. Ann. Neurol. *80*, 797–810.

Deun, J. Van, Roux, Q., Deville, S., Acker, T. Van, Rappu, P., Miinalainen, I., Heino, J., Vanhaecke, F., Geest, B.G. De, Wever, O. De, et al. (2020). Feasibility of Mechanical Extrusion to Coat Nanoparticles with Extracellular Vesicle Membranes. Cells 2020, Vol. 9, Page 1797 *9*, 1797.

Dibbens, L.M., Michelucci, R., Gambardella, A., Andermann, F., Rubboli, G., Bayly, M.A., Joensuu, T., Vears, D.F., Franceschetti, S., Canafoglia, L., et al. (2009). SCARB2 mutations in progressive myoclonus epilepsy (PME) without renal failure. Ann. Neurol.

Dityatev, A. (2010). Remodeling of extracellular matrix and epileptogenesis. In Epilepsia, p.

Dubeau, F., Tampieri, D., Lee, N., Andermann, E., Carpenter, S., Leblanc, R., Olivier, A., Radtke, R., Villemure, J.G., and Andermann, F. (1995). Periventricular and subcortical nodular heterotopia. A study of 33 patients. Brain *118*, 1273–1287.

Ekşioğlu, Y.Z., Scheffer, I.E., Cardenas, P., Knoll, J., DiMario, F., Ramsby, G., Berg, M., Kamuro, K., Berkovic, S.F., Duyk, G.M., et al. (1996). Periventricular heterotopia: An X-linked dominant epilepsy locus causing aberrant cerebral cortical development. Neuron *16*, 77–87.

Elkabetz, Y., Panagiotakos, G., Al Shamy, G., Socci, N.D., Tabar, V., and Studer, L. (2008). Human ES cell-derived neural rosettes reveal a functionally distinct early neural stem cell stage. Genes Dev. *22*, 152–165.

Ercegovac, M., Jovic, N., Sokic, D., Savic-Radojevic, A., Coric, V., Radic, T., Nikolic, D., Kecmanovic, M., Matic, M., Simic, T., et al. (2015). GSTA1, GSTM1, GSTP1 and GSTT1 polymorphisms in progressive myoclonus epilepsy: A Serbian case-control study. Seizure.

Ericson, J., Muhr, J., Placzek, M., Lints, T., Jessel, T.M., and Edlund, T. (1995). Sonic hedgehog induces the differentiation of ventral forebrain neurons: A common signal for ventral patterning within the neural tube. Cell *81*, 747–756.

Escrevente, C., Grammel, N., Kandzia, S., Zeiser, J., Tranfield, E.M., Conradt, H.S., and Costa, J. (2013). Sialoglycoproteins and N-Glycans from Secreted Exosomes of Ovarian Carcinoma Cells. PLoS One *8*, 1–11.

Feng, Y., Chen, M.H., Moskowitz, I.P., Mendonza, A.M., Vidali, L., Nakamura, F., Kwiatkowski, D.J., and Walsh, C.A. (2006). Filamin a (FLNA) is required for cell-cell contact in vascular development and cardiac morphogenesis. PNAS *103*, 19836–19841.

Ferland, R.J., Batiz, L.F., Neal, J., Lian, G., Bundock, E., Lu, J., Hsiao, Y.C., Diamond, R., Mei, D., Banham, A.H., et al. (2009). Disruption of neural progenitors along the ventricular and subventricular zones in periventricular heterotopia. Hum. Mol. Genet. *18*, 497–516.

Ferrara, E., Cefaliello, C., Eyman, M., De Stefano, R., Giuditta, A., and Crispino, M. (2009). Synaptic mRNAs are modulated by learning. J. Neurosci. Res. *87*, 1960–1968.

Fietz, S.A., and Huttner, W.B. (2010). Cortical progenitor expansion , self-renewal and neurogenesis — a polarized perspective. Curr. Opin. Neurobiol. 1–13.

Fietz, S.A., Kelava, I., Vogt, J., Wilsch-Bräuninger, M., Stenzel, D., Fish, J.L., Corbeil, D., Riehn, A., Distler, W., Nitsch, R., et al. (2010). OSVZ progenitors of human and ferret neocortex are epithelial-like and expand by integrin signaling. Nat. Neurosci. *13*, 690–699.

Fietz, S.A., Lachmann, R., Brandl, H., Kircher, M., Samusik, N., Schröder, R., Lakshmanaperumal, N., Henry, I., Vogt, J., Riehn, A., et al. (2012). Transcriptomes of germinal zones of human and mouse fetal neocortex suggest a role of extracellular matrix in progenitor self-renewal. Proc. Natl. Acad. Sci. U. S. A. *109*, 11836–11841.

Fish, J.L., Dehay, C., Kennedy, H., and Huttner, W.B. (2008). Making bigger brains - The evolution of neural-progenitor-cell division. J. Cell Sci. *121*, 2783–2793.

Flames, N., Long, J.E., Garratt, A.N., Fischer, T.M., Gassmann, M., Birchmeier, C., Lai, C., Rubenstein, J.L.R., and Marín, O. (2004). Short- and long-range attraction of cortical GABAergic interneurons by neuregulin-1. Neuron *44*, 251–261.

Flames, N., Pla, R., Gelman, D.M., Rubenstein, J.L.R., Puelles, L., and Marín, O. (2007). Delineation of multiple subpallial progenitor domains by the combinatorial expression of transcriptional codes. J. Neurosci. *27*, 9682–9695.

Flandin, P., Zhao, Y., Vogt, D., Jeong, J., Long, J., Potter, G., Westphal, H., and Rubenstein, J.L.R. (2011). Lhx6 and Lhx8 Coordinately Induce Neuronal Expression of Shh that Controls the Generation of Interneuron Progenitors. Neuron *70*, 939–950.

Fleck, J.S., Sanchís-Calleja, F., He, Z., Santel, M., Boyle, M.J., Camp, J.G., and Treutlein, B. (2021). Resolving organoid brain region identities by mapping single-cell genomic data to reference atlases. Cell Stem Cell *28*, 1148-1159.e8.

Florio, M., and Huttner, W.B. (2014). Neural progenitors , neurogenesis and the evolution of the neocortex. 2182–2194.

Florio, M., Borrell, V., and Huttner, W.B. (2017). Human-specific genomic signatures of neocortical expansion. Curr. Opin. Neurobiol. *42*, 33–44.

Fogeron, M.L., Müller, H., Schade, S., Dreher, F., Lehmann, V., Kühnel, A., Scholz, A.K., Kashofer, K., Zerck, A., Fauler, B., et al. (2013). LGALS3BP regulates centriole biogenesis and centrosome hypertrophy in cancer cells. Nat. Commun. *4*.

Fox, J.W., Lamperti, E.D., Ekşioğlu, Y.Z., Hong, S.E., Feng, Y., Graham, D.A., Scheffer, I.E., Dobyns, W.B., Hirsch, B.A., Radtke, R.A., et al. (1998). Mutations in filamin 1 prevent migration of cerebral cortical neurons in human Periventricular heterotopia. Neuron *21*, 1315–1325.

Frantz, C., Stewart, K.M., and Weaver, V.M. (2010). The extracellular matrix at a glance. J. Cell Sci. *123*, 4195–4200.

Fuccillo, M., Rutlin, M., and Fishell, G. (2006). Removal of Pax6 partially rescues the los of ventral structures in Shh null mice. Cereb. Cortex *16*, 96–102.

Gertz, C.C., and Kriegstein, A.R. (2015). Neuronal migration dynamics in the developing ferret cortex. J. Neurosci. *35*, 14307–14315.

Gilmore, E.C., and Walsh, C.A. (2013). Genetic causes of microcephaly and lessons for neuronal development. Wiley Interdiscip. Rev. Dev. Biol. *2*, 461–478.

Gomes, J., Gomes-Alves, P., Carvalho, S.B., Peixoto, C., Alves, P.M., Altevogt, P., and Costa, J. (2015). Extracellular vesicles from ovarian carcinoma cells display specific glycosignatures. Biomolecules *5*, 1741–1761.

Gong, J., Körner, R., Gaitanos, L., and Klein, R. (2016). Exosomes mediate cell contact-independent ephrin-Eph signaling during axon guidance. J. Cell Biol. *214*, 35–44.

Götz, M., and Huttner, W.B. (2005). The cell biology of neurogenesis. Nat. Rev. Mol.

Cell Biol. *6*, 777–788.

Götz, M., Stoykova, A., and Gruss, P. (1998). Pax6 controls radial glia differentiation in the cerebral cortex. Neuron *21*, 1031–1044.

Grace-Dutton, K.H. (2005). Exploring the brain Fourth Edition. Pharm. J. *275*, 283.

Grassadonia, A., Tinari, N., Iurisci, I., Piccolo, E., Cumashi, A., Innominato, P., D'Egidio, M., Natoli, C., Piantelli, M., and Iacobelli, S. (2002). 90K (Mac-2 BP) and galectins in tumor progression and metastasis. Glycoconj. J. *19*, 551–556.

Guerrini, R., and Dobyns, W.B. (2014). Malformations of cortical development: Clinical features and genetic causes. Lancet Neurol. *13*, 710–726.

Gunhanlar, N., Shpak, G., van der Kroeg, M., Gouty-Colomer, L.A., Munshi, S.T., Lendemeijer, B., Ghazvini, M., Dupont, C., Hoogendijk, W.J.G., Gribnau, J., et al. (2017a). A simplified protocol for differentiation of electrophysiologically mature neuronal networks from human induced pluripotent stem cells. Mol. Psychiatry 1–9.

Gunhanlar, N., Shpak, G., van der Kroeg, M., Gouty-Colomer, L.A., Munshi, S.T., Lendemeijer, B., Ghazvini, M., Dupont, C., Hoogendijk, W.J.G., Gribnau, J., et al. (2017b). A simplified protocol for differentiation of electrophysiologically mature neuronal networks from human induced pluripotent stem cells. Mol. Psychiatry 2018 235 *23*, 1336–1344.

Guo, J., and Anton, E.S. (2014). Decision making during interneuron migration in the developing cerebral cortex. Trends Cell Biol. *24*, 342–351.

Guo, W., Shang, D.M., Cao, J.H., Feng, K., He, Y.C., Jiang, Y., Wang, S.P., and Gao, Y.F. (2017). Identifying and analyzing novel epilepsy-related genes using random walk with restart algorithm. Biomed Res. Int.

Hakanen, J., Ruiz-reig, N., Tissir, F., and Francis, F. (2019). Linking Cell Polarity to Cortical Development and Malformations. *13*, 1–22.

Hamasaki, T., Goto, S., Nishikawa, S., and Ushio, Y. (2001). Early-generated preplate neurons in the developing telencephalon: Inward migration into the developing striatum. Cereb. Cortex *11*, 474–484.

Hansen, D. V., Lui, J.H., Parker, P.R.L., and Kriegstein, A.R. (2010). Neurogenic radial glia in the outer subventricular zone of human neocortex. Nature *464*, 554–561.

Haubensak, W., Attardo, A., Denk, W., and Huttner, W.B. (2004). Neurons arise in the basal neuroepithelium of the early mammalian telencephalon: A major site of neurogenesis. Proc. Natl. Acad. Sci. U. S. A. *101*, 3196–3201.

Herz, J., and Chen, Y. (2006). Reelin , lipoprotein receptors and synaptic plasticity. *7*, 850–859.

Hong, S.E., Shugart, Y.Y., Huang, D.T., Shahwan, S. Al, Grant, P.E., Jonathan, O.B., Martin, N.D.T., and Walsh, C.A. (2000). Autosomal recessive lissencephaly with cerebellar hypoplasia is associated with human RELN mutations. *26*, 93–96.

Howard, B.M., Mo, Z., Filipovic, R., Moore, A.R., Antic, S.D., and Zecevic, N. (2008). Radial glia cells in the developing human brain. Neuroscientist *14*, 459–473.

Hu, W.F., Chahrour, M.H., and Walsh, C.A. (2014). The diverse genetic landscape of neurodevelopmental disorders. Annu. Rev. Genomics Hum. Genet. *15*, 195–213.

Hung, L.-Y., Tang, C.-J.C., and Tang, T.K. (2000). Protein 4.1 R-135 interacts with a novel centrosomal protein (CPAP) which is associated with the gamma-tubulin complex. Mol. Cell. Biol. *20*, 7813–7825.

Hyenne, V., Labouesse, M., and Goetz, J.G. (2018). The Small GTPase Ral orchestrates MVB biogenesis and exosome secretion. Small GTPases *9*, 445–451.

Hynes, R.O. (2009). The extracellu. Science

(80-.). *326*, 1216–1219.

Iefremova, V., Manikakis, G., Krefft, O., Jabali, A., Weynans, K., Wilkens, R., Marsoner, F., Brändl, B., Müller, F.J., Koch, P., et al. (2017). An Organoid-Based Model of Cortical Development Identifies Non-Cell-Autonomous Defects in Wnt Signaling Contributing to Miller-Dieker Syndrome. Cell Rep. *19*, 50–59.

Ingham, P.W., and McMahon, A.P. (2001). Hedgehog signaling in animal development: Paradigms and principles. Genes Dev. *15*, 3059–3087.

Ishiuchi, T., Misaki, K., Yonemura, S., Takeichi, M., and Tanoue, T. (2009). Mammalian Fat and Dachsous cadherins regulate apical membrane organization in the embryonic cerebral cortex. J. Cell Biol. *185*, 959–967.

Ismail, F.Y., and Shapiro, B.K. (2019). What are neurodevelopmental disorders? Curr. Opin. Neurol. *32*, 611–616.

Janas, A.M., Sapoń, K., Janas, T., Stowell, M.H.B., and Janas, T. (2016). Exosomes and other extracellular vesicles in neural cells and neurodegenerative diseases. Biochim. Biophys. Acta - Biomembr. *1858*, 1139–1151.

Jansen, A.C., Oostra, A., Desprechins, B., De Vlaeminck, Y., Verhelst, H., Régal, L., Verloo, P., Bockaert, N., Keymolen, K., Seneca, S., et al. (2011). TUBA1A mutations: From isolated lissencephaly to familial polymicrogyria. Neurology *76*, 988–992.

Jessell TM (2000). Neuronal specification in the spinal cord:inductive signals and transcriptional codes. Nat. Rev. Genet. *1*, 20–29.

Jo, J., Xiao, Y., Sun, A.X., Cukuroglu, E., Tran, H.-D., Göke, J., Tan, Z.Y., Saw, T.Y., Tan, C.-P., Lokman, H., et al. (2016). Midbrain-like Organoids from Human Pluripotent Stem Cells Contain Functional Dopaminergic and Neuromelanin-Producing Neurons. Cell Stem Cell *19*, 248–257.

Joensuu, T., Lehesjoki, A., Kopra, O., and Lundborg, U. Molecular background of EPM1 — Unverricht – Lundborg disease.

Johansson, P.A., Dziegielewska, K.M., Ek, C.J., Habgood, M.D., Liddelow, S.A., Potter, A.M., Stolp, H.B., and Saunders, N.R. (2006). Blood-CSF barrier function in the rat embryo. Eur. J. Neurosci.

Kadoshima, T., Sakaguchi, H., Nakano, T., Soen, M., Ando, S., Eiraku, M., and Sasai, Y. (2013). Self-organization of axial polarity, inside-out layer pattern, and species-specific progenitor dynamics in human ES cell-derived neocortex. Proc. Natl. Acad. Sci. *110*, 20284–20289.

Kalluri, R., and LeBleu, V.S. (2020). The biology, function, and biomedical applications of exosomes. Science (80-.). *367*.

Kälviäinen, R., Khyuppenen, J., Koskenkorva, P., Eriksson, K., Vanninen, R., and Mervaala, E. (2008). Clinical picture of EPM1-Unverricht-Lundborg disease. Epilepsia.

Kanton, S., Boyle, M.J., He, Z., Santel, M., Weigert, A., Sanchís-Calleja, F., Guijarro, P., Sidow, L., Fleck, J.S., Han, D., et al. (2019). Organoid single-cell genomic atlas uncovers human-specific features of brain development.

Karzbrun, E., Kshirsagar, A., Cohen, S.R., Hanna, J.H., and Reiner, O. (2018). Human brain organoids on a chip reveal the physics of folding. Nat. Phys. *14*, 515–522.

Katz, L.C., and Shatz, C.J. (1996). Synaptic activity and the construction of cortical circuits. Science (80-.). *274*, 1133–1138.

Keays, D.A., Tian, G., Poirier, K., Huang, G.J., Siebold, C., Cleak, J., Oliver, P.L., Fray, M., Harvey, R.J., Molnár, Z., et al. (2007). Mutations in α-Tubulin Cause Abnormal Neuronal Migration in Mice and Lissencephaly in Humans. Cell *128*, 45–57.

Kepecs, A., and Fishell, G. (2014).

Interneuron cell types are fit to function. Nature *505*, 318–326.

Kielar, M., Tuy, F.P., Bizzotto, S., Lebrand, C., de Juan Romero, C., Poirier, K., Oegema, R., Mancini, G.M., Bahi-Buisson, N., Olaso, R., et al. (2014). Mutations in Eml1 lead to ectopic progenitors and neuronal heterotopia in mouse and human. Nat Neurosci *17*, 923–933.

Klaus, J., Kanton, S., Kyrousi, C., Cristina Ayo-Martin, A., Di Giaimo, R., Riesenberg, S., O, A.C., Gray Camp, J., Tocco, C., Santel, M., et al. Altered neuronal migratory trajectories in human cerebral organoids derived from individuals with neuronal heterotopia. Nat. Med.

Klaus, J., Kanton, S., Kyrousi, C., Ayo-Martin, A.C., Di Giaimo, R., Riesenberg, S., O'Neill, A.C., Camp, J.G., Tocco, C., Santel, M., et al. (2019). Altered neuronal migratory trajectories in human cerebral organoids derived from individuals with neuronal heterotopia. Nat. Med.

Klingler, E., Francis, F., Jabaudon, D., and Cappello, S. (2021). Mapping the molecular and cellular complexity of cortical malformations. Science (80-.). *371*.

Kodaka, M., and Hata, Y. (2015). The mammalian Hippo pathway: Regulation and function of YAP1 and TAZ. Cell. Mol. Life Sci. *72*, 285–306.

Koskenkorva, P., Khyuppenen, J., Niskanen, E., Könönen, M., Bendel, P., Mervaala, E., Lehesjoki, A.E., Kälviäinen, R., and Vanninen, R. (2009). Motor cortex and thalamic atrophy in Unverricht-Lundborg disease: Voxel-based morphometric study. Neurology.

Kriegstein, A.R., and Noctor, S.C. (2004). Patterns of neuronal migration in the embryonic cortex. Trends Neurosci. *27*, 392–399.

Kriegstein, A., Noctor, S., and Martínez-cerdeño, V. (2006). Embryonic day. *7*, 883–890.

Krienen, F.M., Goldman, M., Zhang, Q., C. H. del Rosario, R., Florio, M., Machold, R., Saunders, A., Levandowski, K., Zaniewski, H., Schuman, B., et al. (2020). Innovations present in the primate interneuron repertoire. Nature *586*, 262–269.

Kyrousi, C., and Cappello, S. (2019). Using brain organoids to study human neurodevelopment, evolution and disease. Wiley Interdiscip. Rev. Dev. Biol. e347.

Kyrousi, C., O'Neill, A.C., Brazovskaja, A., He, Z., Kielkowski, P., Coquand, L., Di Giaimo, R., D' Andrea, P., Belka, A., Forero Echeverry, A., et al. (2021). Extracellular LGALS3BP regulates neural progenitor position and relates to human cortical complexity. Nat. Commun. *12*, 1–22.

Lafrenière, R.G., Rochefort, D.L., Chrétien, N., Rommens, J.M., Cochius, J.I., Kälviäinen, R., Nousiainen, U., Patry, G., Farrell, K., Söderfeldt, B., et al. (1997). Unstable insertion in the 5' flanking region of the cystatin B gene is the most common mutation in progressive myoclonus epilepsy type 1, EPM1. Nat. Genet.

Lalioti, M.D., Scott, H.S., Buresi, C., Rossier, C., Bottani, A., Morris, M.A., Malafosse, A., and Antonarakis, S.E. (1997). Dodecamer repeat expansion in cystatin B gene in progressive myoclonus epilepsy. Nature.

Lancaster, M.A., and Knoblich, J. (2015). Generation of Cerebral Organoids from Human Pluripotent Stem. Nat. Protoc.

Lancaster, M.A., and Knoblich, J.A. (2014a). Generation of cerebral organoids from human pluripotent stem cells. Nat. Protoc. *9*, 2329–2340.

Lancaster, M.A., and Knoblich, J.A. (2014b). Generation of cerebral organoids from human pluripotent stem cells. Nat Protoc *9*, 2329–2340.

Lancaster, M.A., Renner, M., Martin, C.-A., Wenzel, D., Bicknell, L.S., Hurles, M.E., Homfray, T., Penninger, J.M., Jackson, A.P., and Knoblich, J.A. (2013a). Cerebral

organoids model human brain development and microcephaly.

Lancaster, M.A., Renner, M., Martin, C.A., Wenzel, D., Bicknell, L.S., Hurles, M.E., Homfray, T., Penninger, J.M., Jackson, A.P., and Knoblich, J.A. (2013b). Cerebral organoids model human brain development and microcephaly. Nature.

Larsen, L., Chen, H.Y., Saegusa, J., and Liu, F.T. (2011). Galectin-3 and the skin. J. Dermatol. Sci. *64*, 85–91.

Lavdas, A.A., Grigoriou, M., Pachnis, V., and Parnavelas, J.G. (1999). The medial ganglionic eminence gives rise to a population of early neurons in the developing cerebral cortex. J. Neurosci. *19*, 7881–7888.

Lee, J. (2017). Malformations of cortical development: Genetic mechanisms and diagnostic approach. Korean J. Pediatr. *60*, 1–9.

Lee, J.H., Bae, J.A., Lee, J.H., Seo, Y.W., Kho, D.H., Sun, E.G., Lee, S.E., Cho, S.H., Joo, Y.E., Ahn, K.Y., et al. (2010). Glycoprotein 90K, downregulated in advanced colorectal cancer tissues, interacts with CD9/CD82 and suppresses the Wnt/β-catenin signal via ISGylation of β-catenin. Gut *59*, 907–917.

Lehesjoki, A. (2003). NEW EMBO MEMBER ' S REVIEW Molecular background of progressive myoclonus epilepsy. *22*.

Lehtinen, M.K., Tegelberg, S., Schipper, H., Su, H., Zukor, H., Manninen, O., Kopra, O., Joensuu, T., Hakala, P., Bonni, A., et al. (2009). Cystatin B deficiency sensitizes neurons to oxidative stress in progressive myoclonus epilepsy, EPM1. J. Neurosci.

Lepiemme, F., Stoufflet, J., Javier-Torrent, M., Mazzucchelli, G., Silva, C.G., and Nguyen, L. (2022). Oligodendrocyte precursors guide interneuron migration by unidirectional contact repulsion. Science (80-.). *376*.

Leppik, I.E. (2003). Classification of the Myoclonic Epilepsies. Epilepsia *44*, 2–6.

Létard, P., Drunat, S., Vial, Y., Duerinckx, S., Ernault, A., Amram, D., Arpin, S., Bertoli, M., Busa, T., Ceulemans, B., et al. (2018). Autosomal recessive primary microcephaly due to ASPM mutations: An update. Hum. Mutat. *39*, 319–332.

Leventer, R.J., Jansen, A., Pilz, D.T., Stoodley, N., Marini, C., Dubeau, F., Malone, J., Mitchell, L.A., Mandelstam, S., Scheffer, I.E., et al. (2010). Clinical and imaging heterogeneity of polymicrogyria: A study of 328 patients. Brain *133*, 1415–1427.

Liang, Y., Eng, W.S., Colquhoun, D.R., Dinglasan, R.R., Graham, D.R., and Mahal, L.K. (2014). Complex N-linked glycans serve as a determinant for exosome/microvesicle cargo recruitment. J. Biol. Chem. *289*, 32526–32537.

Lim, B.C., Matsumoto, S., Yamamoto, H., Mizuno, H., Kikuta, J., Ishii, M., and Kikuchi, A. (2016). Prickle1 promotes focal adhesion disassembly in cooperation with the CLASP-LL5β complex in migrating cells. J. Cell Sci.

Lim, L., Mi, D., Llorca, A., and Marín, O. (2018). Development and Functional Diversification of Cortical Interneurons. Neuron *100*, 294–313.

Liu, C., Lin, C., Whitaker, D.T., Bakeri, H., Bulgakov, O. V., Liu, P., Lei, J., Dong, L., Li, T., and Swaroop, A. (2013). Prickle1 is expressed in distinct cell populations of the central nervous system and contributes to neuronal morphogenesis. Hum. Mol. Genet.

Lodato, S., Tomassy, G.S., De Leonibus, E., Uzcategui, Y.G., Andolfi, G., Armentano, M., Touzot, A., Gaztelu, J.M., Arlotta, P., De La Prida, L.M., et al. (2011). Loss of COUP-TFI alters the balance between caudal ganglionic eminence- and medial ganglionic eminence-derived cortical interneurons and results in resistance to epilepsy. J. Neurosci. *31*, 4650–4662.

Loimaranta, V., Hepojoki, J., Laaksoaho,

O., and Pulliainen, A.T. (2018). Galectin-3-binding protein: A multitask glycoprotein with innate immunity functions in viral and bacterial infections. J. Leukoc. Biol. *104*, 777–786.

Long, K.R., and Huttner, W.B. (2019). How the extracellular matrix shapes neural development. Open Biol. *9*.

Long, K.R., Newland, B., Florio, M., Kalebic, N., Langen, B., Kolterer, A., Wimberger, P., and Huttner, W.B. (2018). Extracellular Matrix Components HAPLN1, Lumican, and Collagen I Cause Hyaluronic Acid-Dependent Folding of the Developing Human Neocortex. Neuron *99*, 702-719.e7.

López-Bendito, G., Sturgess, K., Erdélyi, F., Szabó, G., Molnár, Z., and Paulsen, O. (2004). Preferential origin and layer destination of GAD65-GFP cortical interneurons. Cereb. Cortex.

Luca, C. De, and Papa, M. (2016). Looking Inside the Matrix : Perineuronal Nets in Plasticity , Maladaptive Plasticity and Neurological Disorders. Neurochem. Res. *41*, 1507–1515.

Lui, J.H., Hansen, D. V., and Kriegstein, A.R. (2011). Development and evolution of the human neocortex. Cell *146*, 18–36.

Luo, M., Zhang, Q., Hu, Y., Sun, C., Sheng, Y., and Deng, C. (2021). Lgals3bp: A potential plasma biomarker associated with diagnosis and prognosis in patients with sepsis. Infect. Drug Resist. *14*, 2863–2871.

Mancini, G.M.S., Schot, R., De Wit, M.C.Y., De Coo, R.F., Oostenbrink, R., Bindels-De Heus, K., Berger, L.P.V., Lequin, M.H., De Vries, F.A.T., Wilke, M., et al. (2016). CSTB null mutation associated with microcephaly, early developmental delay, and severe dyskinesia. Neurology.

Mariani, J., Simonini, M. V., Palejev, D., Tomasini, L., Coppola, G., Szekely, A.M., Horvath, T.L., and Vaccarino, F.M. (2012). Modeling human cortical development in vitro using induced pluripotent stem cells. Proc. Natl. Acad. Sci. *109*, 12770–12775.

Mariani, J., Coppola, G., Pelphrey, K.A., Howe, J.R., and Vaccarino Correspondence, F.M. (2015). FOXG1-Dependent Dysregulation of GABA/ Glutamate Neuron Differentiation in Autism Spectrum Disorders. Cell *162*, 375–390.

Marín, O. (2012). Interneuron dysfunction in psychiatric disorders. Nat. Rev. Neurosci. *13*, 107–120.

Marín, O. (2013). Cellular and molecular mechanisms controlling the migration of neocortical interneurons. Eur. J. Neurosci. *38*, 2019–2029.

Martínez, V.G., Moestrup, S.K., Holmskov, U., Mollenhauer, J., and Lozano, F. (2011). The conserved scavenger receptor cysteine-rich super family in therapy and diagnosis. Pharmacol. Rev. *63*, 967–1000.

Martynoga, B., Morrison, H., Price, D.J., and Mason, J.O. (2005). Foxg1 is required for specification of ventral telencephalon and region-specific regulation of dorsal telencephalic precursor proliferation and apoptosis. Dev. Biol. *283*, 113–127.

Mathieu, M., Martin-Jaular, L., Lavieu, G., and Théry, C. (2019). Specificities of secretion and uptake of exosomes and other extracellular vesicles for cell-to-cell communication. Nat. Cell Biol. *21*, 9–17.

Di Matteo, F., Pipicelli, F., Kyrousi, C., Isabella, T., Ayo Martin, A.C., Giordano, M., Hoffmann, A., Canafoglia, L., Gotz, M., Di Giaimo, R., et al. Cystatin B is essential for proliferation and interneuron migration in individuals with EPM1 epilepsy. EMBO Mol. Med. *2020*.

Di Matteo, F., Pipicelli, F., Kyrousi, C., Tovecci, I., Penna, E., Crispino, M., Chambery, A., Russo, R., Ayo-Martin, A.C., Giordano, M., et al. (2020). Cystatin B is essential for proliferation and interneuron migration in individuals with EPM 1 epilepsy . EMBO Mol. Med. *12*, 1–

21.

Mayer, C., Hafemeister, C., Bandler, R.C., Machold, R., Batista Brito, R., Jaglin, X., Allaway, K., Butler, A., Fishell, G., and Satija, R. (2018). Developmental diversification of cortical inhibitory interneurons. Nature.

Mazurskyy, A., and Howitt, J. (2021). Extracellular Vesicles in Neurological Disorders. Subcell. Biochem. *97*, 411–436.

Megraw, T.L., Sharkey, J.T., and Nowakowski, R.S. (2011). Cdk5rap2 exposes the centrosomal root of microcephaly syndromes. Trends Cell Biol. *21*, 470–480.

Meldolesi, J. (2018). Exosomes and Ectosomes in Intercellular Communication. Curr. Biol. *28*, R435–R444.

Métin, C., Baudoin, J.P., Rakić, S., and Parnavelas, J.G. (2006). Cell and molecular mechanisms involved in the migration of cortical interneurons. Eur. J. Neurosci. *23*, 894–900.

Mirzaa, G.M., Campbell, C.D., Solovieff, N., Goold, C.P., Jansen, L.A., Menon, S., Timms, A.E., Conti, V., Biag, J.D., Olds, C., et al. (2016). Association of MTOR mutations with developmental brain disorders, including megalencephaly, focal cortical dysplasia, and pigmentary mosaicism. JAMA Neurol. *73*, 836–845.

Miura, Y., and Pașca, S.P. (2019). Polarizing brain organoids. Nat. Biotechnol. *37*.

Miura, Y., Li, M.Y., Birey, F., Ikeda, K., Revah, O., Thete, M.V., Park, J.Y., Puno, A., Lee, S.H., Porteus, M.H., et al. (2020). Generation of human striatal organoids and cortico-striatal assembloids from human pluripotent stem cells. Nat. Biotechnol. *38*, 1421–1430.

Miyata, S., and Kitagawa, H. (2017). Formation and remodeling of the brain extracellular matrix in neural plasticity: Roles of chondroitin sulfate and hyaluronan. Biochim. Biophys. Acta - Gen. Subj. *1861*, 2420–2434.

Miyata, T., Kawaguchi, A., Saito, K., Kawano, M., Muto, T., and Ogawa, M. (2004). Asymmetric production of surface-dividing and non-surface-dividing cortical progenitor cells. Development *131*, 3133–3145.

Montecalvo, A., Larregina, A.T., Shufesky, W.J., Stolz, D.B., Sullivan, M.L.G., Karlsson, J.M., Baty, C.J., Gibson, G.A., Erdos, G., Wang, Z., et al. (2012). Mechanism of transfer of functional microRNAs between mouse dendritic cells via exosomes. Blood *119*, 756–766.

Müller, S.A., Sasaki, T., Bork, P., Wolpensinger, B., Schulthess, T., Timpl, R., Engel, A., and Engel, J. (1999). Domain organization of Mac-2 binding protein and its oligomerization to linear and ring-like structures. J. Mol. Biol. *291*, 801–813.

Mullin, A.P., Gokhale, A., Moreno-De-Luca, A., Sanyal, S., Waddington, J.L., and Faundez, V. (2013). Neurodevelopmental disorders: Mechanisms and boundary definitions from genomes, interactomes and proteomes. Transl. Psychiatry *3*.

Muralidharan-Chari, V., Clancy, J.W., Sedgwick, A., and D'Souza-Schorey, C. (2010). Microvesicles: Mediators of extracellular communication during cancer progression. J. Cell Sci. *123*, 1603–1611.

Nadarajah, B., and Parnavelas, J.G. (2002a). Modes of neuronal migration in the developing cerebral cortex. Nat. Rev. Neurosci. *3*, 423–432.

Nadarajah, B., and Parnavelas, J.G. (2002b). Modes of neuronal migration in the developing cerebral cortex. Nat. Rev. Neurosci. *3*, 423–432.

Nadarajah, B., Brunstrom, J.E., Grutzendler, J., Wong, R.O.L., and Pearlman, A.L. (2001). Two modes of radial migration in early development of the cerebral cortex. Nat. Neurosci. *4*, 143–150.

Napolitano, F., De Rosa, A., Russo, R., Di Maio, A., Garofalo, M., Federici, M.,

Migliarini, S., Ledonne, A., Rizzo, F.R., Avallone, L., et al. (2019). The striatal-enriched protein Rhes is a critical modulator of cocaine-induced molecular and behavioral responses. Sci. Rep.

Nicholas, A.K., Swanson, E.A., Cox, J.J., Karbani, G., Malik, S., Springell, K., Hampshire, D., Ahmed, M., Bond, J., Di Benedetto, D., et al. (2009). The molecular landscape of ASPM mutations in primary microcephaly. J. Med. Genet. *46*, 249–253.

Van Niel, G., D'Angelo, G., and Raposo, G. (2018). Shedding light on the cell biology of extracellular vesicles. Nat. Rev. Mol. Cell Biol. *19*, 213–228.

Nigri, A., Visani, E., Bertolino, N., Nanetti, L., Mariotti, C., Panzeri, M., Bruzzone, M.G., Franceschetti, S., and Canafoglia, L. (2017). Cerebellar Involvement in Patients with Mild to Moderate Myoclonus Due to EPM1: Structural and Functional MRI Findings in Comparison with Healthy Controls and Ataxic Patients. Brain Topogr.

Noctor, S.C., Martinez-Cerdeño, V., Ivic, L., and Kriegstein, A.R. (2004). Cortical neurons arise in symmetric and asymmetric division zones and migrate through specific phases. Nat. Neurosci. *7*, 136–144.

Nowakowski, T.J., Pollen, A.A., Sandoval-Espinosa, C., and Kriegstein, A.R. (2016). Transformation of the Radial Glia Scaffold Demarcates Two Stages of Human Cerebral Cortex Development. Neuron *91*, 1219–1227.

O'Neill, A.C., Kyrousi, C., Einsiedler, M., Burtscher, I., Drukker, M., Markie, D.M., Kirk, E.P., Götz, M., Robertson, S.P., and Cappello, S. (2018a). Mob2 Insufficiency Disrupts Neuronal Migration in the Developing Cortex. Front. Cell. Neurosci.

O'Neill, A.C., Kyrousi, C., Klaus, J., Leventer, R.J., Kirk, E.P., Fry, A., Pilz, D.T., Morgan, T., Jenkins, Z.A., Drukker, M., et al. (2018b). A Primate-Specific Isoform of PLEKHG6 Regulates Neurogenesis and Neuronal Migration. Cell Rep. *25*, 2729-2741.e6.

Oberst, P., Fièvre, S., Baumann, N., Concetti, C., Bartolini, G., and Jabaudon, D. (2019). Temporal plasticity of apical progenitors in the developing mouse neocortex. Nature *573*, 370–374.

Ohnuma, S.I., and Harris, W.A. (2003). Neurogenesis and the cell cycle. Neuron *40*, 199–208.

Ostrowski, M., Carmo, N.B., Krumeich, S., Fanget, I., Raposo, G., Savina, A., Moita, C.F., Schauer, K., Hume, A.N., Freitas, R.P., et al. (2010). Rab27a and Rab27b control different steps of the exosome secretion pathway. Nat. Cell Biol. *12*, 19–30.

Pang, T., Atefy, R., and Sheen, V. (2008). Malformations of cortical development. Neurologist *14*, 181–191.

Parrini, E., Ramazzotti, A., Dobyns, W.B., Mei, D., Moro, F., Veggiotti, P., Marini, C., Brilstra, E.H., Bernardina, B.D., Goodwin, L., et al. (2006). Periventricular heterotopia: Phenotypic heterogeneity and correlation with Filamin a mutations. Brain *129*, 1892–1906.

Parrini, E., Conti, V., Dobyns, W.B., and Guerrini, R. (2016). Genetic basis of brain malformations. Mol. Syndromol. *7*, 220–233.

Parsons, J.T., Horwitz, A.R., and Schwartz, M.A. (2010). Cell adhesion: Integrating cytoskeletal dynamics and cellular tension. Nat. Rev. Mol. Cell Biol.

Paşca, A.M., Sloan, S.A., Clarke, L.E., Tian, Y., Makinson, C.D., Huber, N., Kim, C.H., Park, J.-Y., O'Rourke, N.A., Nguyen, K.D., et al. (2015). Functional cortical neurons and astrocytes from human pluripotent stem cells in 3D culture. Nat. Methods *12*, 671–678.

Penna, E., Cerciello, A., Chambery, A., Russo, R., Cernilogar, F.M., Pedone, E.M., Perrone-Capano, C., Cappello, S., Di Giaimo, R., and Crispino, M. (2019). Cystatin B Involvement in Synapse Physiology of Rodent Brains and Human

Cerebral Organoids. Front. Mol. Neurosci.

Pennacchio, L.A., Lehesjoki, A.E., Stone, N.E., Willour, V.L., Virtaneva, K., Miao, J., D'Amato, E., Ramirez, L., Faham, M., Koskiniemi, M., et al. (1996). Mutations in the gene encoding cystatin B in progressive myoclonus epilepsy (EPM1). Science (80-.).

Perez-Hernandez, D., Gutiérrez-Vázquez, C., Jorge, I., López-Martín, S., Ursa, A., Sánchez-Madrid, F., Vázquez, J., and Yañez-Mó, M. (2013). The intracellular interactome of tetraspanin-enriched microdomains reveals their function as sorting machineries toward exosomes. J. Biol. Chem. *288*, 11649–11661.

Peruzzotti-Jametti, L., Bernstock, J.D., Willis, C.M., Manferrari, G., Rogall, R., Fernandez-Vizarra, E., Williamson, J.C., Braga, A., van den Bosch, A., Leonardi, T., et al. (2021). Neural stem cells traffic functional mitochondria via extracellular vesicles.

Peyre, E., Silva, C.G., and Nguyen, L. (2015). Crosstalk between intracellular and extracellular signals regulating interneuron production, migration and integration into the cortex. Front. Cell. Neurosci. *9*, 1–18.

Pfennig, S., Weiss, A., Burk, K., Acker-palmer, A., and Sentu, A. (2011). pathway to regulate neuronal migration. 0–7.

Pikkarainen, T., Nurmi, T., Sasaki, T., Bergmann, U., and Vainio, S. (2017). Role of the extracellular matrix-located Mac-2 binding protein as an interactor of the Wnt proteins. Biochem. Biophys. Res. Commun. *491*, 953–957.

Pilz, D. (1998). LIS1 and XLIS (DCX) mutations cause most classical lissencephaly, but different patterns of malformation. Hum. Mol. Genet. *7*, 2029–2037.

Pilz, G.A., Shitamukai, A., Reillo, I., Pacary, E., Schwausch, J., Stahl, R., Ninkovic, J., Snippert, H.J., Clevers, H., Godinho, L., et al. (2013). Amplification of progenitors in the mammalian telencephalon includes a new radial glial cell type. Nat. Commun. *4*, 1–11.

Pilz, G.A., Bottes, S., Betizeau, M., Jörg, D.J., Carta, S., Simons, B.D., Helmchen, F., and Jessberger, S. (2018). Live imaging of neurogenesis in the adult mouse hippocampus. Science (80-.). *359*, 658–662.

Piñero, J., Bravo, Á., Queralt-Rosinach, N., Gutiérrez-Sacristán, A., Deu-Pons, J., Centeno, E., García-García, J., Sanz, F., and Furlong, L.I. (2017). DisGeNET: A comprehensive platform integrating information on human disease-associated genes and variants. Nucleic Acids Res. *45*, D833–D839.

Pipicelli, F., Baumann, N., Giaimo, R. Di, Kyrousi, C., and Bonrath, R. (2022). Extrinsic regulation of interneuron specification and migration.

Pirozzi, F., Nelson, B., and Mirzaa, G.M. (2018). From microcephaly to megalencephaly: determinants of brain size. Dialogues Clin. Neurosci. *20*, 267–282.

Pleasure, S.J., Anderson, S., Hevner, R., Bagri, A., Marin, O., Lowenstein, D.H., and Rubenstein, J.L.R. (2000). Cell migration from the ganglionic eminences is required for the development of hippocampal GABAergic interneurons. Neuron *28*, 727–740.

Polajnar, M., Zavašnik-Bergant, T., Škerget, K., Vizovišek, M., Vidmar, R., Fonović, M., Kopitar-Jerala, N., Petrovič, U., Navarro, S., Ventura, S., et al. (2014). Human stefin B role in cell's response to misfolded proteins and autophagy. PLoS One.

Pollen, A.A., Nowakowski, T.J., Chen, J., Retallack, H., Sandoval-Espinosa, C., Nicholas, C.R., Shuga, J., Liu, S.J., Oldham, M.C., Diaz, A., et al. (2015). Molecular Identity of Human Outer Radial Glia during Cortical Development. Cell *163*, 55–67.

Prianichnikov, N., Koch, H., Koch, S., Lubeck, M., Heilig, R., Brehmer, S., Fischer, R., and Cox, J. (2020). Maxquant software for ion mobility enhanced shotgun proteomics. Mol. Cell. Proteomics *19*, 1058–1069.

Puts, N.A.J., Wodka, E.L., Harris, A.D., Crocetti, D., Tommerdahl, M., Mostofsky, S.H., and Edden, R.A.E. (2016). Reduced GABA and Altered Somatosensory Function in Children with Autism Spectrum Disorder. 1–12.

Qian, X., Nguyen, H.N., Song, M.M., Hadiono, C., Ogden, S.C., Hammack, C., Yao, B., Hamersky, G.R., Jacob, F., Zhong, C., et al. (2016). Brain-Region-Specific Organoids Using Mini-bioreactors for Modeling ZIKV Exposure. Cell *165*, 1238–1254.

Quadrato, G., Nguyen, T., Macosko, E.Z., Sherwood, J.L., Min Yang, S., Berger, D.R., Maria, N., Scholvin, J., Goldman, M., Kinney, J.P., et al. (2017). Cell diversity and network dynamics in photosensitive human brain organoids. Nature *545*, 48–53.

Rakic, P. (1972). Mode of cell migration to the superficial layers of fetal monkey neocortex. J. Comp. Neurol. *145*, 61–83.

Rakic, P. (2009). Evolution of the neocortex: A perspective from developmental biology. Nat. Rev. Neurosci. *10*, 724–735.

Rashighi, M., and Harris, J.E. (2017). 乳鼠心肌提取 HHS Public Access. Physiol. Behav. *176*, 139–148.

Reczek, D., Schwake, M., Schröder, J., Hughes, H., Blanz, J., Jin, X., Brondyk, W., Van Patten, S., Edmunds, T., and Saftig, P. (2007). LIMP-2 Is a Receptor for Lysosomal Mannose-6-Phosphate-Independent Targeting of β-Glucocerebrosidase. Cell.

Rhinn, M., and Dollé, P. (2012). Retinoic acid signalling during development. Development *139*, 843–858.

Rinne, R., Saukko, P., Järvinen, M., and Lehesjoki, A.E. (2002). Reduced cystatin B activity correlates with enhanced cathepsin activity in progressive myoclonus epilepsy. Ann. Med. *34*, 380–385.

Rivière, J., Mirzaa, G.M., Roak, B.J.O., Beddaoui, M., Conway, R.L., St-onge, J., Schwartzentruber, J.A., Karen, W., Nikkel, S.M., Worthylake, T., et al. (2013). De novo germline and postzygotic mutations in AKT3, PIK3R2 and PIK3CA cause a spectrum of related megalencephaly syndromes. Nat. Genet. *44*, 934–940.

Romero-grimaldi, C., and Moreno-lo, B. (2008). Age-Dependent Effect of Nitric Oxide on Subventricular Zone and Olfactory Bulb. J. Comp. Neurol. *346*, 339–346.

Rubenstein, J.L.R., and Merzenich, M.M. (2003). Model of autism: Increased ratio of excitation/inhibition in key neural systems. Genes, Brain Behav.

Rubin, A.N., Alfonsi, F., Humphreys, M.P., Choi, C.K.P., Rocha, S.F., and Kessaris, N. (2010). The germinal zones of the basal ganglia but not the septum generate GABAergic interneurons for the cortex. J. Neurosci. *30*, 12050–12062.

Russo, R., Matrone, N., Belli, V., Ciardiello, D., Valletta, M., Esposito, S., Pedone, P.V., Ciardiello, F., Troiani, T., and Chambery, A. (2019). Macrophage migration inhibitory factor is a molecular determinant of the anti-EGFR monoclonal antibody cetuximab resistance in human colorectal cancer cells. Cancers (Basel).

Saito, T. (2006). In vivo electroporation in the embryonic mouse central nervous system. Nat. Protoc.

Sakaguchi, H., Kadoshima, T., Soen, M., Narii, N., Ishida, Y., Ohgushi, M., Takahashi, J., Eiraku, M., and Sasai, Y. (2015). Generation of functional hippocampal neurons from self-organizing human embryonic stem cell-derived dorsomedial telencephalic tissue. Nat. Commun. *6*, 8896.

Sarmast, S.T., Abdullahi, A.M., and Jahan, N. (2020). Current Classification of Seizures and Epilepsies: Scope, Limitations and Recommendations for Future Action. Cureus *12*.

Savasta, S., Verrotti, A., Spartà, M.V., Foiadelli, T., Villa, M.P., and Parisi, P. (2015). Unilateral periventricular heterotopia and epilepsy in a girl with Ehlers-Danlos syndrome. Epilepsy Behav. Case Reports.

Scherer, C., Schuele, S., Minotti, L., Chabardes, S., Hoffmann, D., and Kahane, P. (2005). Intrinsic epileptogenicity of an isolated periventricular nodular heterotopia. Neurology *65*, 495–496.

Schneider, C.A., Rasband, W.S., and Eliceiri, K.W. (2012). NIH Image to ImageJ: 25 years of image analysis. Nat. Methods 2012 97 *9*, 671–675.

Sekine, K., Honda, T., Kawauchi, T., Kubo, K. ichiro, and Nakajima, K. (2011). The outermost region of the developing cortical plate is crucial for both the switch of the radial migration mode and the dab1-dependent "inside-out" lamination in the neocortex. J. Neurosci. *31*, 9426–9439.

Sessa, A., Mao, C.A., Colasante, G., Nini, A., Klein, W.H., and Broccoli, V. (2010). Tbr2-positive intermediate (basal) neuronal progenitors safeguard cerebral cortex expansion by controlling amplification of pallial glutamatergic neurons and attraction of subpallial GABAergic interneurons. Genes Dev. *24*, 1816–1826.

Shah, R., Patel, T., and Freedman, J.E. (2018). Circulating Extracellular Vesicles in Human Disease. N. Engl. J. Med. *379*, 958–966.

Shang, W., Liu, W.H., Zhao, X.H., Sun, Q.J., Bi, J.Z., and Chi, Z.F. (2008). Expressions of glutathione S-transferase alpha, mu, and pi in brains of medically intractable epileptic patients. BMC Neurosci.

Shannon, P., Pennacchio, L.A., Houseweart, M.K., Minassian, B.A., and Myers, R.M. (2002). Neuropathological changes in a mouse model of progressive myoclonus epilepsy: Cystatin B deficiency and Unverricht-Lundborg disease. J. Neuropathol. Exp. Neurol.

Sharma, P., Mesci, P., Carromeu, C., McClatchy, D.R., Schiapparelli, L., Yates, J.R., Muotri, A.R., and Cline, H.T. (2019). Exosomes regulate neurogenesis and circuit assembly. Proc. Natl. Acad. Sci. U. S. A. *116*, 16086–16094.

Shi, Y., Kirwan, P., and Livesey, F.J. (2012a). Directed differentiation of human pluripotent stem cells to cerebral cortex neurons and neural networks. Nat. Protoc. *7*, 1836–1846.

Shi, Y., Kirwan, P., Smith, J., Robinson, H.P.C., and Livesey, F.J. (2012b). Human cerebral cortex development from pluripotent stem cells to functional excitatory synapses. Nat. Neurosci. *15*, 477–486.

Siegenthaler, J.A., and Pleasure, S.J. (2011). We have got you "covered": How the meninges control brain development. Curr. Opin. Genet. Dev. *21*, 249–255.

Silva, C.G., Peyre, E., and Nguyen, L. Cell migration promotes dynamic cellular interactions to control cerebral cortex morphogenesis.

Silva, C.G., Peyre, E., Adhikari, M.H., Tielens, S., Tanco, S., Van Damme, P., Magno, L., Krusy, N., Agirman, G., Magiera, M.M., et al. (2018). Cell-Intrinsic Control of Interneuron Migration Drives Cortical Morphogenesis. Cell *172*, 1063-1078.e19.

Sloan, S.A., Andersen, J., Paşca, A.M., Birey, F., and Paşca, S.P. (2018). Generation and assembly of human brain region–specific three-dimensional cultures. Nat. Protoc. *13*, 2062–2085.

Soleman, S., Filippov, M.A., Dityatev, A., and Fawcett, J.W. (2013). Targeting the neural extracellular matrix in neurological

disorders. Neuroscience *253*, 194–213.

Song, Y., Wang, M., Tong, H., Tan, Y., Hu, X., Wang, K., and Wang, K. (2020). Plasma exosomes from endometrial cancer patients contain LGALS3BP to promote endometrial cancer progression. Oncogene.

Staerk, J., Dawlaty, M.M., Gao, Q., Maetzel, D., Hanna, J., Sommer, C.A., Mostoslavsky, G., and Jaenisch, R. (2010). Reprogramming of human peripheral blood cells to induced pluripotent stem cells. Cell Stem Cell *7*, 20–24.

Stahl, R., Walcher, T., De Juan Romero, C., Pilz, G.A., Cappello, S., Irmler, M., Sanz-Aquela, J.M., Beckers, J., Blum, R., Borrell, V., et al. (2013). Trnp1 regulates expansion and folding of the mammalian cerebral cortex by control of radial glial fate. Cell.

Stampolidis, P., Ullrich, A., and Iacobelli, S. (2015). LGALS3BP , lectin galactoside-binding soluble 3 binding protein , promotes oncogenic cellular events impeded by antibody intervention. 39–52.

Steinecke, A., Gampe, C., Zimmer, G., Rudolph, J., and Bolz, J. (2014). EphA / ephrin A reverse signaling promotes the migration of cortical interneurons from the medial ganglionic eminence. 460–471.

Stiles, J., and Jernigan, T.L. (2010). The basics of brain development. Neuropsychol. Rev. *20*, 327–348.

Sun, T., and Hevner, R.F. (2014). Growth and folding of the mammalian cerebral cortex: from molecules to malformations. Nat. Rev. Neurosci. *15*, 217–232.

Takahashi, K., and Yamanaka, S. (2006). Induction of pluripotent stem cells from mouse embryonic and adult fibroblast cultures by defined factors. Cell *126*, 663–676.

Talebian, A., Britton, R., Ammanuel, S., Bepari, A., Sprouse, F., Birnbaum, S.G., Szabó, G., Tamamaki, N., Gibson, J., and Henkemeyer, M. (2017). Autonomous and non-autonomous roles for ephrin-B in interneuron migration. Dev. Biol.

Tamamaki, N., Yanagawa, Y., Tomioka, R., Miyazaki, J.I., Obata, K., and Kaneko, T. (2003). Green Fluorescent Protein Expression and Colocalization with Calretinin, Parvalbumin, and Somatostatin in the GAD67-GFP Knock-In Mouse. J. Comp. Neurol.

Tanaka, T., Serneo, F.F., Higgins, C., Gambello, M.J., Wynshaw-Boris, A., and Gleeson, J.G. (2004). Lis1 and doublecortin function with dynein to mediate coupling of the nucleus to the centrosome in neuronal migration. J. Cell Biol. *165*, 709–721.

Tatti, R., Haley, M.S., Swanson, O.K., Tselha, T., and Maffei, A. (2017). Neurophysiology and Regulation of the Balance Between Excitation and Inhibition in Neocortical Circuits. Biol. Psychiatry *81*, 821–831.

Taverna, E., and Huttner, W.B. (2010). Neural progenitor nuclei IN motion. Neuron *67*, 906–914.

Taverna, E., and Magdalena, G. (2014). The Cell Biology of Neurogenesis : Toward an Understanding of the Development and Evolution of the Neocortex.

Telley, L., Agirman, G., Prados, J., Amberg, N., Fièvre, S., Oberst, P., Bartolini, G., Vitali, I., Cadilhac, C., Hippenmeyer, S., et al. (2019). Temporal patterning of apical progenitors and their daughter neurons in the developing neocortex. Science (80-.). *364*.

Theil, T., Alvarez-Bolado, G., Walter, A., and Rüther, U. (1999). Gli3 is required for Emx gene expression during dorsal telencephalon development. Development *126*, 3561–3571.

Thom, M., Martinian, L., Parnavelas, J.G., and Sisodiya, S.M. (2004). Distribution of cortical interneurons in grey matter heterotopia in patients with epilepsy. Epilepsia *45*, 916–923.

Thomson, J.A. (1998). Embryonic stem cell lines derived from human blastocysts. Science (80-.). *282*, 1145–1147.

Thornton, G.K., and Woods, C.G. (2009). Primary microcephaly: do all roads lead to Rome? Trends Genet. *25*, 501–510.

Tiveron, M.C., Rossel, M., Moepps, B., Yong, L.Z., Seidenfaden, R., Favor, J., König, N., and Cremer, H. (2006). Molecular interaction between projection neuron precursors and invading interneurons via stromal-derived factor 1 (CXCL12)/CXCR4 signaling in the cortical subventricular zone/intermediate zone. J. Neurosci. *26*, 13273–13278.

Tole, S., Ragsdale, C.W., and Grove, E.A. (2000). Dorsoventral patterning of the telencephalon is disrupted in the mouse mutant extra-toes. Dev. Biol. *217*, 254–265.

Trapnell, C., Cacchiarelli, D., Grimsby, J., Pokharel, P., Li, S., Morse, M., Lennon, N.J., Livak, K.J., Mikkelsen, T.S., and Rinn, J.L. (2014). The dynamics and regulators of cell fate decisions are revealed by pseudotemporal ordering of single cells. Nat. Biotechnol. *32*, 381–386.

Turk, B., Turk, D., and Turk, V. (2000). Lysosomal cysteine proteases: More than scavengers. Biochim. Biophys. Acta - Protein Struct. Mol. Enzymol. *1477*, 98–111.

Turrero García, M., and Harwell, C.C. (2017). Radial glia in the ventral telencephalon. FEBS Lett. *591*, 3942–3959.

Tyanova, S., Temu, T., and Cox, J. (2016). The MaxQuant computational platform for mass spectrometry-based shotgun proteomics. Nat. Protoc. *11*, 2301–2319.

Urbanelli, L., Buratta, S., Sagini, K., Tancini, B., and Emiliani, C. (2016). Extracellular vesicles as new players in cellular senescence. Int. J. Mol. Sci. *17*.

Villar-Cerviño, V., Molano-Mazón, M., Catchpole, T., Valdeolmillos, M., Henkemeyer, M., Martínez, L.M., Borrell, V., and Marín, O. (2013). Contact Repulsion Controls the Dispersion and Final Distribution of Cajal-Retzius Cells. Neuron *77*, 457–471.

Virtaneva, K., D'Amato, E., Miao, J., Koskiniemi, M., Norio, R., Avanzini, G., Franceschetti, S., Michelucci, R., Tassinari, C.A., Omer, S., et al. (1997). Unstable minisatellite expansion causing recessively inherited myoclonus epilepsy, EPM1. Nat. Genet.

Vyas, N., and Dhawan, J. (2017). Exosomes: mobile platforms for targeted and synergistic signaling across cell boundaries. Cell. Mol. Life Sci. *74*, 1567–1576.

Wamsley, B., and Fishell, G. (2017). Genetic and activity-dependent mechanisms underlying interneuron diversity. Nat. Rev. Neurosci. *18*, 299–309.

Wang, P., Mokhtari, R., Pedrosa, E., Kirschenbaum, M., Bayrak, C., Zheng, D., and Lachman, H.M. CRISPR/Cas9-mediated heterozygous knockout of the autism gene CHD8 and characterization of its transcriptional networks in cerebral organoids derived from iPS cells.

Watanabe, K., Taskesen, E., Van Bochoven, A., and Posthuma, D. (2017). Functional mapping and annotation of genetic associations with FUMA. Nat. Commun. *8*, 1–10.

Wen, T.H., Binder, D.K., Ethell, I.M., and Razak, K.A. (2018). The Perineuronal 'Safety' Net? Perineuronal Net Abnormalities in Neurological Disorders. Front. Mol. Neurosci. *11*, 270.

Wight, T.N. (2002). Versican: A versatile extracellular matrix proteoglycan in cell biology. Curr. Opin. Cell Biol. *14*, 617–623.

Wiśniewski, J.R., Zougman, A., Nagaraj, N., and Mann, M. (2009). Universal sample preparation method for proteome analysis. Nat. Methods 2009 65 *6*, 359–362.

Wojcik-Stanaszek, L., Gregor, A., and Zalewska, T. (2011). Regulation of neurogenesis by extracellular matrix and integrins. Acta Neurobiol. Exp. (Wars). *71*, 103–112.

Xiang, Y., Tanaka, Y., Patterson, B., Kang,

Y.J., Govindaiah, G., Roselaar, N., Cakir, B., Kim, K.Y., Lombroso, A.P., Hwang, S.M., et al. (2017). Fusion of Regionally Specified hPSC-Derived Organoids Models Human Brain Development and Interneuron Migration. Cell Stem Cell *21*, 383-398.e7.

Xu, Q., Guo, L., Moore, H., Waclaw, R.R., Campbell, K., Anderson, A., Cornell, W., College, M., Ave, Y., and York, N. (2011). NIH Public Access. *65*, 328–340.

Yingling, J., Youn, Y.H., Darling, D., Toyo-oka, K., Pramparo, T., Hirotsune, S., and Wynshaw-Boris, A. (2008). Neuroepithelial stem cell proliferation requires LIS1 for precise spindle orientation and symmetric division. Cell *132*, 474–486.

Yu, J., Vodyanik, M.A., Smuga-Otto, K., Antosiewicz-Bourget, J., Frane, J.L., Tian, S., Nie, J., Jonsdottir, G.A., Ruotti, V., Stewart, R., et al. (2007). Induced pluripotent stem cell lines derived from human somatic cells. Science (80-.). *318*, 1917–1920.

Yu, Y., Zeng, Z., Xie, D., Chen, R., Sha, Y., Huang, S., Cai, W., Chen, W., Li, W., Ke, R., et al. (2021). Interneuron origin and molecular diversity in the human fetal brain. Nat. Neurosci.

Yun, K., Garel, S., Fischman, S., and Rubenstein, J.L.R. (2003). Patterning of the lateral ganglionic eminence by the Gsh1 and Gsh2 homeobox genes regulates striatal and olfactory bulb histogenesis and the growth of axons through the basal ganglia. J. Comp. Neurol. *461*, 151–165.

Žerovnik, E. (2019). Possible Mechanisms by which Stefin B could Regulate Proteostasis and Oxidative Stress. Cells.

Zhang, X., Ding, H., Lu, Z., Ding, L., Song, Y., Jing, Y., Hu, Q., Dong, Y., and Ni, Y. (2019). Increased LGALS3BP promotes proliferation and migration of oral squamous cell carcinoma via PI3K/AKT pathway. Cell. Signal. *63*, 109359.

Zhao, Y., Yin, L., Zhang, H., Lan, T., Li, S., and Ma, P. (2018). Eph/ephrin family anchored on exosome facilitate communications between cells. Cell Biol. Int. *42*, 1458–1462.

Zhong, J., Kim, H.T., Lyu, J., Yoshikawa, K., Nakafuku, M., and Lu, W. (2011). The Wnt receptor Ryk controls specification of GABAergic neurons versus oligodendrocytes during telencephalon development. Development *138*, 409–419.

Zhou, J., Flores-Bellver, M., Pan, J., Benito-Martin, A., Shi, C., Onwumere, O., Mighty, J., Qian, J., Zhong, X., Hogue, T., et al. (2021). Human retinal organoids release extracellular vesicles that regulate gene expression in target human retinal progenitor cells. Sci. Reports 2021 111 *11*, 1–17.

Zhou, L., Xiao, X., Li, S., Jia, X., Wang, P., Sun, W., Zhang, F., Li, J., Li, T., and Zhang, Q. (2018). Phenotypic characterization of patients with early-onset high myopia due to mutations in COL2A1 or COL11A1: Why not stickler syndrome? Mol. Vis.

Zimmer, G., Garcez, P., Rudolph, J., Niehage, R., Weth, F., Lent, R., and Bolz, J. (2008). Ephrin-A5 acts as a repulsive cue for migrating cortical interneurons. Eur. J. Neurosci. *28*, 62–73.

Zimmer, G., Rudolph, J., Landmann, J., Gerstmann, K., and Gampe, C. (2011). Bidirectional EphrinB3 / EphA4 Signaling Mediates the Segregation of Medial Ganglionic Eminence- and Preoptic Area-Derived Interneurons in the Deep and Superficial Migratory Stream. *31*, 18364–18380.

9 Acknowledgment

This thesis is the result of an intense and incredibly important period of my life, where I grew up scientifically, but also personally. All of this would have not been possible without the people that have been on my side during these years.

First of all, thank you Silvia from believe in me since the beginning, when in 2017 I came to your lab for a 4 months internship. Thank you for giving me the chance to pursue my interests and passion in science, to support me all along this long journey and to push me to always do better.

I would also like to thank the members of my thesis advisor committee, Elisabeth and Moritz, for all the suggestions and discussions that helped to improve the quality of this work.

Being part of the IMPRS-TP graduation school gave me the great opportunity of meeting other students of the program, attending courses and gave me chances to travel to conferences and meetings around the world. Special thanks to the coordinators that have assisted me in these past years, Bettina, Andre and, of course, Isabel.

I would also like to thank all the people that contributed and collaborated to this thesis.
Christina, thank you for all the help, especially during the first year of my Ph.D., for teaching me how to perform in utero electroporation and live imaging experiments.
Francesco thank you for the huge support and fun we had working for the revision of the CSTB paper.
Rossella, thank you for all the support during the Ph.D. (and before!), for introducing me to the extracellular vesicles world and for always be available to help.
Andrea, my “exo-sister”, thank you for you precious help, for being by my side and for sharing every moment of joy and, sometimes, of frustration. I am really grateful that we could always count on each other!
Thanks to Natalia and Denis for supporting me and giving me the opportunity to learn how to perform single-cell RNAseq analysis all by myself, and thanks to Filippo for the help in the bulkRNA seq analysis. Thanks also to Maik, Anthi, Cristiana and Pablo for helping me with the single-cell experiment. Thanks also to Cinzia, Baerbel and Caro for the excellent technical support.
I would also like to thank all the members of the C-lab, for amazing discussion and support, but also fun.

Special thanks to Francesco, for being my best lab-mate. Thank you for listening to me and for sharing moments of craziness and fun together and to be always there for me!
Veronica, Giovanna and Kyrania thank you for all the laughs, the gossip and the fun in and outside the lab.
Thank you, Rebecca for letting me to be your master thesis supervisor, I have learnt a lot from this great experience we had together.
I would also like to thank Ane and Isabel, for welcoming me in the lab and supporting me at the beginning of my PhD.
Also, Lucia, Ezgi, Christine, thank you for all the great time spent together, most of the time with a bottle of wine and good food!

Sylvain, you can perfectly imagine how grateful I am to have you by my side. You have seen every shade that my mood could possibly have during these years, and yet you have always been there for me! Thank you for always finding the time to listen to me and help me, especially with R or statistics matters. These years would have not been the same without our trips with the van or our cycling tours. Thank you for being my life partner, I am so grateful that I could share this experience with you and I am so looking forward for our next adventures.

Inoltre, vorrei ringraziare la mia famiglia, soprattutto i miei genitori, Mario e Cristina, i miei modelli di riferimento, esempi di duro impegno e responsabilita'. Grazie per avermi sempre ricordato di impegnarmi al massimo per raggiungere i miei obbiettivi, contando sulle mie forze. Grazie il vostro incoraggiamento e supporto in tutti questi anni e per aver, a malincuore, accettato la mia scelta di andare all'estero. Ringrazio anche mia sorella Chiara, mio cognato Alessandro e miei nipoti Alessio e Simone per l'affetto e per esserci sempre.

10 Appendix

10.1 List of figures and tables

10.2 List of tables

10.3 List of abbreviations

ASD	autism spectrum disorder
BP	basal progenitor
CGE	caudal ganglionic eminence
CM	conditioned media
CNS	central nervous system
CO	cerebral organoid
CSF	cerebral spinal fluid
CSTB	cystatin B
CTRL	control
DAPI	4,6-diamidino-2 phenylindole
DCX	double cortin
DE	differential expression
DEP	differential expression package
DMSO	dimethyl sulfoxide
DNA	Deoxyribonucleic acid
DTT	dithiothreitol
EB	embryoid body
ECL	Electrochemiluminescence
ECM	extracellular matrix
EDTA	Ethylenediaminetetraacetic acid
EGFP	enhanced green fluorescent protein
EM	electromicroscopy
EPM1	Epilepsy with Progressive Myoclonus, Type 1
EV	extracellular vesicle
FACS	fluorescence-activated cells sorting
FCD	focal cortical dysplasia
FCS	fetal calf serum
FDR	False discovery rate
GE	ganglionic emincence
ID	intellectual disability

IHC	immunohistochemistry
IN	interneuron
INM	interkinetic nuclear migration
IP	intermediate progenitor
IPSC	induced pluripotent stem cell
IZ	intermediate zone
JME	benign primary epilepsy syndromes
KO	knockout
LFQ	label-free quantification
LGALS3BP	galectin 3 binding protein
LGE	lateral ganglionic eminence
MGE	medial ganglionic eminece
MO	mosaic organoid
MRI	Magnetic resonance imaging
MSN	midy spiny neurons
MVB	multivescicular body
MZ	marginal zone
NDD	neurodevelopmental disorder
NPC	neuronal progenitor cell
NSC	neuronal stem cell
OSVZ	outer subventricular zone
PBMC	peripheral blood mononuclear cells
PBS	phosphate-buffered saline
PCA	Principal component analysis
PFA	paraformaldehyde
PME	progressive myoclonic epilepsies
PMG	polymicrogyria
PVNH	periventricular nodular heterotopia
RFP	red fluorescent protein
RIPA	Radioimmunoprecipitation assay buffer
RNA	ribonucleic acid
RT	room temperature
SBH	subcortical band heterotopia
SCZ	schizophrenia

STED	Stimulated Emission Depletion
SVZ	subventricular zone
TF	transcription factor
UMAP	Uniform Manifold Approximation and Projection
UMI	Unique Molecular Identifier
VIM	vimentin
VIP	vasoactive intestinal peptide
VZ	ventricular zone

10.4 List of publications

10.4.1 First author publications

1. **Pipicelli, F**., Baumann, N., Di Giaimo, R., Kyrousi, C., Bonrath, R., Jabaudon, D., & Cappello, S. (2022). Extrinsic regulation of interneuron specification and migration. bioRxiv.

2. Di Matteo, F.*, **Pipicelli, F.***, Kyrousi, C., Tovecci, I., Penna, E., Crispino, M., Chambery, A., Russo, R., Ayo-Martin, A. C., Giordano, M., Hoffmann, A., Ciusani, E., Canafoglia, L., Götz, M., Di Giaimo, R., & Cappello, S. (2020). Cystatin B is essential for proliferation and interneuron migration in individuals with EPM 1 epilepsy. *EMBO Molecular Medicine*, *12*(6), 1–21. https://doi.org/10.15252/emmm.201911419

3. Kullmann, J. A.*, Meyer, S.*, **Pipicelli, F.***, Kyrousi, C., Schneider, F., Bartels, N., Cappello, S., & Rust, M. B. (2019). *Profilin1-Dependent F-Actin Assembly Controls Division of Apical Radial Glia and Neocortex Development*. 1–16. https://doi.org/10.1093/cercor/bhz321

***The authors contributed equally to the work.**

10.4.2 Other publications

4. Jeroen W. Noordhoek, ‡, **Fabrizia Pipicelli**, Ida Barone, Oscar Franken, Kora Montagne-Wajer, Janine Mariën, Rudo A. Verweij, Cornelis A. M. van Gestel, Nico M. van Straalen and Dick Roelofs (2018). *Phenotypic and transcriptional responses associated with multi-generation exposure of Folsomia candida to engineered nanomaterials.* DOI: 10.1039/c8en00456k

10.5 Affidavit

LMU LUDWIG-MAXIMILIANS-UNIVERSITÄT MÜNCHEN

Dean's Office Medical Faculty
Faculty of Medicine

Affidavit

Pipicelli, Fabrizia

Surname, first name

Address

I hereby declare, that the submitted thesis entitled

Non-cell autonomous mechanisms in neurodevelopment and neurological disorders

is my own work. I have only used the sources indicated and have not made unauthorised use of services of a third party. Where the work of others has been quoted or reproduced, the source is always given.

I further declare that the dissertation presented here has not been submitted in the same or similar form to any other institution for the purpose of obtaining an academic degree.

Vienna, 16/03/2023
Place, Date

Fabrizia Pipicelli
Signature doctoral candidate

Affidavit Human Biology

Date: 17.03.2023

10.6 Confirmation of congruency

LMU LUDWIG-MAXIMILIANS-UNIVERSITÄT MÜNCHEN

Dean's Office Medical Faculty
Doctoral Office

Confirmation of congruency between printed and electronic version of the doctoral thesis

Doctoral candidate: Fabrizia Pipicelli

Address:

I hereby declare that the electronic version of the submitted thesis, entitled

Non-cell autonomous mechanisms in neurodevelopment and neurological disorders

is congruent with the printed version both in content and format.

Vienna, 16/03/2023
Place, Date

Fabrizia Pipicelli
Signature doctoral candidate

Congruency of submitted versions Human Biology Date: 17.03.2023